Republic of Iraq
Ministry of Higher Education
and Scientific Research
University of Babylon
Faculty of Materials Engineering
Polymer Department

Effect of MWCNTs and Natural Dye/Polystyrene Composite Nano Fibers for High Sensitivity Applications By Electrospinning Techniques

A thesis submitted in partial fulfillment of the requirements for the degree of Master in the Babylon University/Faculty of Materials Engineering / Polymer

Submitted by

Ahmed Amer Flayeh Hassan

Supervised by:

Prof. Dr. Hanaa Jawad Kadhim

2021-2022 A.D

1442-1443 A.H

بسم الله الرحمن الرحيم

﴿وَقُل رَّبِّ زِدْنِي عِلْمًا﴾

صدق الله العلي العظيم

سورة طه_الآية (١١٤)

Dedication

To

My family

With All love

Ahmed Amer Flayeh

Acknowledgments

In the first, I would like to thank My distinguished family for their great sacrifices to make progress and excellence in various fields, including the field of study, and to thank my distinguished teachers for their great efforts and their support in this work which I hope will develop the reality of our country to the best in the near future.

Ahmed Amer Flayeh

ABSTRACT

In the current work, the electrospinning technique was used to manufacture nanocomposite fibers of polystyrene dissolved in dimethylformamide in concentration (12, 14, 16 wt.%), and multi-walled carbon nanotubes were also added to the prepared samples, to know its effect on the prepared solutions and the properties of the resulting fibers. A plant dye extracted from yellow flower leaves was also used on the best prepared samples to see the extent of its effect on the properties of the solution and the resulting fibers.

Several tests were carried out, including tests for the solution, which include surface tension and viscosity, tests for the prepared films, which include, infrared examination to indicate the type of interaction between the components and to know the resulting bonds and composition, wetting angle examination to determine whether the prepared fibers are hydrophilic or hydrophobic, Atomic force microscopic test to find out the surface roughness and surface bearing index, scanning electron microscope with field emission to study the morphology of the fibers and their distribution and calculating their average diameters, their orientation and the identity of their elements. Ultraviolet technology was also used to know the physical properties of the material such as energy gap, optical conductivity, refractive index, extinction coefficient and absorption.

The results proved that the surface tension increased with increased the polystyrene concentration from (12-14wt.%) and decreased when the concentration was increased (16wt.%), while the addition of multi-walled carbon nanotube (MWCNT), led to a decrease in the surface tension in low concentrations and it increased with high concentrations. As for adding the dye, it led to an increase in the surface tension. The results also proved that the prepared films became hydrophilic by increasing the polystyrene concentration and hydrophobicity when adding the dye to the group with a polymer concentration

(12wt.%). As for the surface roughness, it increased when the concentration of polystyrene increased, as well as with the increase of the multi-walled carbon nanotubes. The surface bearing index was also increased, indicating an increase in the mechanical properties of the prepared films. The results of the electron microscopy examination proved that the average diameter of the fibers increases with the increase in the concentration of polystyrene and the number of beads increases with low concentrations, but when using the dye, the diameter of the resulting fibers will decrease and the number of beads will also decrease, and the produced fibers have higher orientation for the group with a concentration of polystyrene (14wt.%), It was followed by (16wt.%), then (12wt.% ps/ 0.063g dye) group and then (12wt.%ps) group. The constituent elements of the materials were also inferred through energy dispersive X-ray system associated with the scanning electron microscope. The results of the ultraviolet examination showed that the energy gap increased with increase the polystyrene concentration and decreased with the increase in the multi-walled carbon nanotubes and the dye, where the lowest obtained energy gap reached about (0.2ev) for the sample with concentration (12wt.% polystyrene / 0.16wt.% MWCNT/0.063 g dye) and its optical conductivity value is about (6.85×10^{6} S^{-1}). Which indicates that it is the best prepared samples and it has the necessary properties to be used as a optical sensor, and the best prepared group was the (12wt.%ps / dye /MWCNT) group because it contains the lowest energy gap values, as well as the lowest values of fiber diameters, as well as medium viscosity, medium surface tension and humidity resistance, if compared with the rest of the prepared groups.

Table of Contents

List of Figures

List of Tables

List Of Abbreviations

Abbreviate	Meaning
AFM	Atomic Force Microscopy
AgNP	Silver Nano Particle
APS	American Polymers Services
Eg	Energy Gap
BMWD	Broad Molecular Weight Distribution
CA	Contact Angle
CDH	Central Drug House
CL	Chloride
CNT	Carbon Nanotube
Cu	Copper
$CuCl_2H_2O$	Cupric Chloride Dihydrate
CV	Cyclic Voltammetry
DMAc	Dimethylacetamide
DMF	N, N-Dimethylformamide
DNT	Dinitro Toluene
DSC	Differential Scanning Calorimetry
DSSCs	Dye Synthesis Solar Cells
EC	Electrical Conductivity
EDX	Energy Dispersive X-Ray
EF-TEM	Energy-Filtered Transmission Electron Microscopy
EtOH	Ethanol
Ev	Electron Volt
FESEM	Field Emission Scanning Electron Microscopy
FIA	Flow Injection Analysis
FTIR	Fourier Transform Infrared
GCE	Ground Collector Electrode
GPPS	General Purpose Poly Styrene

H_2O_2	Hydrogen Peroxide
H_2S	Hydrogen Sulfide
HCO_3	Bicarbonate
IR	Infrared
K	Potassium
KCL	Potassium Chloride
KH_2PO_4	Monopotassium Phosphate
LEDs	Light Emitting Diodes
MC	Methylene Chloride
MNPs	Metallic Nanoparticles
MW	Molecular Weight
MWCNT	Multiwall Carbon Nanotube
MWD	Molecular Weight Distribution
N	Nitrogen
NaH_2PO_4	Monosodium Phosphate
NFs	Nano Fibers
NH_3	Ammonia
NMR	Nuclear Magnetic Resonance
NMWD	Narrow Molecular Weight Distribution
NNI	National Nanotechnology Initiative
P	Phosphor
PAA	Polyacrylic Acid
PAN	Polyacrylonitrile
PANI	Polyaniline
PLA	Polylactide
PLAGA	Polylactic Acid/Glycolic Acid
ppm	Part Per Million
PPy	Polypyrrole
PS	Polystyrene

PSNF	Polystyrene Nano Fiber
Pt	Platinum
PU	Polyurethane
PUNF	Polyurethane Nanofiber
PVA	Polyvinyl Alcohol
PVDF	Polyvinylidene Fluoride
PVP	Polyvinylpyrrolidone
QCM	Quartz Crystal Microbalances
RIU	Refractive Index Unit
Sa	Roughness Average
Sbi	Surface Bearing Index
SBS	Styrene- Butadiene- Styrene
Sdr	Surface Area Ratio
SEM	Scanning Electron Microscopy
SO_4	Sulfate
Sq	Roughness Mean Square
STEP	Spinneret Tunable Engineering Parameters
STM	Surface Tunneling Microscope
TEM	Transmission Electron Microscope
THF	Tetrahydrofuran
TSM	Thickness Shear Mode
UV	Ultraviolet
VOCs	Volatile Organic Compounds
Wt.%	Weight Percent
XRD	X-Ray Diffraction

Chapter 1

Introduction

1.1 Introduction

Nanotechnology is science-related with the structure of materials at the atomic and molecular levels is formed to the nanoscale scale. One-dimensional nanostructures, like nanowires, nanofibers, and nanotubes have been recently produced for their unique features and their prospective uses in electronics and nanocomposites. Formhals invented the advanced method of the manufacture of ultrafine fibers, electrospinning in 1934. In recent years, Reneker and colleagues pay attention to this technology that has described the electrospinning of numerous polymer solutions [1].

The National Nanotechnology Initiative (NNI) describes nanotechnology as more global if it has at least a dimension of 1 to 100 nanometers, the materials known as nanomaterial.[2]

Carbon nanotubes (CNT), perhaps the most existing material and important Today, nanotechnology, is a special material with mechanical and other properties are expected to make innovative results to current products and devices [3].

From a mechanical and electrical standpoint, the idea of dispersing or aligning carbon nanotubes within a matrix of nanofibers to make composite materials seems very promising. Carbon nanotubes are good candidates for making nanocomposite products because they have a high aspect ratio, high power and rigidity, low density, high conductivity, great durability, and extensibility, as well as the ability to cope with cross-sectional and twisting, and compressive capacity [4].

Over the last few decades, considerable attention has been paid to polymers conducting an electric current. This is due to unique properties, such as lightweight, controlled conductivity, and use in applications of great importance, such as thermal sensors, fuel cells, and so on [5]. The polymers that conduct electricity are conductive. They were made using several methods, Similar to the conductor and classical semiconductors, conductive polymers are distinguished by intermediate electrical resistivity. Special electronic structures are to track for

an effect on electron affinities [6], and thus conductive polymers are considered 21st-century materials. Conductive polymers are also referred to as synthetic metals because they have organic properties and metal like properties. They collected electrical characteristics of metals and semiconductors, with useful behavior of traditional polymers, such as operating scalability, durability, processing ability, environmental stability, and low cost [7-9].

The prepared conductive polymers have gained more interest by attaching MWCNTs to host polymers due to the high surface ratio, the electrical, thermal, and mechanical properties specialized in the resulting nanofilms [10].

It is difficult to manufacture MWCNTs polymer composites with homogeneous dispersion and powerful interfacial adhesion between MWCNTs and the matrix because of the clear effect of Van der Waals forces in MWCNT's structure [11].

In recent years, the quantity of research on uses electrospun conductive nanofiber mats has increased (Figure1.1). However, it should be noted that "eletrical" nanofibers in these studies do not always have conductivities of similar magnitude, but instead span a wide range of conductivities or sheet resistance [12].

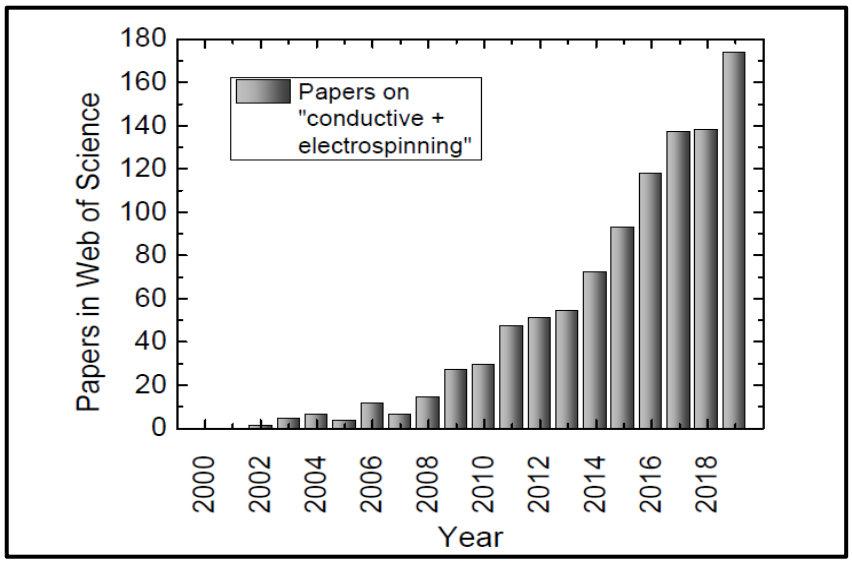

Figure (1.1): Web of Science counts of published research on the terms "conductive" and "electrospinning"[12]

1.2 AIMS

- To produce polymeric nanofibers with lower diameter and less beads
- To produce nanofibers, have ability to withstand humidity.
- To enhance the electrical conductivity of the solution by adding MWCNT and natural dye.
- To make nanofibers used as optical sensors.

Chapter 2

Theoretical Part
&
Literature Review

2.1 Introduction

Nano-materials are substances developed with different physical and chemical properties from various compounds, such as membranes, filaments, nano-fibrous fabrics, or nano-fibrous composites mixed with nanoparticles. However, compared to other chemicals and physical methods to manufacture nanofibers with the following properties, electrospinning regarding as the best technique for creating nanofibers owing the following properties:

1- It is a continuous process where it produces one-dimension nanofibers so It can extend to several meters[20].

2- Extremely large surface area with a regular and more complicated porous structure. Compared to fibers produced using extrusion or the conventional mechanical spinning method, the nanofibers using electrospinning are smaller in diameter and therefore leads to a greater surface to volume ratio. and as a consequence of greater nanofiber entanglements, it may also generate high pore density.

3- The electrospinning method will allow the produced nanofibers to line up, which will give the polymer chain a higher alignment, which may be the result of rapid solvent evaporation that produced high shear strength, which produced crystalline nanofibers as a result [21].

2.2 Nanofibers Techniques

2.2.1 Drawing

Fibers are generated in a specific manner. It works similarly to dry spinning. The fact that this technique just requires a fine tip or a micropipette which limits its main advantages. In this technique, fine tip utilized to pull liquid fibers from the drop of the polymer solution. Due to the large surface area the solvent is gradually evaporated, leaving the liquid fibers to solidify. To solve the problem of shrinkage in volume that affect the continuous pulling of fibers and impacts on their diameter, hollow cylindrical glass micropipettes employed instead of the sharp tip with a consistent dose of the polymer see figure (2.1) [22].

After being submerged into polymer solution droplet, the micropipette is softly removed from the droplet at a lower speed (about 10^{-4} m/s). as a consequence, nanofibers are formed by contact the nanofibers drawn from the needle end with the substrate, this process repeated many times on each drop of polymer solution [23].

This method may be used to make continuous nanofibers in any configuration. Furthermore, accurate control of main drawing parameters like viscosity and drawing velocity may be achieved, allowing for repeatability and control of generated fiber measurements [24].

Although this technique is simple, it is restricted to the laboratory level because nanofibers formed singly. It is a discontinuous method with low productivity, and it can also control the fiber diameter. Only viscoelastic materials can withstand the tension generated by the dragging, and depending on the orifice size, just fibers with diameters above 100 nm may be formed.

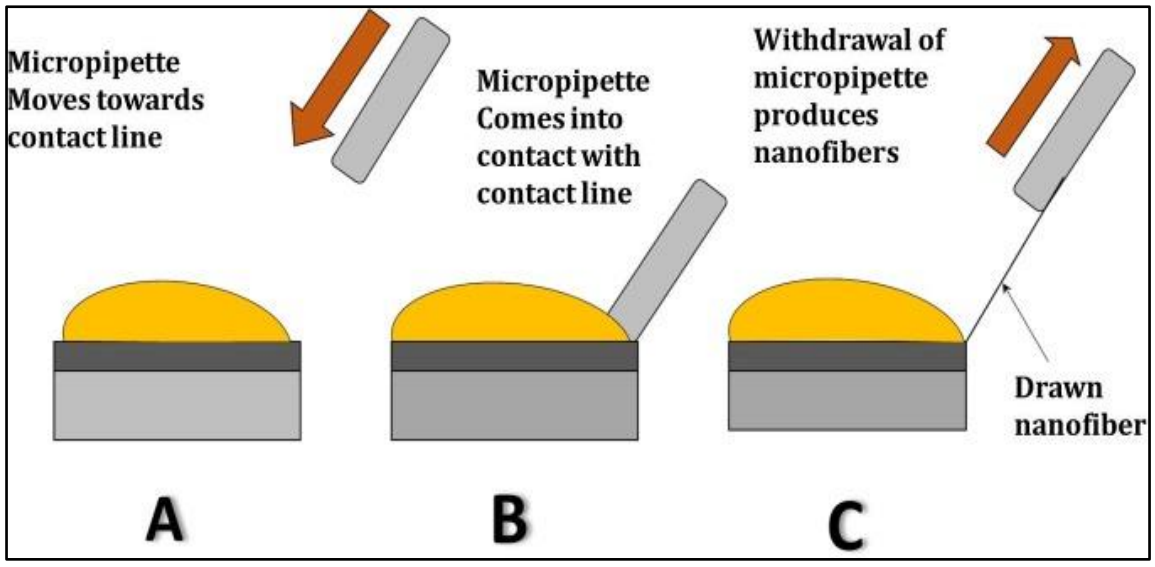

Figure (2.1) Drawing method steps [30]

2.2.2 Template Synthesis method

This operation generated various polymeric, metallic, semiconductors, or ceramic nanofibers by utilizing chemical or electrochemical oxidative polymerization also uses nano porous membrane having many cylindrical holes varying from (5-50 mm) thickness. This method produces nanofibers by using mold or template made from aluminum oxide (AL_2O_3) to get final structure. Nanofibers are created by pumping the polymer solution across nano diameter holes by the effect of water pressure on one side, enabling the polymer to extrude and form nanofibers when it comes into contact with a solidifying solution as shown in (figure 2.2). This method not able to form large length nanofibers. Only few micrometers lengthy fibers are produced from this method, also the fiber diameter is connected to the membrane's pore sizes [27 and 28]. Some benefits of using this technique are the capability to produce nanofibers with various diameters using multiple templates.

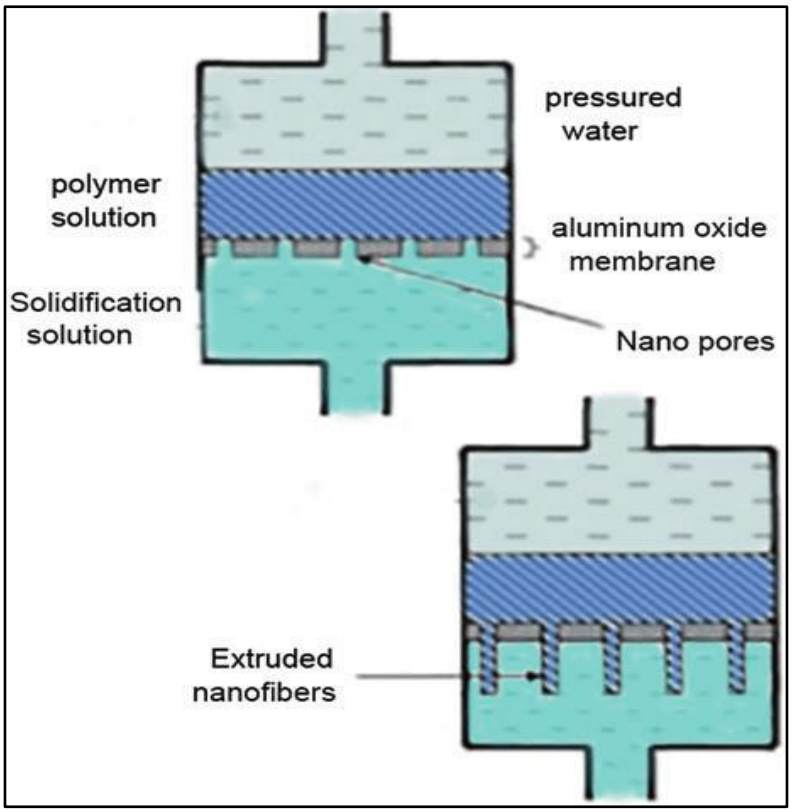

Figure (2.2) Obtaining nanofibers by template synthesis Technique [27 and 28]

2.2.3 Phase Separation

Phases will separate in this process. The solvent layer is then separated from the solution, leaving behind the other phase. there are four main stages in this method: [29]

1. Dissolve the polymer with using convenient solvent a room temperature or upper it.
2. Gelation step and it regarded as difficult step because of difficult regulating the porosity of nanofibers.
3. Extraction of solvent step to separate and remove the solvent from the produced gel by using water.
4. Freezing followed by drying under vacuum step.

The characteristics of nanofiber are determined by the concentration of polymer used; if the polymer percentage rises, porosity of the fiber decreases, and the mechanical properties of the fiber increase [28].

The first step in this method is dissolving the polymer at room temperature to make homogeneous solution, after that removing the gel from the solution by holding it to temperature of gelation, where nanofibrous matrixes are formed due to phase separation, and eventually the solvent will be extracting followed by the matrix drying step, this eventually leads to the formation of nanofibers. As shown in figure (2.3)

This method requires minimal equipment, it may produce a nanofiber matrix directly, with mechanical properties adjusted by altering the polymer concentration [30].

The phase separation technique has only been utilized to create nanofibers from few polymers, like “polylactide (PLA)” and “polyglycolide” [27]. This technique also cannot create long continuous fibers, and not all polymers can undergo phase separation and form nanofibers since it needs gelation capacity, which restricts the application of this technology.

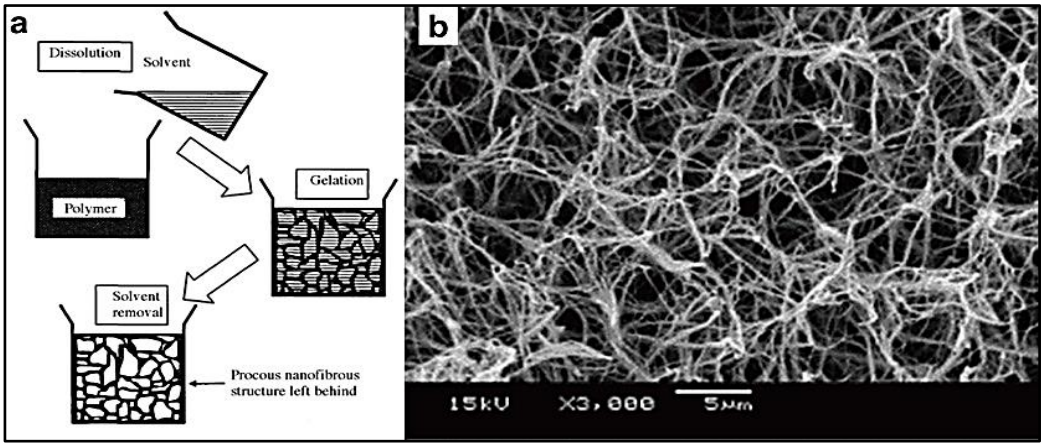

Figure (2.3) (a) Phase separation process, (b) SEM image of final form nanofiber [30]

2.2.4 Self Assembly

This method involves rearrangement and reassembly of the molecules by themselves to form different shapes and configurations through non covalent forces like hydrogen bond forces and electrostatic interactions, figure (2.4) [22].

This method is suitable for manufacturing smaller diameter nanofibers with average diameter lower than 100 nm and length in micrometer scale. Mechanism of his method is by the intermolecular forces which hold the molecules together. Orientation of the molecules determined the final shape of it. The main disadvantages of this method is the complexity, slow, low production scale and complex in maintaining fiber diameters produced [27 and 31].

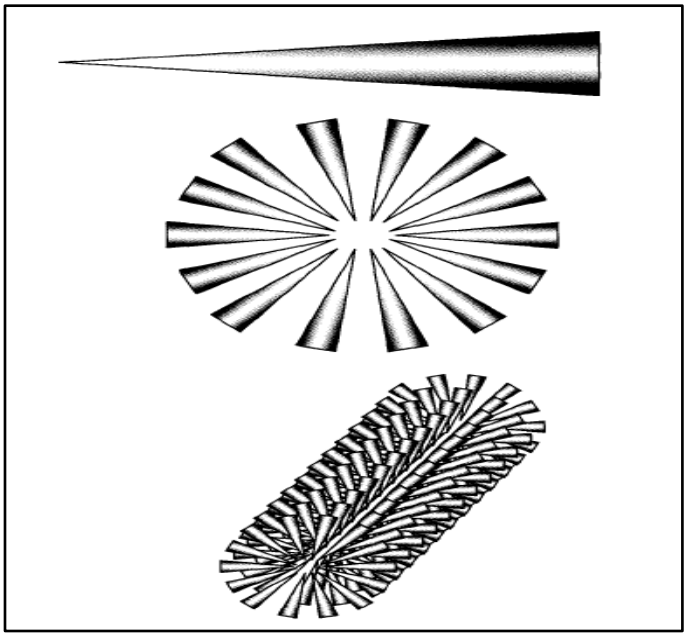

Figure (2.4) Self-assembly process to create nanofibers [30]

2.2.5 Electrospinning technique

The electrospinning method includes utilizing a high voltage delivered to polymer solution in which charges will induce inside the solution. When critical limit is exceeded by the charge's addition, jet is generated first from drop that is located in the needle tip leading to the construction the "Taylor cone". The jets run to the region of lowest voltage which is the grounded collector. as shown in (Figure 2.5) [30].

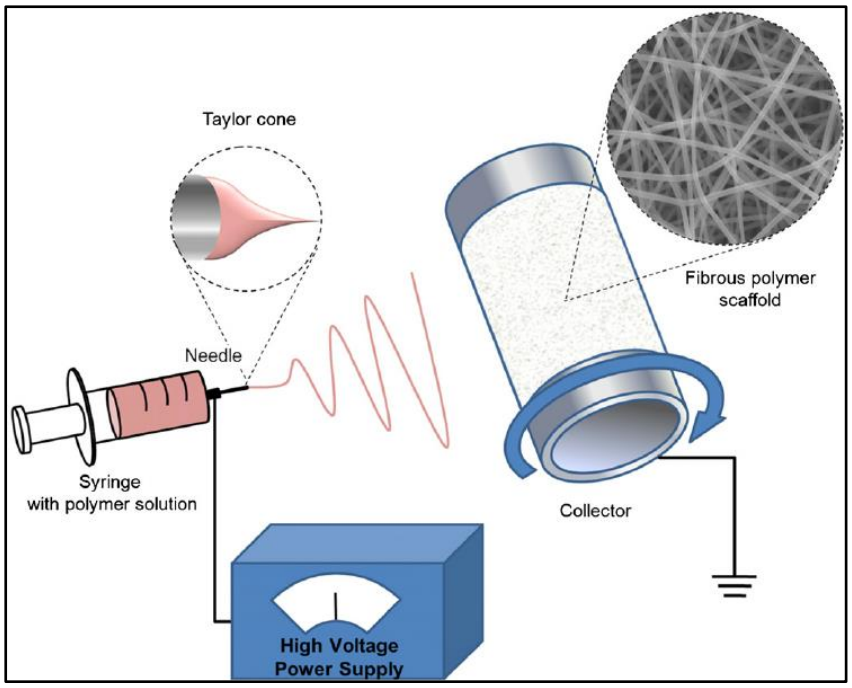

Figure (2.5) Electrospinning Setup [25]

All the above-mentioned techniques and their advantages and disadvantages and limitations listed in the tables (2.1 and 2.2).

Table (2.1) Comparison between different nanofibers techniques [15]

Process	Technological advances	Can be scaled?	Repeatability	Convenient to process	Controlling fiber dimensions
Drawing	Laboratory	NO	Yes	Yes	NO
Template Synthesis	Laboratory	NO	Yes	Yes	Yes
Phase Separation	Laboratory	NO	Yes	Yes	NO
Self-Assembly	Laboratory	NO	Yes	NO	NO
Electrospinning	Laboratory and industrial	Yes	Yes	Yes	Yes

Table (2.2) Advantages and Disadvantages of nanofibers processes [15]

Process	Advantages	Disadvantages
Drawing	Lower equipment needs	Discontinuous process
Template Synthesis	Produces fibers with different diameters	
Phase Separation	Directly manufacture nanofiber matrix using minimum equipment. Consistency from batch to batch is easy to achieve. The matrix's mechanical characteristics may be modified by adjusting the polymer concentration.	Limited to specific polymers.
Self-Assembly	Suitable for producing a smaller nanofiber	Complicated process
Electrospinning	Can produce long and continuous nanofibers, cost-effective	Instability of jet

2.3 Factors affecting electrospinning technique

To obtain fibers with high orientation and desirable properties, several factors must be controlled, some of which are specific to the prepared solution, some are specific to the process, and some are specific to ambient conditions.

2.3.1 Effect of solution characteristics

The final formed nanofibers are mostly affected and depend on the solution prepared and its physical properties, such as the effect of surface tension influence on the prepared fibers in which beads may occur, also the viscosity can play important role in elongation of the solution, which change the average fiber diameters.

2.3.1.1 Molecular weight and viscosity of solution

Basically, polymer solution most has appropriate molecular weight and adequate viscosity. These parameters are very important in electrospinning which are necessary to make jet formation occurring. Viscosity making the polymer solution to be stretched and molecular weight play an important role in entanglement and determines the chain length so that, when increased the chain length, the entanglement chance increase leading to make jet solution breakage not to be occur [45].

Molecular weight affects the polymeric solution viscosity, thereby increasing the molecular weight will increase the chain length and this increase from the probability of the chains to be entangled leading to raise the solution viscosity. Another method to increase the viscosity by means increasing the polymer concentration which leads to more chains entanglements inside the solution. This is benefit to ensure the continuous jet formation occur during electrospinning process, entanglements of the chains have also an impact on the jet whether it will breakup into droplets or not [46].

So, the need of smaller amount of chain entanglements and also high viscosity is required to form jets without beads but not too high in which difficulties in pumping the solution occurs [47]. Another problem of too high viscosity is that the solution before electrospinning process maybe facing drying in needle tip [48].

when the viscosity is high there is a strongly interaction occurs between the molecules of solvent and the molecules of polymer as shown in the figure (2.6).

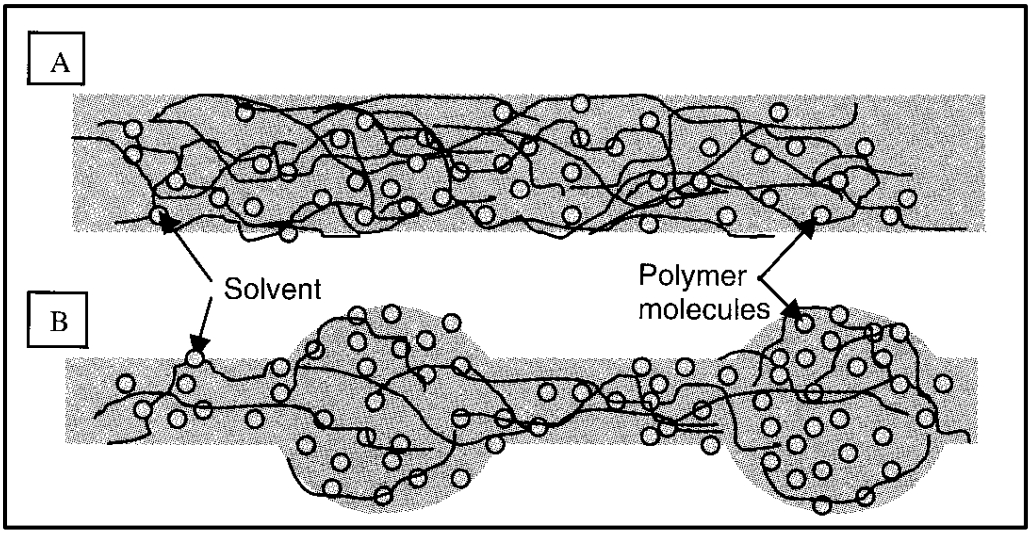

Figure (2.6) [A] High viscosity, solvent molecules aligned and orientate across polymer molecules[B] Lower viscosity, solvent molecules tend to aggregate under surface tension effect [30]

2.3.1.2 Surface tension

The charges that are developed in the polymeric solution should be highly enough in electrospinning to overcome the solution's surface tension. The solution is stretched as the solution jet speeds from the source's tip to the collector, and the solution's surface tension may cause the solution to split up into droplets [49 and 50]. If droplets produced on collector, the process will be called as electrospraying instead of electrospinning [51], in which fibers are assembled.

If a very tiny drop of water dropped in the air, it usually exhibits sphere form. Surface tension regarded as a characteristic of a solution’s surface that make this phenomenon. A homogeneous attractive force is produced on a liquid molecule immersed inside a solution by the surrounded liquid molecules. molecules which to found near the surface of liquid affected by the two forces one of them is the attractive forces come from the bulk molecules and the other is from the gas molecules and the later stronger than the former as shown in the figure (2.7).

As a result, the surface becomes in tension, causing the surface of the solution contracted, which is counterbalanced by repulsive forces arising the impacts of

molecules that exist in the inner of the solution. The total impact of all the surface liquid molecules pushing on each other leads the liquid surface to shrink, decreasing the surface area. As a result, a spherical form has the lowest ratio of surface area to volume for a droplet of water.

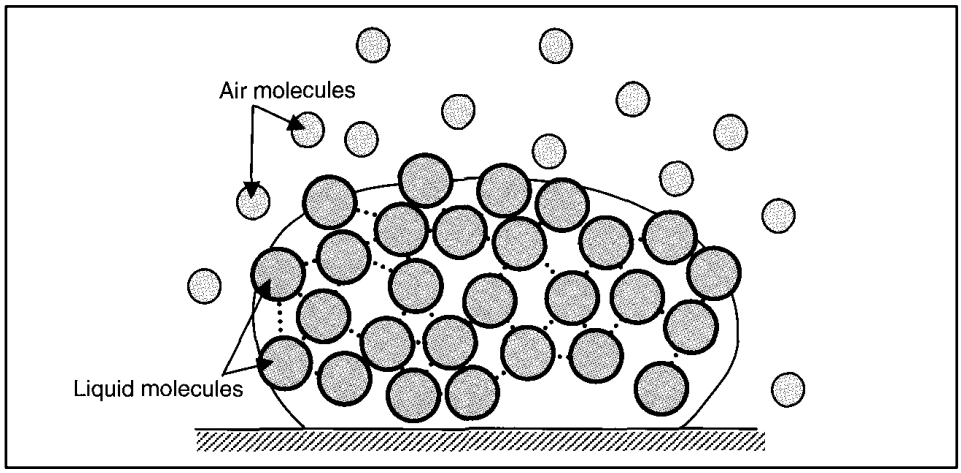

Figure (2.7) Forces exerted by the air and liquid

2.3.1.3 Electrical conductivity of solution

The conductivity of solution is necessary property to get smoother fibers with small and high diameters so, charges increased in solution and on the transferred jets if the electrical conductivity of the solution improves. Improving conductivity of solution may be done by adding salts or ions, most of the protein and medicines create ions when dissolved in water. Charges, also play an important role in stretching the solution so that increasing the charges has effect to increase the stretching of solution also tends to form smoother fiber diameter [48]. Furthermore, when ions enhancing the electrical conductivity of solution this will reducing the amount of critical voltage required in electrospinning process [53].

Another advantage of increasing charges in the solution in which bending instability improved this leads to increase the area where fibers being deposited [52]. This is also giving a fine fiber dimeter owing to increasing jet paths. For solutions with zero electrical conductivity value there is no fibers

formed [54]. Table (2.3) shows the electrical conductivities values of some solvent.

Table (2.3) Electrical conductivity of solvents [30]

Solvent	Conductivity (µS/cm)	Reference
1,2-Dichloroethan	0.034	[54]
Aceton	0.0202	[55]
Butanol	0.0036	[56]
Dichloromethane/Dimethylformamide (40/60)	0.505	[55]
Dichloromethane/Dimethylformamide (75/25)	0.273	[55]
Dimethylformamide	1.090	[54]
Distilled Water	0.447	[55]
Ethanol	0.0554	[56]
Ethanol (95%)	0.0624	[55]
Ethanol/Water (40/60)	0.150	[55]
Methanol	0.1207	[56]
Propanol	0.0385	[56]
Tetrahydrofuran/ Ethanol (50/50)	0.037	[55]

The size of ions dissolved in the solution may also affects o the morphology of the final formed fibers for example using (KCl) give a lowest fiber diameter on the other hand when solution has (KH_2PO_4), the final fibers possess a maximum diameter and when uses NaH_2PO_4 medium fiber dimeter obtained. This is because sodium, chloride ions possess lower radius of atoms from potassium, phosphate ions, they might possess higher velocities under the effect of the electrostatic field, as a result stretching forces will develop on electrospinning jets owing to the mobility of the small ions and eventually smaller diameter achieved [48].

2.3.1.4 Solvent dielectric constant effect

Higher dielectric constant gives lesser beads formation and smaller diameter of nanofibers [53]. N, N-Dimethylformamide (DMF) solvent usually added to the solution to enhance fibers morphology due to its higher dielectric constant [57].

With a larger dielectric constant, the electrospinning jet's bending instability improves as well. This may also assist the decrease of the fiber diameter owing to the larger jet path [58]. The dielectric constant for many familiar solvents utilized in electrospinning given in Table (2.4). Nevertheless, if the solvent possesses high dielectric constant used in the solution for enhancing its electrospinnability, the interaction between the mixes, such as the polymer's solubility, the morphology of resulting fibers will be affected. When DMF solvent added to the solution of polystyrene this will eventually causes beads in the formed fibers, this may be due to the molecules of polystyrene have weaker interaction with DMF solvent’s molecules [59].

Table (2.4) Popular solvents and their dielectric constant values

Solvents	Dielectric constant	Reference
2-Propanol	183	MERCK technical datasheet
Acetic acid	6.15	[59]
Acetone	20.7	[60]
Acetonitrile	35.92 - 37.06	[59]
Chloroform	4.8	[60]
Dichloromethane	8.93	[61]
Dimethylformamide	36.71	[61]
Ethyl acetate	6.0	[60]
Ethanol	24.55	[61]
m-Cresol	11.8	[59]

Methanol	32.6	MERCK technical data sheet
Pyridine	12.3	MERCK technical data sheet
Tetrahydrofuran	7.47	[59]
Toluene	2.438	[59]
Trifluoroethanol	27.0	[60]
Water	80.2	MERCK technical data sheet

2.3.2 Processing parameters

The different external variables exerting on the electrospinning jet are another significant parameter that impacts the electrospinning nanofibers production process. This comprises the voltage applied, the flow rate, the solution temperature, the type of collector, the needle's diameter, and the space between tip-collector. All these parameters have an effect on fiber morphology; however, they are not as significant as the solution parameters.

2.3.2.1 Applied Voltage

The high voltage will cause charged solution leading to overcome the surface tension of the solution. Generally, both the positive and negative high voltage with 6 Kv can form a drop at the needle tip to yield the Taylor cone at the end [62].

For the Taylor Cone to be stable, a high voltage may be required. The viscoelastic solution will subsequently be stretched by the columbic repulsive force in the jet. When increased the applied voltage, number of charges will increase and make the jet to produce faster, pulling solution increased from needle's tip. This probably leads the Taylor Cone be smaller and less stable [48]. The morphology of the fibers obtained will be influenced by the applied voltage also affected by resultant electric field, both can change the jet stretching and their speeds. Because of increasing columbic forces developed in jets also

because of the higher electric field, a higher voltage will usually result in more stretching of the solution. The diameter of the fibers is reduced as a result of them [53,45,63].

High voltage has an effect on nanofibers crystallinity as well as the it's physical shape. During electrospinning, the electrostatic forces may lead the polymer molecules being well organized, crystallinity then improves in nanofibers. The crystallinity of the fiber is decreased over a specified voltage. Furthermore, Higher voltage has a disadvantage in which fibers will not have adequate time to orientate and align themselves when travel to collector and the crystallinity reduced because of that [64].

2.3.2.2 Flow rate effect on nanofibers

Increasing the flow rate will cause the diameter of nanofibers to be increased and beads formation chance increased as shown in the figure (2.8) [48].

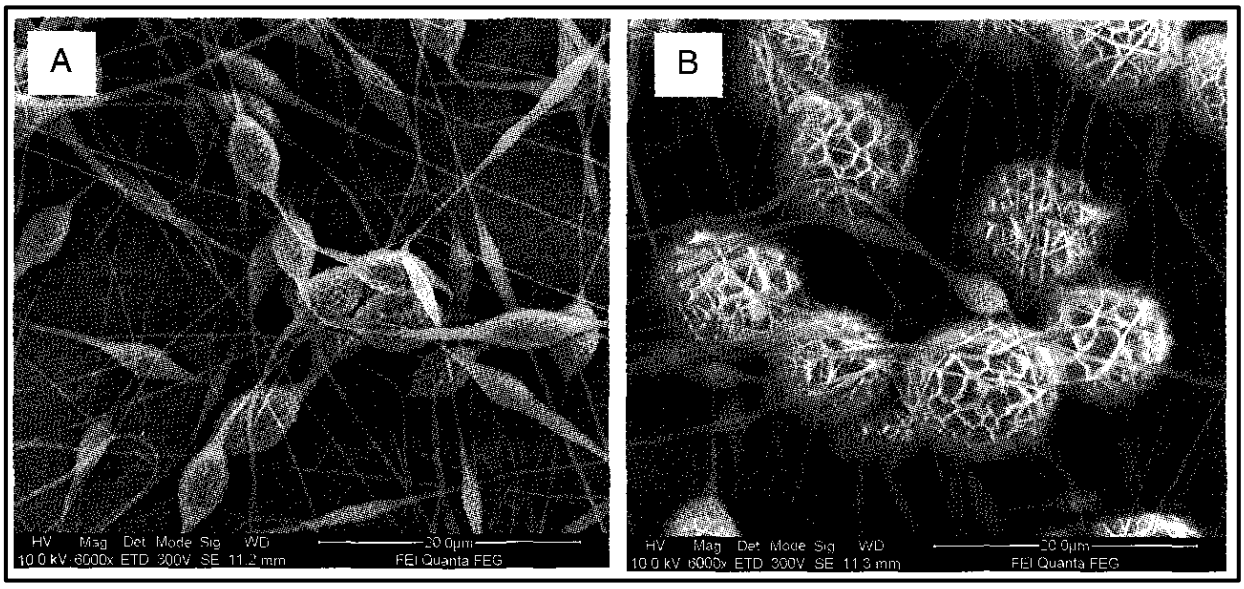

Figure (2.8) Effect of flow rate in Polycaprolactone nanofibers where; [A] 0.5ml/hr and [B] 2ml/hr in which the size of beads increased with flow rate [30]

2.3.2.3 Effect of collector

The collector plate in most electrospinning setups is comprised of conductive material like aluminum foil that is electrically grounded to maintain a steady potential differential between tip and collector. If nonconducting material is

utilized as a collector, it will leads to fewer fibers being deposited on it [67]. The packing density of fibers produced on insulating surface is usually lower than that of fibers produced on conducting collector. This is produced because of accumulation charges will cause a repulsive force to the continuous deposited fibers on the collector. Discharge of charges occur on conducting collector, allowing new fibers of being drawn to the collected. Consequently, the fibers can pack tightly with each other [68].

Rather than the conductivity of the collector, its shape is also more important in the improvement of the morphology of the yielded deposited fibers, many shapes and the pattering of a collector such as cylindrical collector, rotating mandrel, rotating wire drum, knife-edge disk, etc. each of them gives different properties to the other types of the resultant electrospun deposited nanofibers figure (2.9) shows these types of collectors.

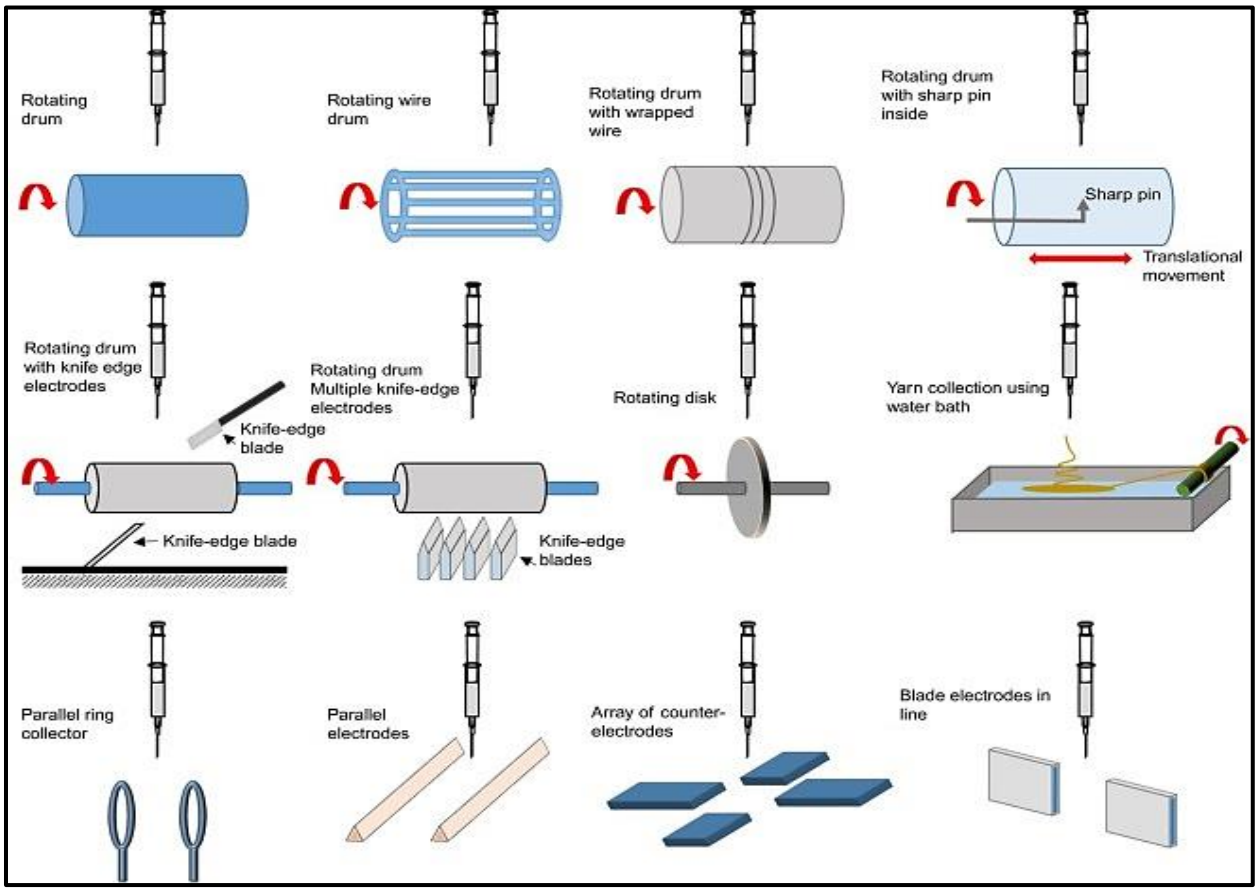

Figure (2.9) Collector type in electrospinning technique [13]

2.3.2.4 Needle diameter

The electrospinning process is influenced by the interior needle diameter. Clogging and beads were shown to be reduced with a lower internal diameter [70]. The diameter of the electrospun fibers was found to be reduced when the internal diameter of needle was reduced. The surface tension of the drop increases as the droplet size at the needle tip is reduced, like when the orifice's internal diameter is reduced. To cause jet start at the same voltage, a higher columbic force is necessary. As a result, the velocity of the jet slows down, giving the solution more time to stretch and extend before being collected. However, if the orifice's diameter is too small, a droplet of solution may not be able to extrude from the orifice's tip [64].

2.3.2.5 Tip-Collector distance

The electrospinning process and the resulting fibers are affected by electrical field amount and travelling time to collector. The flight time and the electric field strength will both be affected by changing the space between the tip and collector. Adequate time must be given to the jet to make the solvent evaporated leaving behind dry fibers. If the space from the tip to the collector is lowered, the jet flight time is lowered and reach the collector rapidly, if the tip-collector space is too short, the fibers excessive solvent might induce leading the adjacent fibers to be merged and welded together, as shown in figure (2.10) [45]. This interlinked fiber mesh could provide the resulting scaffold more strength.

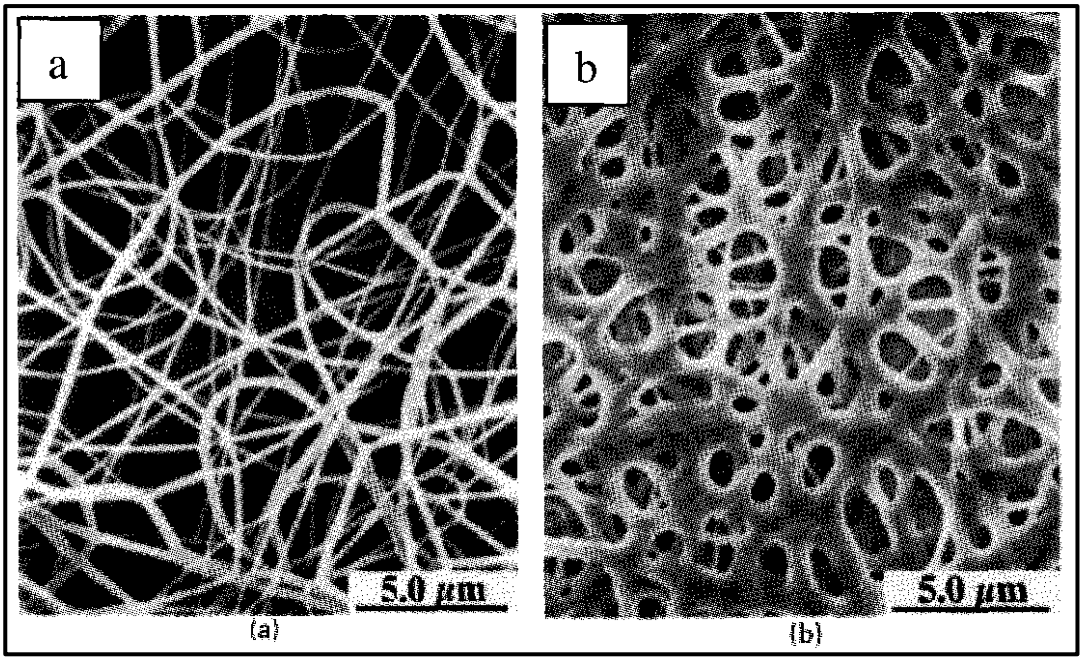

Figure (2.10) Nanofibers deposited in various distances (a) 2 cm (b) 0.5cm [45]

2.3.3 Ambient parameters

The electrospun fiber shape can be affected by reaction between the surrounding and the electrospinning solution prepared. The creation of holes on the surface of the nanofibers was discovered to be caused by high humidity, for example. Because the electrospinning process is impacted by the external electric field, any changes in the electrospinning environment will have an impact [30].

2.3.3.1 Humidity

The electrospinning environment's humidity affects the solution of polymer during electrospinning. When electrospinning is done at normal atmosphere, water is likely to condense on the fiber's surface at high humidity. As a result, the fiber morphology, particularly polymer dissolved in volatile solvents, may be affected [63,71]. Humidity has a direct effect on nanofiber porosity and in which increasing the humidity will increase the porosity [14 and 26] as shown in the figure (2.11).

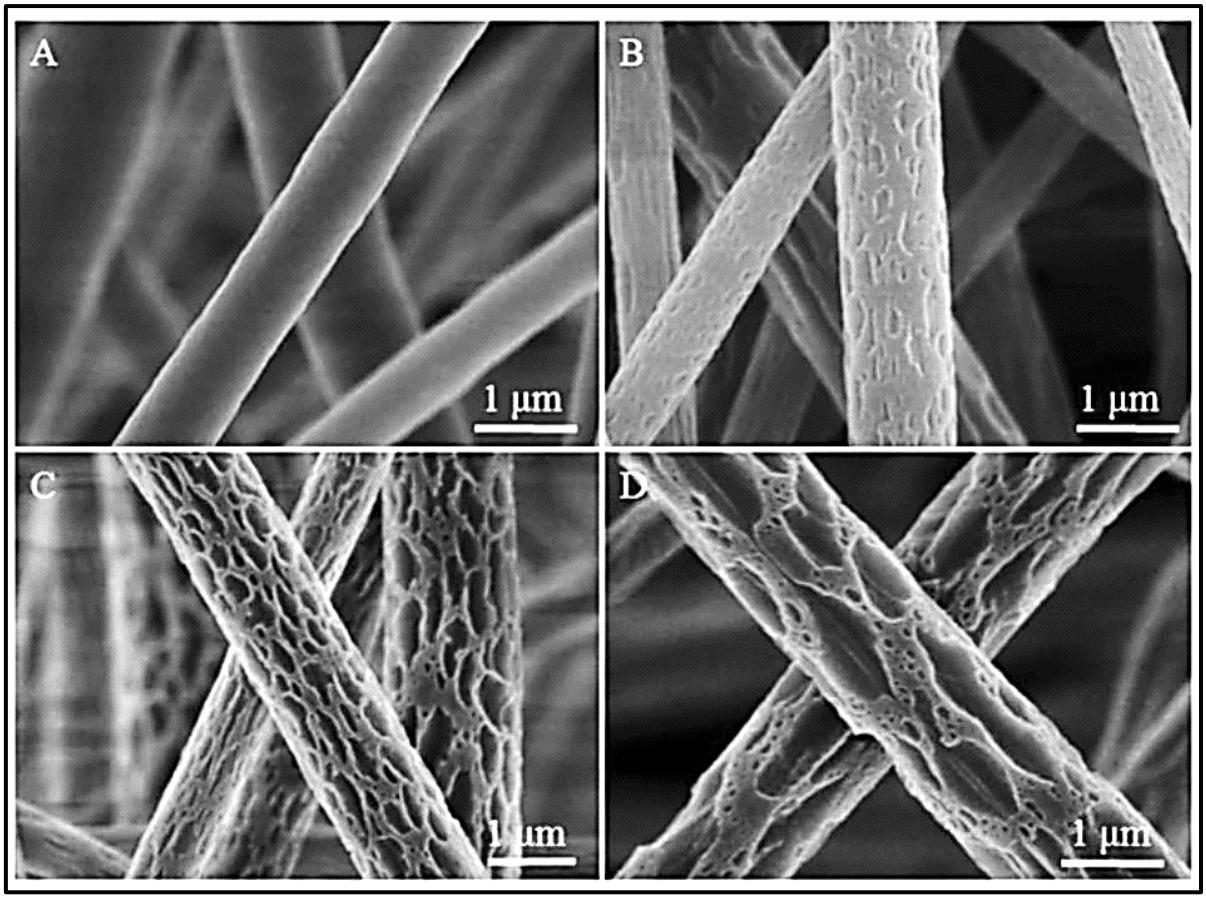

Figure (2.11) Representative SEM images of samples fabricated by electrospinning 18% (w/v) PVDF solution from acetone at different levels of relative humidity. (a 5%, b 25%, c 45%, and d 65%) [26]

2.3.3.2 Atmosphere type

The electrospinning process is influenced by the air composition in the electrospinning environment. Under a high electric field, different gases behave differently. Helium, for example, will decompose in a strong electric field, making electrospinning impossible. When Freon®-12gas is used instead of air, the fibers produced double the diameter of the nanofibers produced in air [73].

2.3.3.3 Temperature

The temperature of the solution increases the rate of evaporation, also increasing it will decrease the viscosity of the polymer solution. The fibers formed at a higher temperature when polyurethane is electrospun have a more uniform diameter [65]. This maybe because the solution has a lower viscosity and the polymer is more soluble, permit the solution from being stretched

equally. Columbic forces can generate a larger stretching force on the solution with a lower viscosity, resulting in smaller diameter fibers [66].

Increased temperature increases the mobility of polymer molecules, facilitate the columbic forces to further stretching the polymeric solution. When biological substances like enzymes and proteins used in electrospinning solution, the use of high temperature make these components to lose its benefits. The table (2.5) also indicates the effect of the above-mentioned factors on the electrospinning process and the deposited nanofibers [69].

Table (2.5) A brief table of parameters that effect on the electrospinning process [69]

Solution Properties	Symbol	Effect on morphology and structure	Effects on diameter
Concentration	C ↑	Increasing concentration leads to increase in fiber diameter.	Nanofiber diameter ↑
Viscosity	η ↑	Increasing viscosity leads to thicker nanofibers without beads, but too high viscosity causes generation of beds.	Nanofiber diameter ↑
Solution Electrical conductivity	σ ↑	Increasing conductivity leads to thinner nanofibers.	Nanofiber diameter ↓
Surface tension	ϒ	No conclusive correlation has been established between the surface tension and the nanofiber morphology.	-
Molecular weight of polymer	Mr ↑	Increasing polymer molecular weight leads to formation of a nanofiber with fewer beads.	-
Volatility of solvent	$\alpha_{solvent}$	Higher volatility requires higher flow rate and leads to formation of a nanofiber with fewer beads.	-
Solution relative volatility	α	Porous microstructure appears because of higher volatility.	-
Dielectric constant	ε	Sufficient dielectric constant of the solvent in needed for successful electrospinning.	-
Process parameters	**Symbol**	**Effect on morphology and structure**	**Effects on diameter**
Flow rate	Q↑	Higher flow rate results in thicker nanofibers. Too high	Nanofiber diameter ↑

		flow rate causes the generation of beads.	
Applied voltage	V↑	Higher applied voltage leads to thinner nanofibers.	Nanofiber diameter ↓
Needle diameter	D	Minimum in required to get smoother nanofibers	Nanofiber diameter ↓
Needle tip to collector distance	D↑	Beaded morphology occurs when the distance is too short and the electric field is too strong.	Nanofiber diameter ↓
Geometry of collector	-	Metal collectors with conductive frame or rotating drum are preferred	-
Environmental conditions	**Symbol**	**Effect on morphology and structure**	**Effects on diameter**
Relative humidity	Ψ	Porous microstructure appears due to evaporation-cooling effects.Lower humidity enables higher flow rate and the generation of beads is reduced.	-
Temperature	T↑	Higher temperature leads to thinner nanofibers	Nanofiber diameter ↓

2.4 Literature theory about the materials used

2.4.1 Polystyrene

Polystyrene regarded as an aromatic synthetic polymer synthesized from monomer styrene [96]. Polystyrene may be solid or foamed. General purpose polystyrene is clear, hard, and brittle. Polystyrene regarded as a good barrier to oxygen and water and also has a lower melting point [97]. Structure of polystyrene consist from long hydrocarbon chain made from centered carbon atom with alternated phenyl group as shown in the figure (2.12) [44].

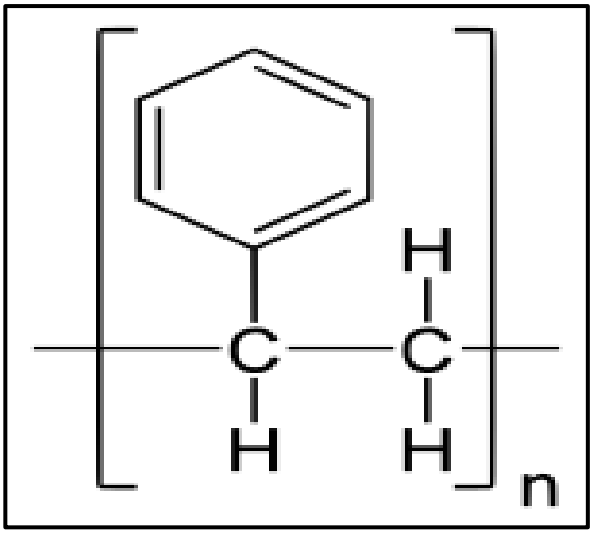

Figure (2.12) Polystyrene structure [44]

Polystyrene produces from the addition polymerization of styrene monomer, in which the carbon-carbon (π-bonds) of the vinyl group will broke and formed new carbon-carbon (σ-bonds) as shown in the figure (2.13) .

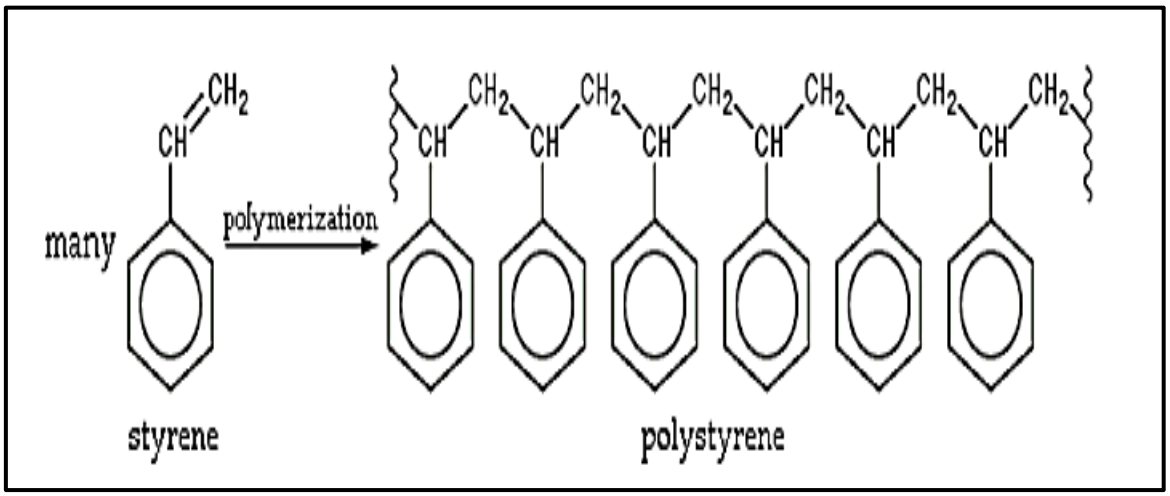

Figure (2.13) Polymerization of polystyrene [101]

According the position of phenyl group around the carbon chains of polystyrene there are three tacticity structures the (isotactic structure syndiotactic structure atactic structure) as shown in the figure (2.14), each one of them has different properties from the other types [99].

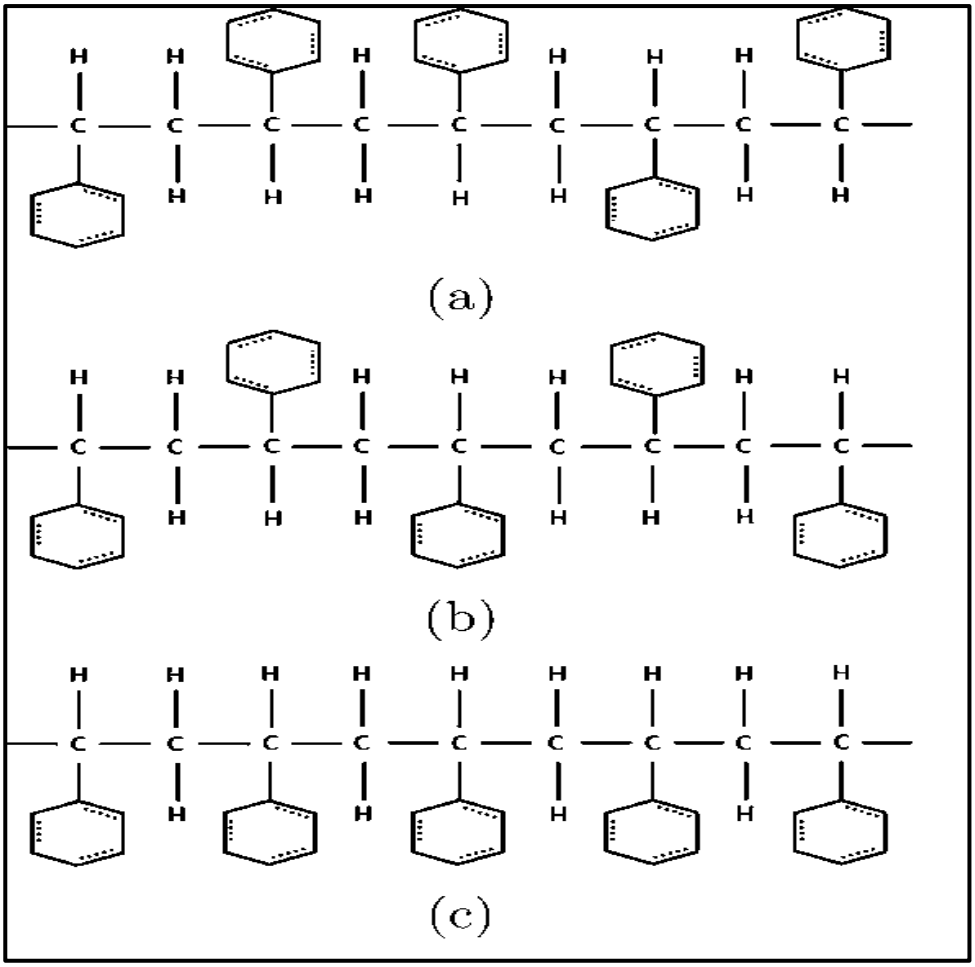

Figure (2.14) Stereochemistry of (a) atactic, (b) syndiotactic, and (c) isotactic polystyrene [100]

Polystyrene has a wide range of applications in our life such as I food packaging, laboratory, electronics, automobile parts, toys, medical uses, petri dishes, egg cartons ...etc.[99].

2.4.2 Multiwall carbon nanotubes

It is a type of carbon nanotube (CNT). It consists at least from two concentric different diameters of carbon nanotubes as shown in the figure (2.15) [102]. The diameters of Multiwall carbon nanotubes varying from 2 nm for the inner nanotube diameter to over 50 nm for the outer nanotube and lengths up to centimeters. They exhibit higher electrical, thermal, and mechanical properties [103].

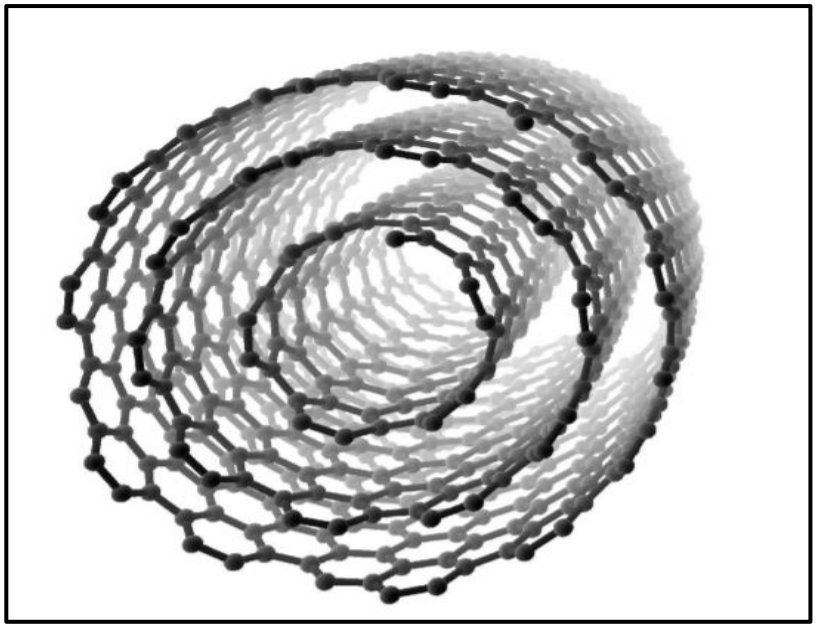

Figure (2.15) Multiwall carbon nanotubes [102]

CNTs are manufactured by the process catalytic chemical vapor (CVD) decomposition at moderate temperature (600 - 1000°C) [104], by using direct-current arc discharge under helium at high temperature (2000 - 4000°C) [105], also by laser vaporization [106].

The different between the multiwall carbon nanotubes and the other types of carbon nano tubes shown in the table (2.6).

Different applications of MWCNTs owing to their unique characteristics, especially in solar cells, batteries, nano electronics, transistors, energy storage, and in flat panel displays.

Table (2.6) Properties of different types of CNTs [104]

Property	SWNT	DWNT	MWNT
Tensile Strength (GPa)	50 - 500	23 -63	10-60
Elastic Modulus (Tpa)	~ 1	_	0.3 - 1
Elongation at break (%)	5.8	28	_
Density (g/cm^3)	1.3 – 1.5	1.5	1.8 - 2
Electrical Conductivity (S/cm)		~ 10	
Thermal Stability		> 700°C (in air)	

Typical diameter	1nm	~ 5 nm	~ 20 nm
Specific Surface Area		10-20 m^2/g	

2.5 Applications of nanofibers

There are many different applications of polymeric nanofibers in many fields such as applications found in cosmetics, military, filtration, industrial, sensors. as shown in figure (2.16).

current thesis focus on the applications of polymeric nanofibers made with the electrospinning technique as optical sensor application.

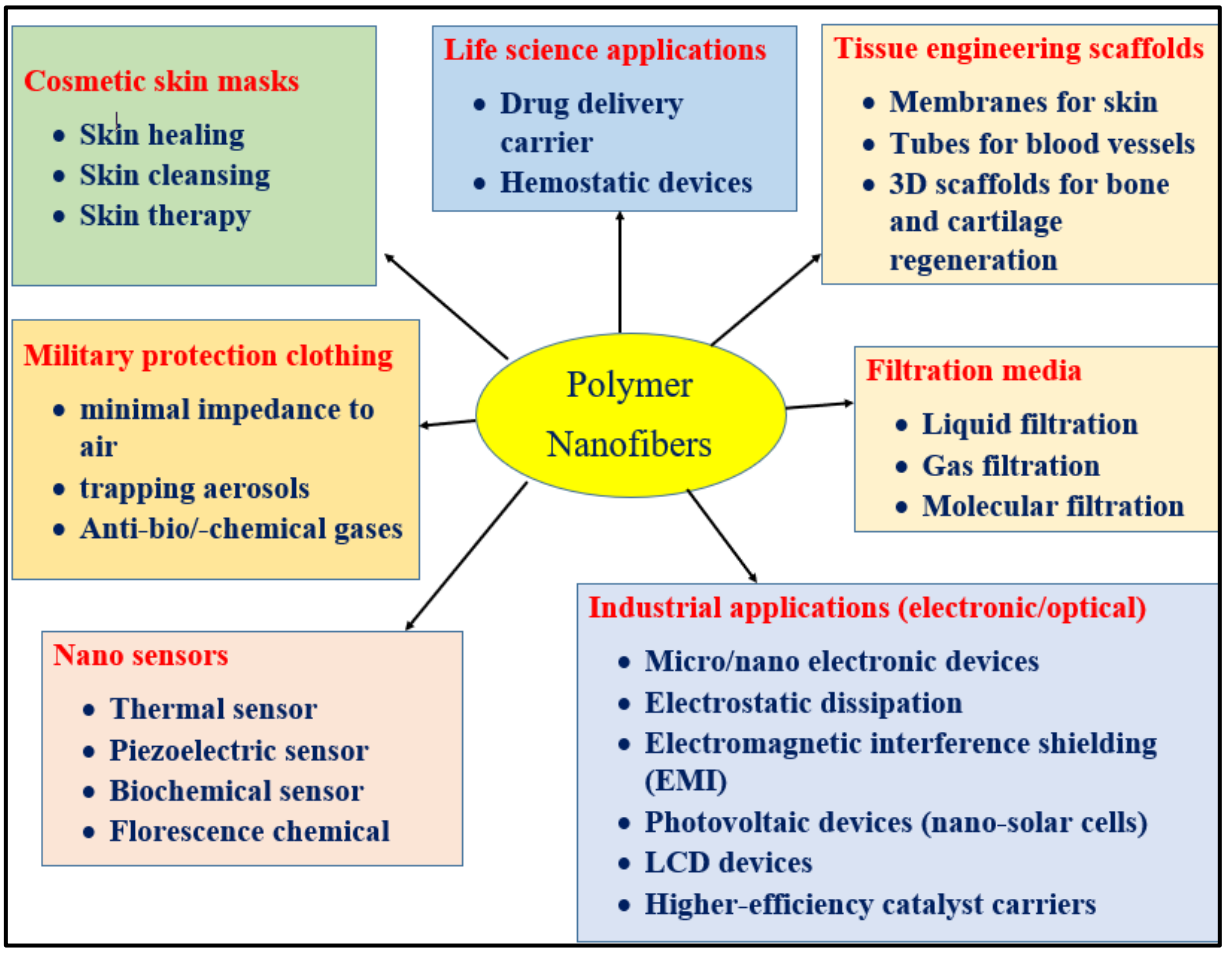

Figure (2.16) Applications of polymeric nanofibers [30]

2.5.1 Gas sensors

In recent years, pollution caused by gases generated by industrial companies has grown. The gases are hazardous to the human body. Therefore, in order to ensure people's safety, detecting and removing these gases have become a

necessary task in our life. The most hazardous gases are the ammonia gas, hydrogen sulfide gas, carbon monoxide gas, and nitrogen dioxide gas [74].

Several researches have been made to detect these gases, one of them by using "quartz crystal microbalances QCM" detectors together with electrospun sensors. QCM sensor used to detect mass changes by presence of coating material so that it will react with the gas as shown in the figure (2.17).

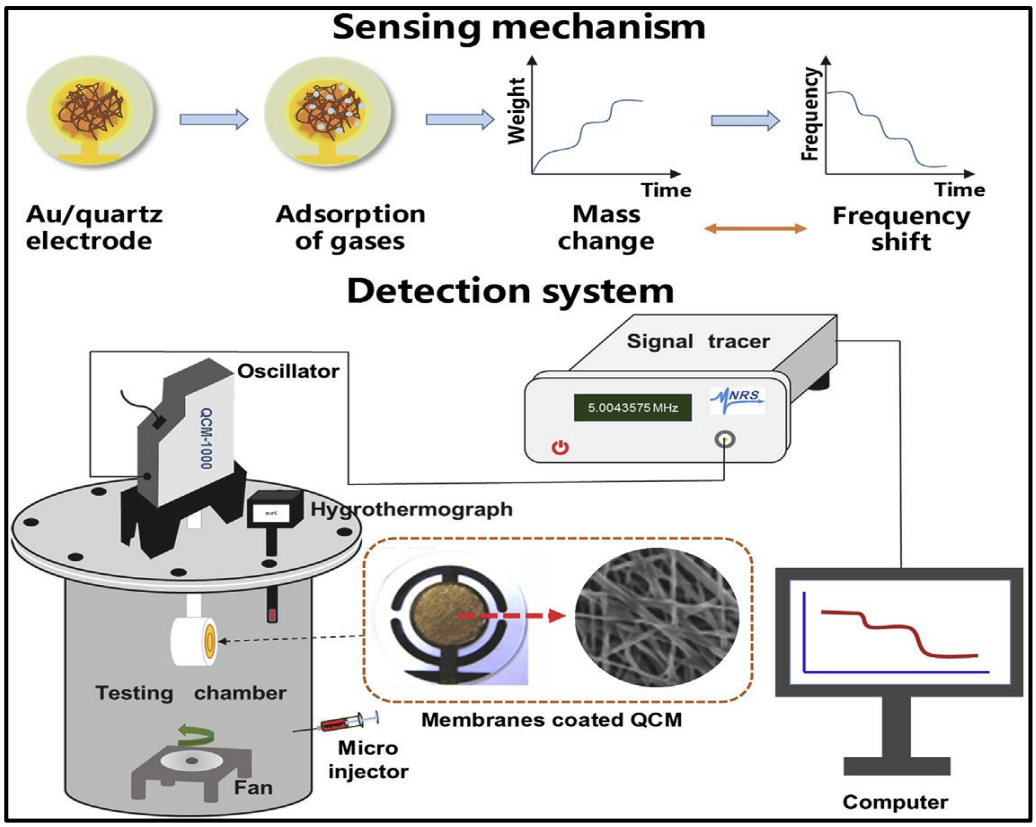

Figure (2.17) A scheme to illustrate the working principle of the quartz crystal microbalance (QCM).

There are many nanofibers used as coating materials to QCM sensors such as "polyacrylic acid PAA" because it has a carboxylic group which adsorbe the ammonia gas and increase the weight of nanofibers which indicate in increasing the sensitivity of the nanofibers to the detected gas [75]. For NH_3 gas detecting with QCM higher molecular weight PAA used [76], polyaniline used also as NH_3 sensor with various detecting limits [77].

H_2S gas is also harmful one to be detected is using "Cu-doped Zno" nanofibers through using electrospinning technique where various limits of H_2S observed and the sensitivity of the sensor increased with increasing amount of the H_2S gas as shown in figure (2.18) [78].

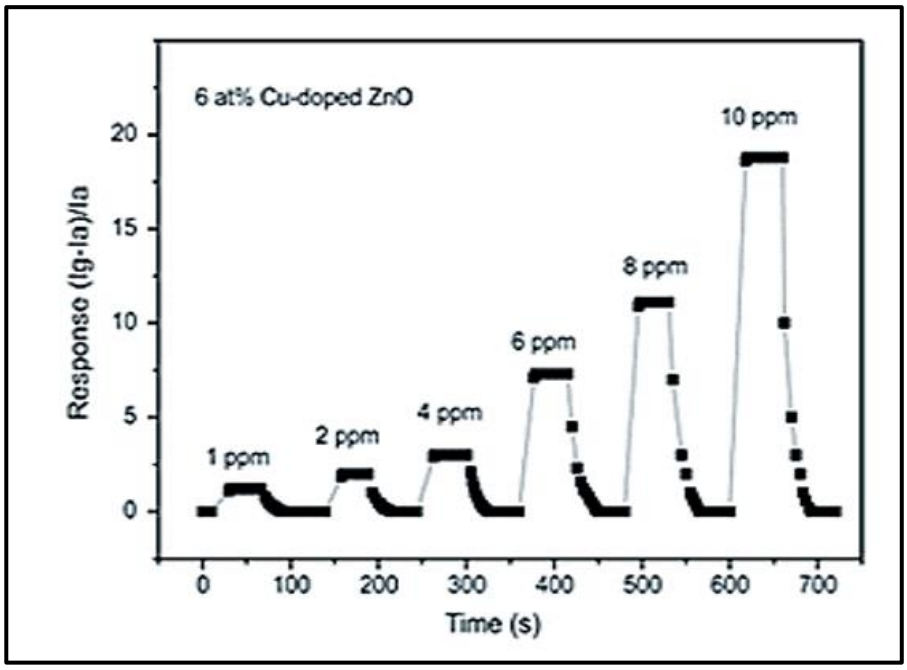

Figure (2.18) H_2S sensing using Cu /ZnO nanofiber sensor

2.5.2 Electrochemical sensors

Based on the electrochemical properties of the analyte and the associated changes in the solution, the electrochemical sensor is employed as an analysis method to determine the concentration of the analyte. The electrocatalytic reaction typically creates a measurable current (amperometry sensing) in an electrochemical sensor [79].

Electrochemical sensors for H_2O_2 and glucose have been developed in using poly vinyl difluoride (PVDF) and poly urethane (PU) doped with metallic nano particles (MNPs) and multi-wall carbon nanotubes (MWCNTs). Given AgNPs' outstanding electrocatalytic activity and MWCNTs' superior conductivity, the generated hybrid of (Polyurethan/MWCNT/AgNP) nanofibers are predicted to

be best from Polyurethan/MWCNT or (Polyurethan/AgNP) nanofibers individuals in the manufacturing electrochemical sensors.

Performance of the prepared Nanofiber-modified ground collector electrode(GCE) for hydrogen peroxide detecting was examined after (Polyurethan/MWCNT/AgNP) nanofibers were immediately electrospun to the GCE surface polished. The results reveal that, there are no redox reactions in pure electrospun PUNF-modified GCE owing to catalytically active surfaces of MWCNTs, they could enhance the active surface area of treated electrode when modified with electrospun Polyurethan/MWCNT, diffused current enhanced significantly. There are no noticeable peaks of redox current in the cyclic voltammetry (CV) of (Poly urethan/MWCNT/modified ground collecting electrode (GCE)), just as there aren't in the CV of pure Polyurethan nanofiber-modified GCE. Due to the lowering of H_2O_2, a strong response of the current and peak decreased clearly from (-0.65 to -0.4 V) for the (Polyurethan–AgNPs nanofibers)/modified GCE.

The CV results clarify that the Polyurethan/MWCNT/Ag-modified GCE has greater electrocatalytic activity toward the reduction of H_2O_2 from indiviuals (Polyurethan/MWCNT) or (Polyurethan/Ag) nanofibers with modified GCE, confirming the harmonious effect of multiwalled carbon nanotubes and silver nanoparticles. GCE modified with (Polyurethan/MWCNT/AgNP) displays a linear response to H_2O_2. The biosensor possesses a sensing range of 0.5 to 30 mM (R = 0.9999), a sensing of 18.6 µM (S/N = 3), and a sensitivity of 160.6 µA mM^{-1} cm^{-1} [80, 81].

2.5.3 Sensing of urea

Urea was adsorbed onto polyaniline nanofibers combined with Pt nanoflowers (PANi/Pt) and by using flow-injection-analysis (FIA) method the composite utilized as sensor for urea detection. The detection of urea has a large linear range and good anti-interference

properties against the chloride ion. Furthermore, the response to urea was revealed to be dependent not only to the conductivity variation of polyaniline because of contact it with ammonia but also depends on the interaction that occurs between amine groups in urea and Pt nanoflowers. The typical flow injection analysis amperometry response of the polyaniline/Pt/GCE to following injections of urea have made at maximum applied voltage about -0.1 V is shown in the inset of figure (2.19). urea biosensor formed has a linear range of up to 20 mM, a correlation coefficient of 0.9968, a sensitivity of 115.6 nA mM^{-1} cm^{-2}, and a detection limit of 10 mM (S/N = 3) [82]. It also has a sensitivity of 115.6 nA mM^{-1} cm^{-2} and a detection limit of 10 mM (S/N = 3).

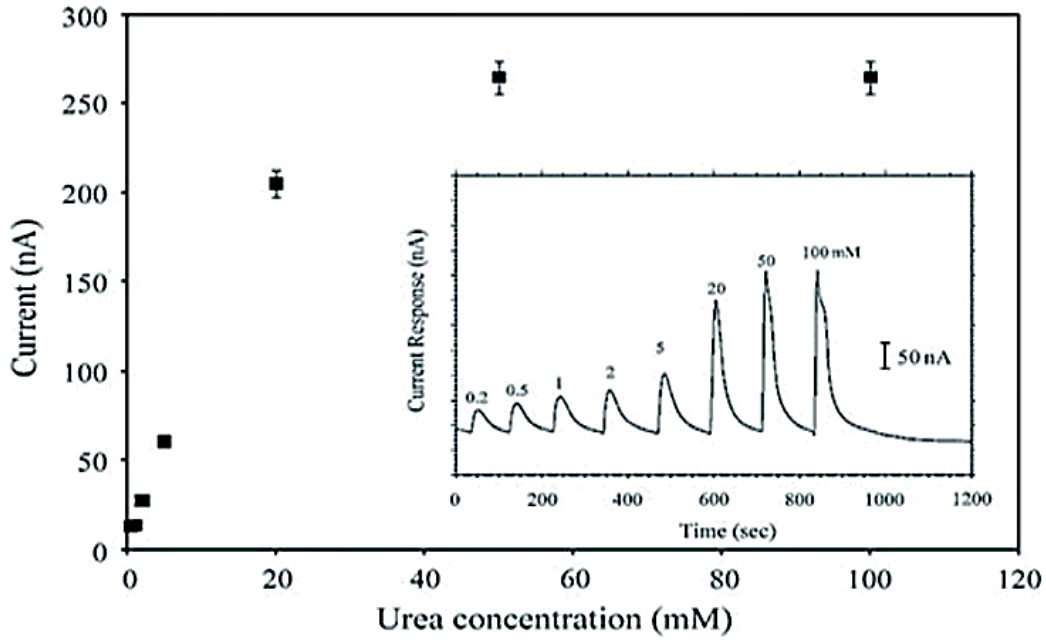

Figure (2.19) polyaniline–Pt urea biosensor

2.5.4 Optical Sensors

In the optical sensors, the "fluorescence quenching" principal of sensitive material is used against the targeted chemical molecules. for example, an attempt to manufacture the florescent monomer as well as further polymerized with methacrylate monomer. The produced polymer has a high photosensitive pyrene content, as illustrated in figure (2.20 a). The fluorescence emission response of the nanofibers formed from this polymer with average fiber diameter equal (300-1000 nm) was examined using dinitro toluene (DNT). DNT is a hazardous chemical component that has been found in drinking water occasionally. Humans are affected by "dinitro toluene", in which anemia will caused, methemoglobinemia, and liver affected [83]. As a result, detecting DNT in the water is critical. The intensity of the produced nanofiber's fluorescence lowered with DNT content, as shown in figure (2.20 b).

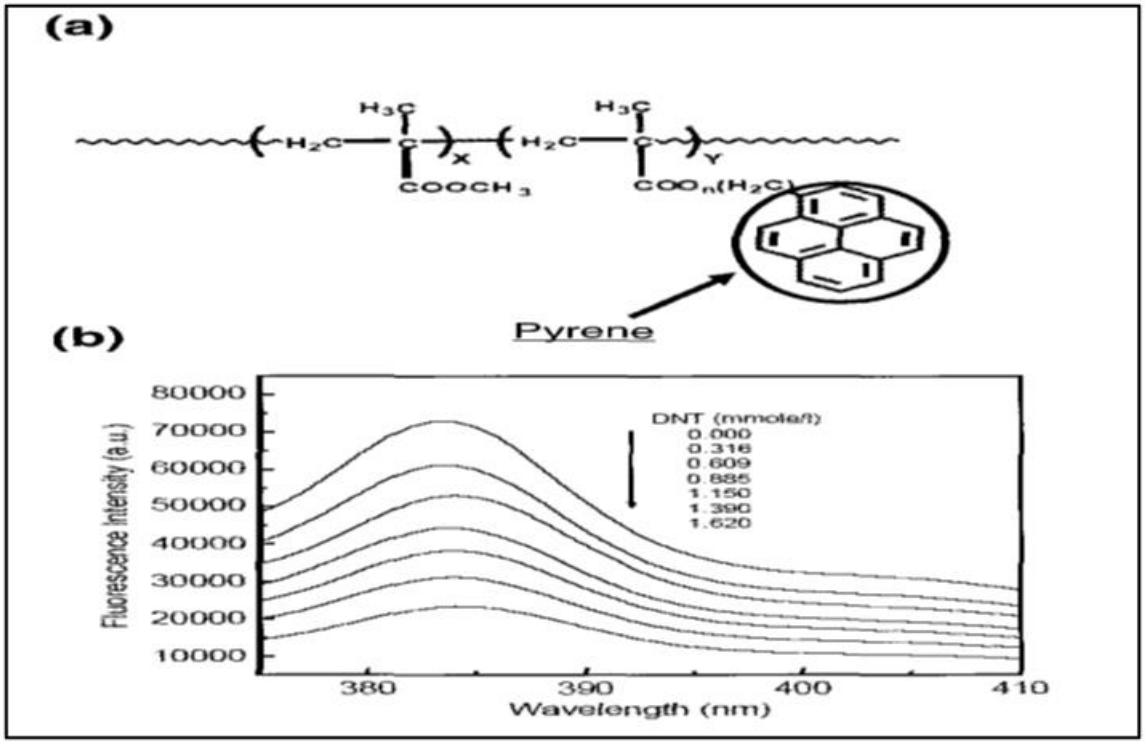

Figure (2.20) (a) electrospun fluorescent polymer Structure (b) decreasing in fluorescent intensity of nanofibers as result from concentration of DNT increasing

2.5.5 Bio sensors

Biosensors are devices that can detect and track biological changes in the human body. Because the percent of old people is expected to increase rapidly in the near future, one of the most important disciplines today is bioengineering. Biosensors have become a prominent topic because to the growing need for therapy using bioengineering technology. cytochrome c is a heme-containing respiratory protein that can be detected. This protein is associated with the myocardial infarction confirmation, and detecting it is necessary for patient monitoring.

The fluorescent layer of poly[2-(3-thienyl) ethanol butoxy carbonyl-methyl urethane] that covers the cellulose acetate nanofibers were also utilized to monitor cytochrome c and methyl viologen. Average fiber diameter of nanofibers made was 100 to 400 nanometers. The fluorescence intensity was found to decrease when the concentration of cytochrome c and methyl viologen increased. The higher surface area of nanofibers and good interaction between the fluorescent polymer and the targeted material to be analyzed are responsible to higher fluorescence sensitivity [84].

2.5.6 Chemical sensors

Chemical sensors are used to detect a specific chemical element or variation in pH value in a material system. Many attempts have been made in this area of application. The initial attempt used electrospun nano fiber membrane to modify traditional piezoelectric sensors, resulting in Thickness Shear Mode (TSM) sensors. Nanofibers of polylactic acid/glycolic acid (PLAGA) were coated over the interface sensing of TSM sensors and characterized with various liquid loading conditions [85]. Another attempt to make use of PLAGA's unique characteristic, which is that the PLAGA polymer is moderately hydrophobic against water and moderately hydrophilic against propanol. Sensors of TSM covered with PLAGA nanofibers responded in distinct ways in water and

propanol, and the notion of sensors is extremely beneficial for detecting specific chemical components [85].

2.6 Literature Review

There are several studies done to investigate the electrical conductivity of nanocomposites using the electrospun device, "Electrospinning" regarded as the most preferred technique for the manufacturing of continuous polymer 1D nanostructures with controllable diameter and compositions [15 and16].

In the year 2005, H. Hou et. al, added MWCNTs to the polyacrylonitrile suspended solution to make nanofibers using electrospinning technique. Then PAN nanofibers with MWCNT was created. The nanofiber sheets were characterized using scanning electron microscopy, atomic force microscopy, transmission electron microscopy (TEM), IR spectroscopy, Raman spectroscopy, X-ray scattering, and the Instron test. The MWCNTs were parallel and orientated along the axis of the nanofibers, according to TEM observations. MWCNT fillers were used to improve the mechanical properties of the composite nanofibers. Heat shrinkage of nanofibers composites improved with higher concentration of MWCNTs addition [41].

In the year 2008, T. Uyar, et.al, studied the conductivity of the solvent which is a critical factor in electrospinning homogenous polystyrene (PS) fibers from dimethylformamide (DMF) solutions in a uniform fashion. The shape of the resulting PS fibers can be dramatically influenced by even minor changes in conductivity. The solution conductivities of different solvent grades are slightly different. The researchers discovered that solutions with a higher conductivity produced bead-free fibers from lower polymer concentrations, confirming that solution conductivity is a key factor in developing uniform fibers free of beads [42].

In the year 2008, Wei Wang, et.al, used zinc oxide nanofibers having diameters about (150 nm) formed using electrospinning method. Various characterizations methods used for the final form nanotextiles for the

morphology and composition were examined using “SEM”, “TEM”, and “XRD”. The prepared ZnO nanofibers tests revealed to excellent usage of ZnO as ethanol detectors at 300°C and the fabricated nanofilms have rapid response time (3 sec.) and (8 sec.) as a recovery time and has enormous sensitivity, this makes it best candidate for usage as gas sensor [35].

In 2009, S. Mazinani, A. Ajji, et.al, studied the polystyrene (PS)/Carbon Nanotube (CNT) conductive electrospun mat, (PS/CNT with different ratios and types/DMF solvent) this solution showed that the dispersion of CNT depends on the morphology and characteristics of nanocomposite fibers, also used copolymer (SBS” styrene- butadiene- styrene”) as an interfacial agent to enhancing the dispersion of carbon nanotubes in polystyrene solution prior electrospinning. as a consequence, adding CNT to the copolymer prior to electrospinning considerably increased its dispersion. Additionally, adding CNT to the solution reduces the creation of beads along the fiber's axis before the percolation threshold, while raising above it. Electrical conductivity calculations on nanocomposite mats with a thickness of 15–300 μm revealed an electrical percolation threshold of roughly 4 wt percent MWCNT, whereas samples including SBS had greater values of conductivities below percolation than samples without a compatibilizer. The inclusion of CNTs at concentrations below percolation resulted in improvements in mechanical characteristics [17].

In the year 2009, Z. Zhang, et.al, utilized electrospinning a precursor solution including polyacrylonitrile (PAN), polyvinylpyrrolidone (PVP), and zinc acetate composite through a simple single capillary, ZnO hollow nanofibers with diameters of 120-150 nm were effectively produced. Due to their unique one-dimensional nano structural characteristics, the as-prepared nanofiber has outstanding ethanol sensing capabilities. Zinc oxide (ZnO) nanofibers might be used as a structural direction template during the calcination procedure to prepare them [37].

In the year 2010, K. Ketpang, et.al, fabricated PVDF/PPy/MWCNT composites using a highly porous electrospun (e-spun) nonwoven web as the host polymer PVDF and $CuCl_2H_2O$ in a solvent of N, N-dimethylacetamide were electrospun together in a solvent of N, N-dimethylacetamide (DMAc). The manufacturing process and oxidant content in the nonwoven web had an impact on the electrical conductivity of the PPy composites. If adding modified MWCNT to the PPy, the mechanical strength and the electrical conductivity of the PPy composites will enhanced. The MWCNTs were properly organized and incorporated in the e-spun fibers, according to the results of energy-filtered transmission electron microscopy (EF-TEM). The conducting PPy-MWCNTs composite has a conductivity of (101 S/cm) [18].

In the year 2010, J. C. C. Lima, et.al, used electrospinning technique to create composite fibers of poly vinyl butyral and zinc nitrate. Nanostructured zinc oxide fibers were obtained after a heat treatment at 600°C. X-ray diffraction was used to identify the fibers. The photocatalytic behavior of the nanostructured fibers was tested using a methyl orange solution photodegradation. The photoactivity of zinc oxide reduces as the heat treatment temperature rises. The physical, chemical, and photocatalytic behavior of zinc oxide are affected by heat treatment, phases, and surface area [33].

In the year 2011, J. Yun, J. S. Im, et.al, produced poly (vinyl alcohol)/poly (acrylic acid/ MWCNTs nanocomposites to construct an electro-responsive transdermal medication delivery system. Oxyfluorination improved the dispersion and compatibility of MWCNTs with polymer matrices. Swelling and drug release properties of nanofibers were affected by MWCNTs material and oxyfluorination settings. The researchers say their findings could lead to a new type of drug delivery system in the future [32].

In the year 2012, G. A. Zamora-P?rez, et.al, studied the Poly(vinylideneflouride) (PVDF) pellets which dissolved in N, N-

dimethylformamide (DMF). After that, they utilized the electrospinning method to produce ultrafine fibers (mats) that may be used in a number of biological applications. Here's an example of a humidity sensor. PVDF films have demonstrated excellent results when employed as a soil moisture sensor, allowing them to be utilized as control sensors in biological applications such as bioreactors, assisted ventilation devices, and also industrial applications [34].

In the year 2015, F. A. Chayad, A. R. Jabur et.al, added MWCNT in different ratios (0, 0.1, 0.2, 0.4, 0.6, and 0.8) wt. percent to electrospun nylon6 films to improve electrical conductivity and activation energy. The electrical conductivity test reveals that when the MWCNTs concentration increases, the electrical conductivity was improved significantly from (2.9×10^{-9} S/cm) to (1.04×10^{-6} S/cm) for the pure nylon6 and nylon6/0.8 wt.% MWCNT nanotextiles. There is also improvement in activation energy of (pure nylon6, nylon6/0.1, 0.2, 0.4, 0.6, 0.8 percent wt. percent MWCNTs) films decreased as the MWCNTs percentages increased. The activation energy values were (0.068, 0.057, 0.0536, 0.0523, 0.045, 0.077) eV for (pure nylon6, nylon6/0.1, 0.2, 0.4, 0.6, 0.8 wt.% percent MWCNTs. The estimated activation energy of 0.077 eV is greater than that of the pure sample, which is 0.068 eV. This might because the manner of dispersion of MWCNTs in the nylon6 nanofibers varies as the amounts of MWCNTs increased [19].

In the year 2017, N. Amariei, L. R. Manea, et.al, Polyaniline is a conductive polymer with various applications as detecting (mineral acids, ammonia, volatile organic compounds (VOCs)) etc. the results from electrochemical processes related to the surface area, it is predicted that polyaniline nanofibers could offer significant possibilities for electronic nanodevices applications [36].

In the year 2018, S. Ponce-Alcántara and D. Martín-Sánchez, developed porous materials that considered as an excellent candidate for the development

optical sensors capable of achieving higher range of sensitivities, owing high surface area and penetration ability of target materials. In this study, they propose a novel option for the development of optical porous detectors by the utilization of polymeric nanofibers (NFs) layers produced by electrospinning. Polyamide6 nanofibers layers possess average diameter smaller than 30 nm and strong porosities have been utilized for the construction of optical sensing Fabry-Perot structures, which recorded an experimental sensitivity more than 1060 nm/RIU (refractive index unit). This great sensitivity, along with the cheap manufacturing fees and the ability to be produced across vast regions, make NFs-based devices a highly attractive option for the creation optical sensors of cheaper and high-performance properties [38].

In the year 2019, A. R. Jabur, produced conductive polymer sheets of polyvinyl alcohol (PVA) containing (0, 2, 4, 6, 8, and 10) wt.% multiwalled carbon nanotubes (MWCNTs). Scanning electron microscopy (SEM) was utilized to examine the morphologies of the produced films. Average dynamically gauged fiber diameters were (115 nm) for (PVA/10 wt.% MWCNT film) whereas (170 nm) for pure PVA electrospun film. Improve the electrical conductivity (EC) of Polymeric nanofiber films by increasing the extra concentration of MWCNT from (3.69×10^{-7} S / cm) for pure (PVA) nanofibers to (1.24×110^{-2} S / cm) for 10 wt.% MWCNTs film. The ultimate stress of PVA film has been enhanced by increasing the concentration of MWCNT, the elasticity modulus for pure PVA was increased from (12.87 MPa) to (49.89 MPa) for PVA / 8wt.% MWCNT [8].

In the year 2019, S. Kohn, D. Wehlage, I. J. Junger, et.al, Dye-sensitized solar cells employing electrospinning technique provide new opportunities to collect solar energy by using non-toxic cheap materials. While the efficiency is lower than for glass-based cells, potential issues such as short-circuits which frequently arise in fiber-based DSSCs did not occur in this proof-of-concept. There are many methods to improve the efficiency in future investigations, the

researchers suggest. The cells may be used to generate solar energy from photovoltaic cells, LEDs, and other low-cost solar cells [39].

In the year 2020, H. J. Alesa, B. M. Aldabbaget.al, produced Solar cells thin films from polyvinyl alcohol (PVA), with extract of natural dye from local flower. Analysis showed an increase of PVA melting point when adding 15 percent concentration and it lowers with a 50 percent concentration of pigment. Optical characteristics were improved by adding the natural dye, thus the energy gap reduced from 3 eV to 2.3 eV for the PVA with a high concentration dye [40].

2.7 Summary of literature reviews

Previous studies showed that there is a possibility to synthesized and utilizing the nanofibers by electrospinning technique in sensors applications, owing to their high surface area to volume ratio, as compared with traditional nano fibers methods. Some of the studies showed the incorporation effect of MWCNTs to the polymeric nanofibers which will lead to improve its sensitivity values, other studies showed the effect of addition of natural dye on polymeric nanofibers which will cause improvement in the electrical conductivity of the solutions because if increasing the dissolved ions. This thesis will investigate what happened if MWCNTs and natural dye added individually and together on the properties of polystyrene nanofibers, and investigation of the possibility of using the prepared samples as optical sensors

Chapter 3

Experimental Part

3.1 Introduction

This chapter describes the experimental work of preparing and testing the electrospun nanocomposites, as well as the characteristics of the materials used. In this work, polymer nanocomposite of polystyrene with different concentrations (12, 14, 16 wt.%) reinforced with a multiwall carbon nanotube at different weight percentages were prepared via the electrospinning technique to produce nanocomposite thin textiles. Structural properties, bonds between MWCNT and polystyrene nanofibers were studied via Fourier transform infrared spectroscopy (FTIR) analysis. Morphology, tribology, porosity, and roughness of thin films by atomic force microscopy (AFM) were tested. Energy band gap measured using the ultraviolet spectroscopy test, the morphology of manufactured films has been conducted with Field emission Scanning electron microscopy (FESEM), and many other tests mentioned in this chapter.

3.2 Materials used

3.2.1 General purpose Poly Styrene (GPPS)

Polystyrene grains with a purity of 99% were obtained from American polymers services Inc. (APS) made in the USA, general properties of polystyrene illustrated in table (3.1).

Table (3.1) General purpose polystyrene Properties.[44]

No.	Property	Information
1	Melting Point	180-260 ˚C
2	density	1.04 - 1.05 g mL^{-1}
3	Thermal conductivity	0.35 W/m.K
4	Tensile Strength, break at 23 ˚C	47MPa

5	solvents	Benzene, toluene, DMF, Chloroform, cyclohexane, THF
6	Volume resistivity	> 6 * 10 ^{15}
7	Dielectric strength	2.1 - 3.5 V/mm *10^4
8	Dielectric Constant	2.20 – 2.35 n/a
9	Processing temperature	170 – 240 ˚C
10	Continuous service temperature	-73 – 82 ˚C

3.2.2 Multi-walled Carbon Nanotube

Multi-Walled Nanotubes obtained from SKY spring nanomaterials Inc. with outside diameter: <8nm, internal diameter: 2–5nm, , table 3.2 shows its properties.

Table (3.2) Properties of Multiwall carbon nanotube

No.	Property	Information
1	Purity	> 95 wt.%
2	Outside diameter	< 8nm
3	Inside diameter	2-5 nm
4	Length	5-20 µm
5	Specific Surface Area (SSA)	> 500 m^2/g
6	Ash	< 1.5 wt.%
7	Electrical Conductivity	> 100 S/cm
8	Bulk density	0.27 g/cm^3
9	True density	~ 2.1 g/cm^3
10	Manufacturing Method	CVD

3.2.3 Natural Dye

Natural dye from sunflower leaves of euryops daisy flower extracted with DMF solvent has the contents shown in the table (3.3) and has (36 S/cm) electrical conductivity value.

Table (3.3) Natural dye content analysis

Element	Value
N	17.5 ppm
P	5.5 ppm
K	12.1 ppm
Cl	0.3 Meq/L
HCO_3	0.1 Meq/L
SO_4	4.5 Meq/L

3.3 Samples Preparation

In this work, The solutions are prepared by dissolving polystyrene in dimethylformamide (DMF) solvent with three concentrations (12, 14, 16 wt.%) by using a hot plate stirrer at room temperature (25℃) for three hours, until we have a homogeneous solution. Then we added multiwall carbon nanotubes into the prepared solutions with different weight percentages according to the polymer weight by (0, 0.08 wt.%, 0.11 wt.%, 0.16 wt.%), (0, 0.07 wt.%, 0.1 wt.%, 0.14 wt.%), and (0, 0.06 wt.%, 0.8 wt.%, 0.125 wt.%) for (12, 14, 16 wt.%) polystyrene respectively, then dispersion process occurred using the ultrasonic device to get well dispersion of MWCNTs in the polymeric solutions at (40℃) for (15 min) then 1 ml from the syringe was taken to be pumped in electrospinning device.

For the natural dye addition, after we extract the best group from the results, we made which is (12 wt.%) group after we make ultrasonication we added two drops (0.063g) from the dye solution and make the solution to be

stirred well before the electrospinning process to it to get more homogeneity dissolved in the solution. As shown in table (3.4) and figure (3.1).

Table (3.4) Materials used percentages

Polymer (wt.%)	MWCNT (wt.%)
12	0
12	0.08
12	0.11
12	0.16
14	0
14	0.07
14	0.1
14	0.14
16	0
16	0.06
16	0.08
16	0.125
12 + 0.063 g dye	0
12 + 0.063 g dye	0.08
12 + 0.063 g dye	0.11
12 + 0.063 g dye	0.16

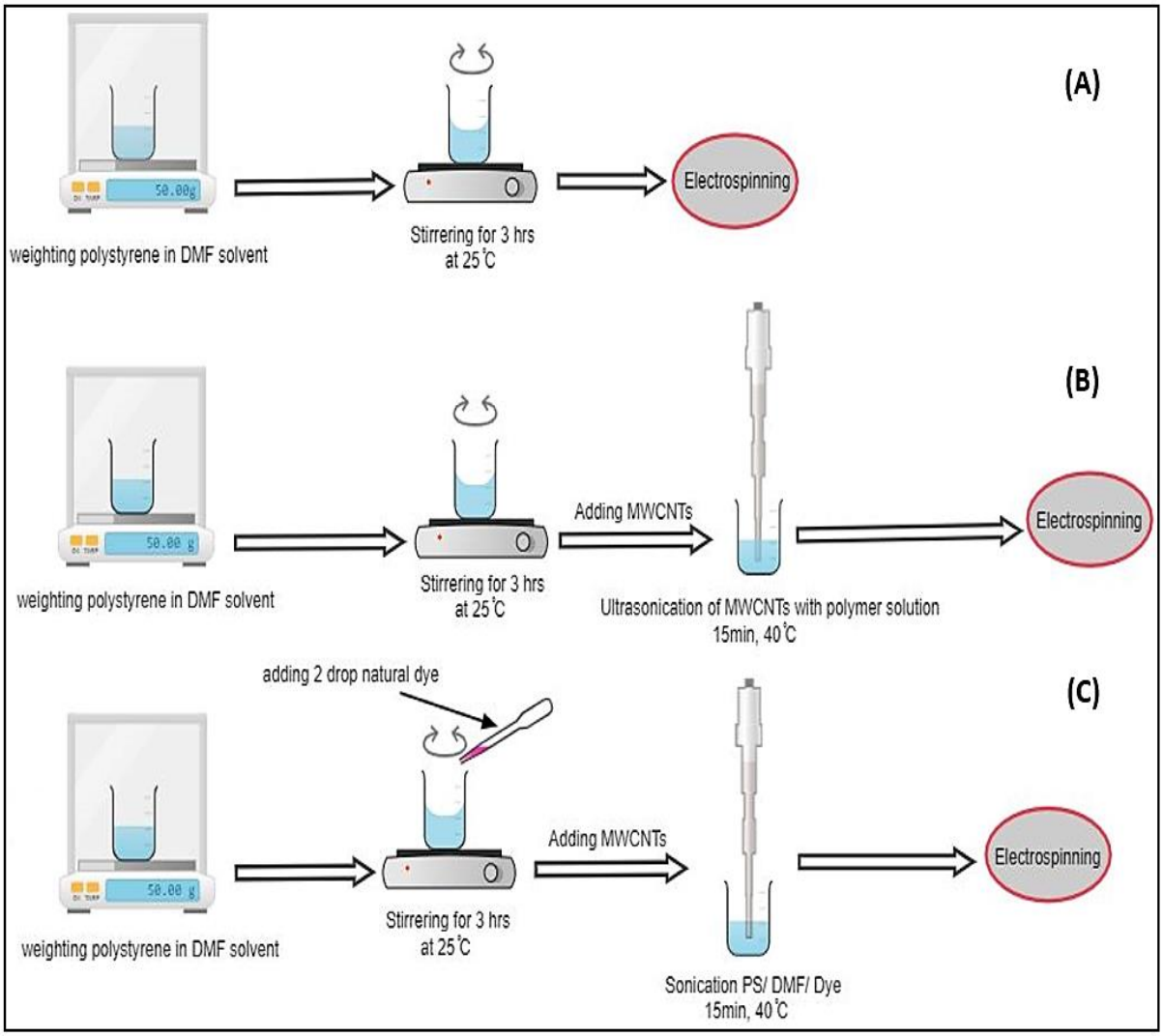

Figure (3.1) Procedure of sample preparation were (a) for pure polystyrene (b) polystyrene/MWCNTs (c) polystyrene/MWCNTs/Dye

3.4 Electrospinning process

After mixing the components by using the stirrer and ultrasonic for dispersing the MWCNT through the solution, an electrospinning process occurred to the solution to get nanofiber textiles the device used and its modeling illustrated in figures (3.2, 3.3). the process conditions used were the applied Voltage was 20 KV, tip-collector distance was 20 cm, the temperature was 25℃, rotation speed was 480 rpm, the flow rate was 1ml/hr.

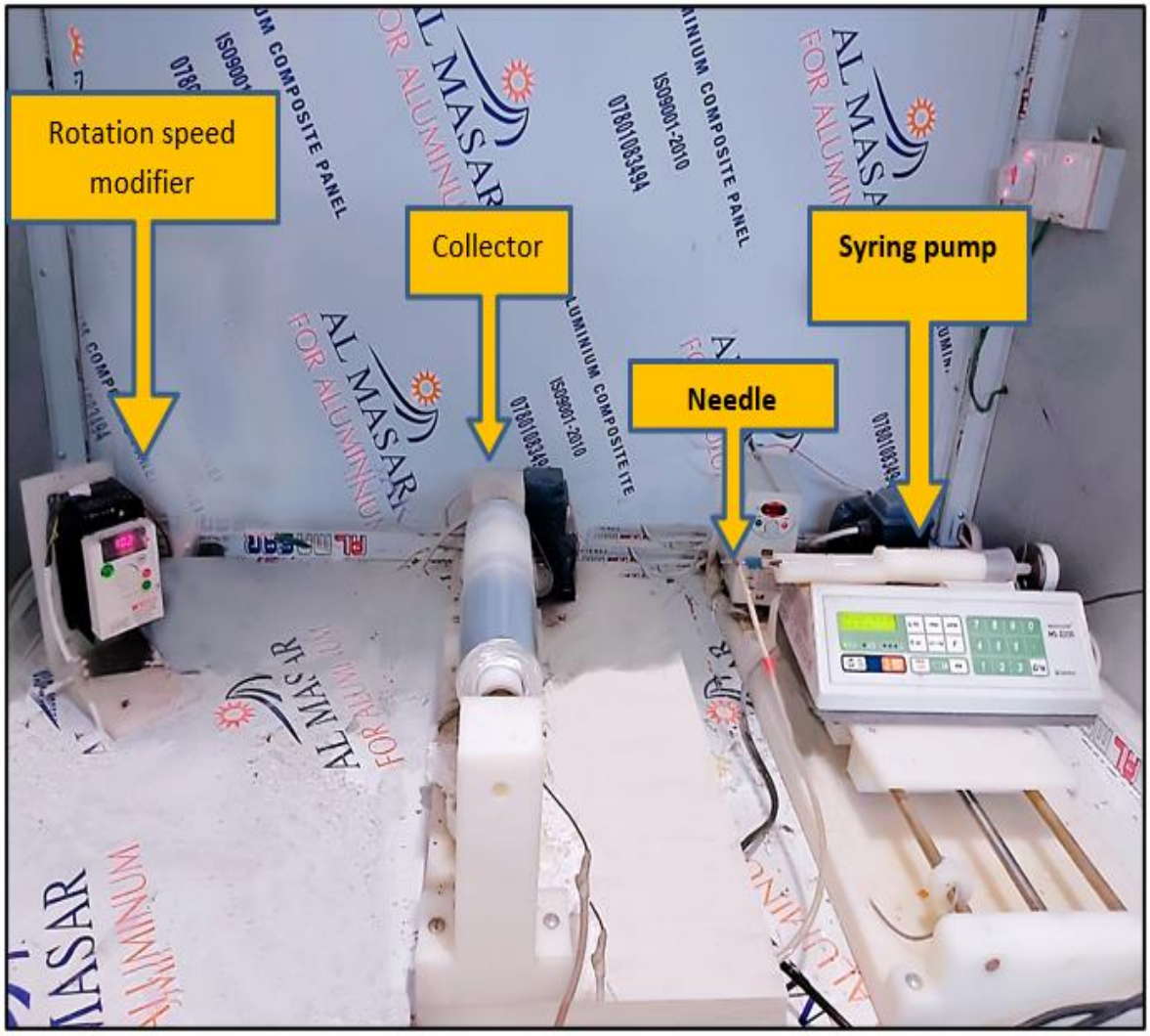

Figure (3.2) Electrospinning device

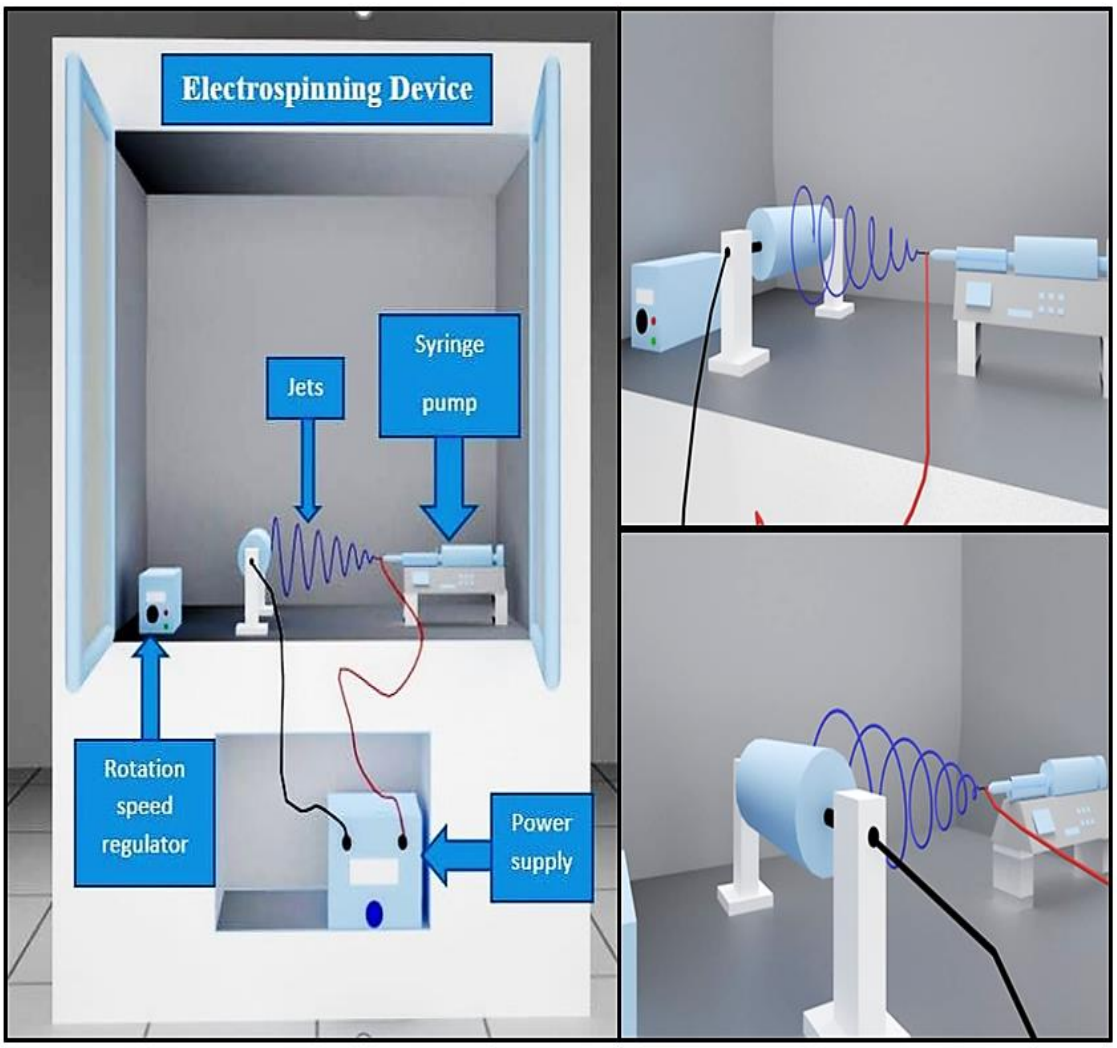

Figure (3.3) Scheme electrospinning device with 3DS Max program

3.5 sampling

after using the electrospinning process nano textiles deposited on the Aluminum foil as shown in the figure (3.4).

Figure (3.4) Final sample deposited on aluminum foil

3.6 Tests

3.6.1 Surface tension test

The surface tension of the PS/MWCNT solutions was measured with a TEN202 Surface Interfacial Tensiometer using a pt ring immersed in a solution mounted in a cylindrical petri dish and the surface tension value of the solutions was measured in mN/m. figure (3.5).

Figure (3.5) Surface tension device

3.6.1 Viscosity test

The viscosity test was done using “Brookfield DV-III Ultra Rheometer” to measure the viscosity of the prepared solutions in cP units as shown in the figure as shown in the figure (3.6).

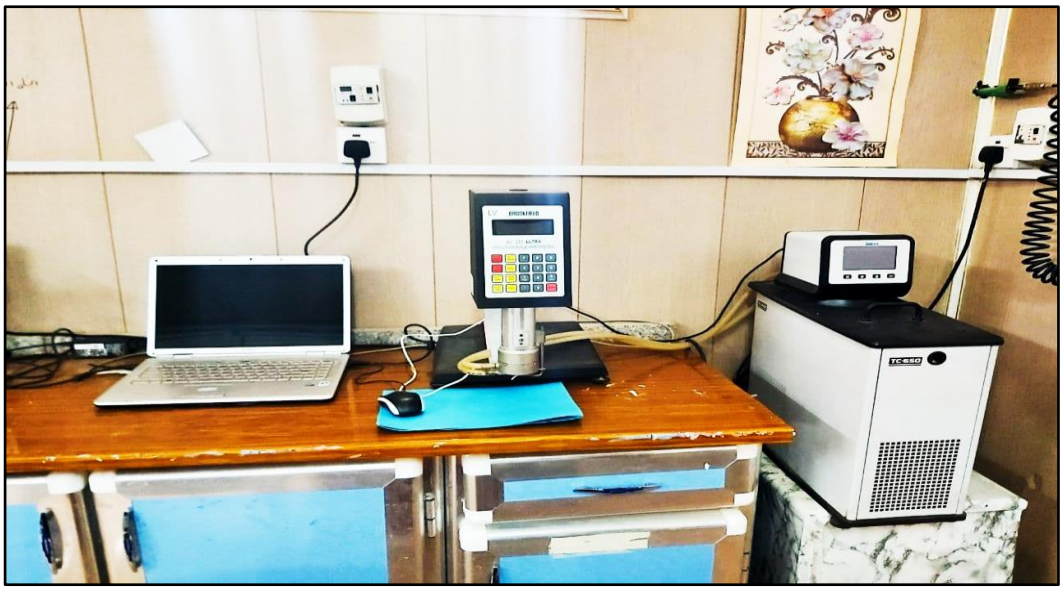

Figure (3.6) Brookfield DV-III Ultra Rheometer

3.6.3 Fourier transform infrared spectroscopy (FTIR) Test:

FTIR test is done by utilizing IR Affinity-1 Shimadzu –Japan Figure (3.7). To know the type of interaction between components and bonds types of it.

Figure (3.7): IR Affinity-1Shimadzu device

3.6.4 Contact Angle Test:

Contact angle (circle fitting mode) was used to evaluate the wettability of the Nanocomposite samples using "SL200B Optical Dynamic / Static Contact Angle Meter" as shown in Figure (3.8).

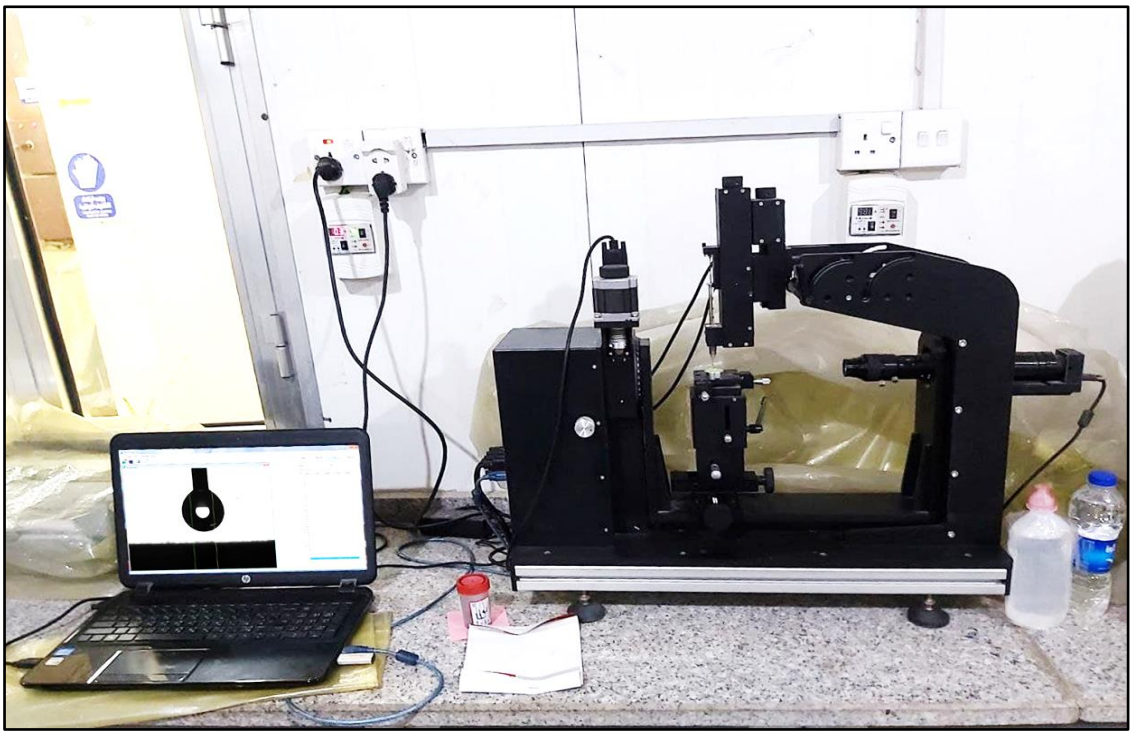

Figure (3.8): Contact Angle Meter (SL200B Optical) device

3.6.5 Atomic Force Microscopy (AFM) Test:

AA3000 Scanning Probe Microscope is a very well device designed for use in research and industry, in which the inspector may do quick, easy analysis. Because the tip is placed into the base, there is no risk of being damaged by handling. tapping mode, contact mode, lateral force microscopy, all possible with the AA3000 Scanning Probe Microscope.

The main function of the standard unit is to see the area of samples prepared up to 10 microns by 10 microns. The device can be adjusted to inspect larger areas of the sample. With the existing "digital signal processor

(DSP)" in the system, the device can treat more complex tasks effectively. The device is shown in figure (3.9)

Figure (3.9) AA3000 Scanning Probe Microscope

3.6.6 Field emission scanning electron microscopy (FESEM)

Field emission scanning electron microscopy and "energy dispersive x-ray (EDX) tests were carried to the prepared films to check the fibers diameter distribution and the smoothness also the chemical components of them using the "FESEM (Zeiss Sigma 300- HV) GERMANY" instrument. figure (3.10)

Figure (3.10) FESEM with Edx instrument

3.6.7 UV-Visible spectroscopy test

Energy band gap, absoption, refractive index,extinction coefficient, optical conductivity results were taken by using the Shimadzu UV-1800 UV/Visible Scanning Spectrophotometer, as shown in figure (3.11).The equation (3.1) was used to calculate the energy gap which is called tauc plot method, equation (3.2) used to calculate the extinction coefficient, equation (3.3) used to calculate the optical conductivity and equations (3.5, 3.6) used to calculate the refractive index.

$$\left[(\alpha hv)^{\frac{1}{2}} = A(hv - Eg)\right] \ldots\ldots\ldots\ldots\ldots\ldots\ldots\ldots\ldots\ldots\ldots\ldots\ldots\ldots\ldots\ldots (3.1)$$

Where:

α = Absorption coefficient

h = Blank constant (4.14x 10^{-5} ev.sec)

v = photon frequency

Eg = Energy gap

A = Absorbance

$$\left[k = \frac{\alpha \lambda}{4 \pi}\right] \ldots\ldots\ldots\ldots\ldots\ldots\ldots\ldots\ldots\ldots\ldots\ldots\ldots\ldots\ldots\ldots\ldots\ldots\ldots\ldots\ldots\ldots (3.2)$$

Where:

K = Extinction coefficient

α = Absorption coefficient

λ = Wavelength

π = 3.14

$$\left[\sigma = \frac{\alpha n c}{4 \pi}\right] \ldots\ldots\ldots\ldots\ldots\ldots\ldots\ldots\ldots\ldots\ldots\ldots\ldots\ldots\ldots\ldots\ldots\ldots\ldots\ldots\ldots\ldots (3.3)$$

Where:

α = Absorption coefficient

n = Refractive index

c = Speed of light in vacuum (3x10^{8} m/sec)

π = 3.14

Absorption coefficient can be calculated from this equation

$$\left[\alpha = \frac{2.303\ x\ A}{l}\right] \ldots\ldots\ldots\ldots\ldots\ldots\ldots\ldots\ldots\ldots\ldots\ldots (3.4)$$

Where :

A = Absorbance

l = thickness of sample

$$\left[n = \frac{1}{Ts} + \sqrt{\frac{1}{Ts}}\right] \ldots\ldots\ldots\ldots\ldots\ldots\ldots\ldots\ldots\ldots\ldots\ldots (3.5)$$

Where :

n = Refractive index

Ts = Percent Transmittance

$$[Ts = 10^{-A}\ x\ 100] \ldots\ldots\ldots\ldots\ldots\ldots\ldots\ldots\ldots\ldots\ldots\ldots (3.6)$$

Where A = Absarbance

Figure (3.11) UV-Visible spectroscopy device

Chapter 4

Results & Discussion

4.1 Solution Characterizations Results

4.1.1 Surface Tension Results

Table (4.1) shows the effect of polymer concentration on the surface tension of (PS/DMF) solutions. surface tension increase when increasing the polymer concentration from (12 to 14 wt.%). This is because increasing the concentration leads to an increase in the attraction of the polymeric chains which leads to increase the cohesive forces of it, and this is also clear from the results of viscosity with concentration, where there is a close relationship between surface tension and viscosity with concentration. This is consistent with [89].

When the concentration is increased to 16 wt.%, the surface tension decreases because the adhesion force between solution and air molecules on the surface is much greater than the cohesive force between solution molecules, which reduces the surface tension [90]

On the other hand, the surface tension decreases after adding carbon nanotubes. This is because the presence of low concentrations of carbon nanotubes works to separate the molecules from each other, and this leads to a reduction in surface tension due to reduces cohesive forces as shown in Table (4.2) [91].

While at high concentrations of carbon nanotubes, it leads to an increase in the surface tension of the solutions due to the convergence between the particles. [91]

As well as, the addition of natural dye with (0.063 g) to the solution at a concentration of 12 wt. %, leads to an increase in the surface tension of the solution compared to solutions without dye. This is due to the generation of two separate surfaces between the dye and the solution due to the lack of total

dissolution of the dye and this leads to increase the surface tension of the solutions.

Table (4.1) Surface tension results of different PS/DMF solutions.

Concentration PS/DMF	Surface tension (mN/m)
12wt.%	25.675
14wt.%	30.55
16wt.%	16
12wt.%+Natural dye	29

Table (4.2) The Surface tension results of the prepared samples

12 wt.% PS	
Sample	Surface tension (mN/m)
Pure polystyrene	25.675
PS/ 0.08 wt.% MWCNT.	23.4
PS/ 0.11 wt.% MWCNT.	23.382
PS/ 0.16 wt.% MWCNT.	22.572
14 wt.% PS	
Sample	Surface tension (mN/m)
Pure polystyrene	30.55
PS/ 0.07 wt.% MWCNT.	32.74
PS/ 0.1 wt.% MWCNT.	32.65
PS/ 0.14 wt.% MWCNT.	32.85
16 wt.% PS	
Sample	Surface tension (mN/m)
Pure polystyrene	16
PS/ 0.06 wt.% MWCNT.	16.88
PS/ 0.08 wt.% MWCNT.	16.44
PS/ 0.125 wt.% MWCNT.	16.48
12 wt.% PS+ 0.063g Dye	
Sample	Surface tension (mN/m)
Dye	29.60
PS/ 0.08 wt.% MWCNTs. /Dye	29.24
PS/ 0.11 wt.% MWCNTs. /Dye	29.18
PS/ 0.16 wt.% MWCNTs. /Dye	27.71
PS/ 0.08 wt.% MWCNTs. /Dye	33.08

4.1.2 Viscosity Results

Figure (4.1) Shows the viscosity of solution increases with increasing the concentration of polymer solution, due to increase the polymeric chains in the solution.

On the other hand, the viscosity results showed that when increasing ratios of MWCNTs will cause reduction in the viscosity of the solutions of groups (12, 14, 16 wt.%). This is because that the MWCNTs have a high surface to volume ratios and high aspect ratios furthermore, they are expected to align themselves in the direction of shear flow (acting as a lubricant), which decrease the resistance to the flow and eventually reduce the viscosity at a constant shear rate (15 Sec^{-1}) this is clear in figure (4.2), table (4.3). Figure (4.3) shows that the adding of the natural Dye to the group of (12 wt.% PS group) will cause a reversible effect of adding MWCNT where the viscosity was increased when added it to the solutions. The reason for the increasing viscosity when adding the dye to the polymeric solutions can be returned to the fact of the dye particles will increases the resistance of the solution molecules to flow, and cause converge of the spaces between the solution molecules which leads to an increase in the viscosity of solutions, this is good to have nanofibers without beads. [92,93]

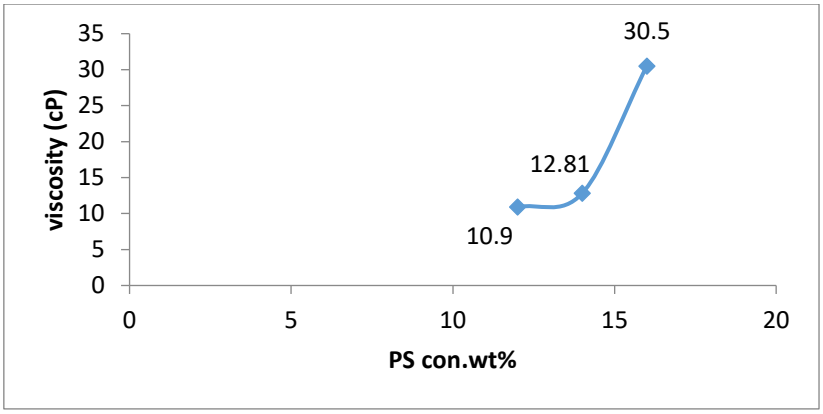

Figure (4.1) The relationship between the viscosity and concentration of polystyrene solution

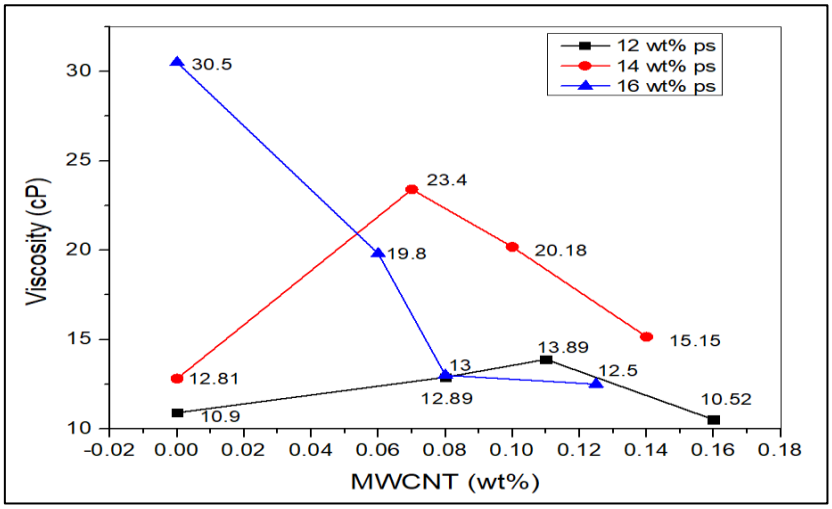

Figure (4.2) The relationship between the viscosity and MWCNT con.wt% under different concentrations of ps solution

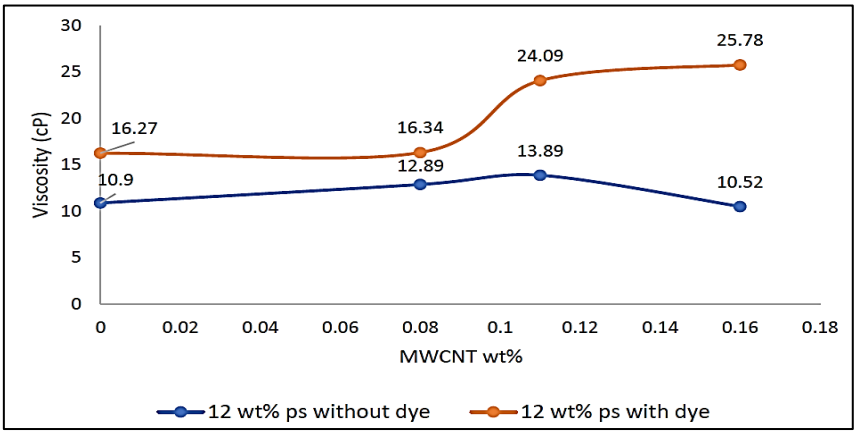

Figure (4.3) The relationship between the viscosity and MWCNT wt.% + (0.063 g) natural dye for 12wt% ps concentration

4.2 Textiles Characterization Results

4.2.1 FTIR Results

Figure (4.4) Shows the FTIR spectrum of (12wt.% PS nanofibers, PS/0.16 wt% MWCNT nanocomposites nanofibers, and 12wt% PS/0.16wt%MWCNT/ yellow natural dye), it can be observed that there is a strong peak at 1100 cm^{-1} compared to free PS nanofibers, this is referred to successful incorporation between PS and MWCNT. As well as, there are clear peaks at (1240) cm^{-1} due to the presence of O-H vibration which happened via incorporation of dye with PS/MWCNT nanocomposites. Also, we can observe that there are strong peaks between (2800 – 3600) cm^{-1} represents both aliphatic and aromatic C-H stretching bands. peaks also become strongly sharp due to the successful joining of carbon nanotubes, yellow dye, and polystyrene fibers. This is matches with [87] and [88].

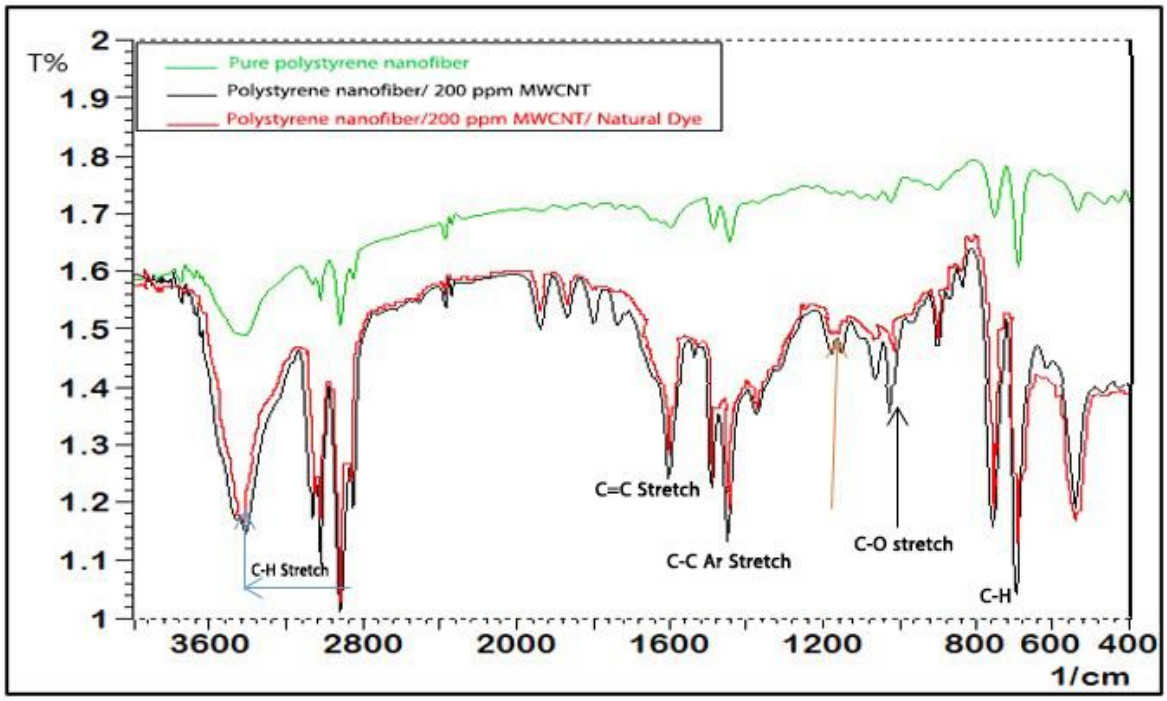

Figure (4.4) The results of FTIR analysis of polystyrene nanofibers and polystyrene reinforced with 0.16wt.% MWCNTs nano textile and with natural dye.

4.2.2 Wettability Results

It can be notice from the contact angle test for the pure polystyrene sample that when the polystyrene concentration increases, the material will be hydrophilic. The value of contact angle dropped from (°134.22 for 12wt.% to °63.50 for 16 wt.% pure polystyrene concentration), this is related to the average surface roughness of the prepared samples as shown from the AFM test result we notice for the pure samples of the three percentages (12wt%, 14wt.%, 16wt.% pure polystyrene nanofiber) the average roughness increase with increasing the polystyrene concentration also it can be notice from the FESEM test results that the gaps between the fibers decrease in the smaller concentration than that of high concentration these gaps can also affect the hydrophilicity and hydrophobicity of the prepared fibers so that when the gaps is small the sample tend to be hydrophobic and restrict the penetration of water droplet to pass through them and if the gaps are larger the water droplet can found spaces to enter over there leading to hydrophilic sample.

It is also possible to return the reason to large diameter of the fibers resulting from increasing concentration, which reduces the contact angle due to the decrease in the compaction between the fibers of the textile, which allows the water droplets to expand more and the surface acquires a hydrophilic character.

The addition effect of MWCNTs on the contact angle shows at polymer concentration (12, 14 wt.%) increase the MWCNTs addition led to decreases the contact angle in concentrations (0.08, 0.11 wt.%), (0.07, 0.1 wt.%) respectively, and it will raising from the contact angle at concentration. and for polymer concentration (16wt.%) the addition of MWCNTs causes the contact angle to increase leading to hydrophobic samples. These results are shown in the figures (4.5, 4.6, 4.7).

For the group of natural dye the prepared samples are hydrophobic as clear from contact angle values from(˚99.65) for pure polystyrene nanofiber with natural dye to (˚127.77) for PSNF/natural dye/ 0.11 wt.% MWCNT and the contact angle start decreased by (˚106.67) for PSNF/0.16wt.% MWCNT / natural dye but still hydrophobic due to its value lower than ˚90 this is indicate that these samples possess the ability to withstand the moisture when they exposure to it in outside applications as shown in the figure (4.8).

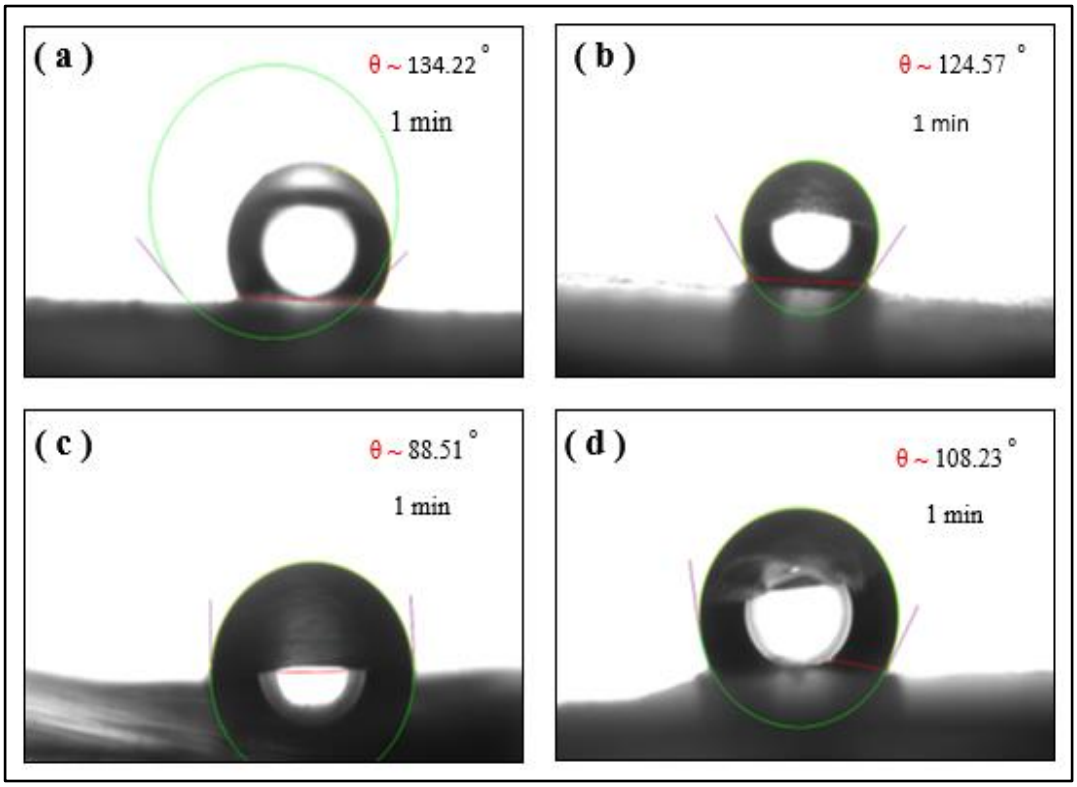

Figure (4.5) Contact angle results for four samples (12wt.% PSNF) in which (a) Pure PSNF (b) PSNF/0.08wt.%. MWCNT (c) PSNF/0.11wt.% MWCNT (d) PSNF/0.16wt.% MWCNT

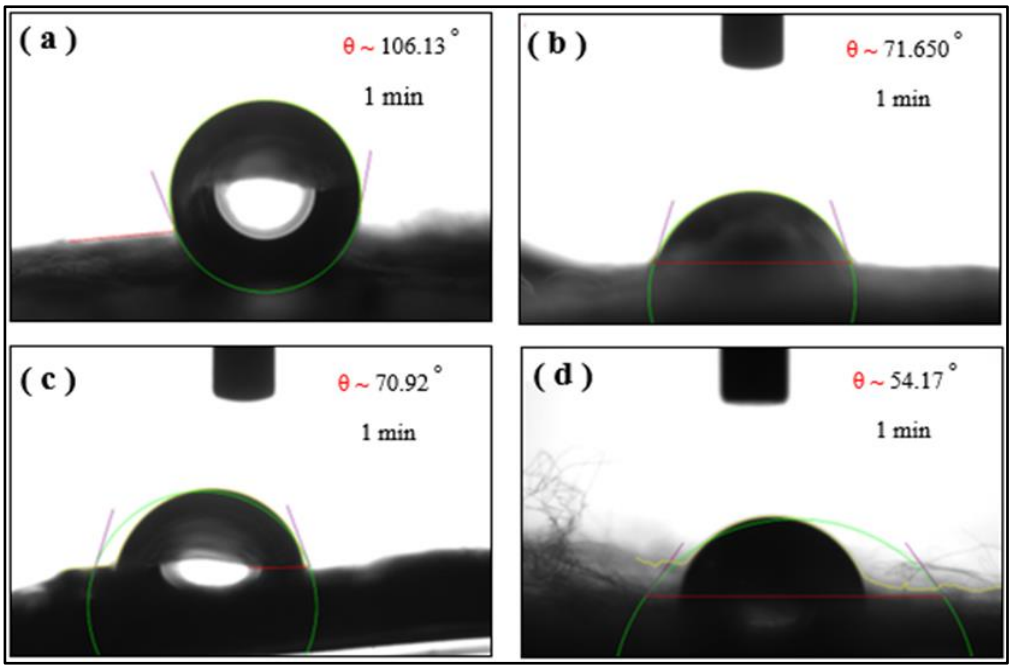

Figure (4.6) Contact angle results for four samples (14 wt.% PSNF) in which (a) Pure PSNF (b) PSNF/0.07wt.% MWCNT (c) PSNF/0.1wt.% MWCNT (d) PSNF/0.14wt.% MWCNT

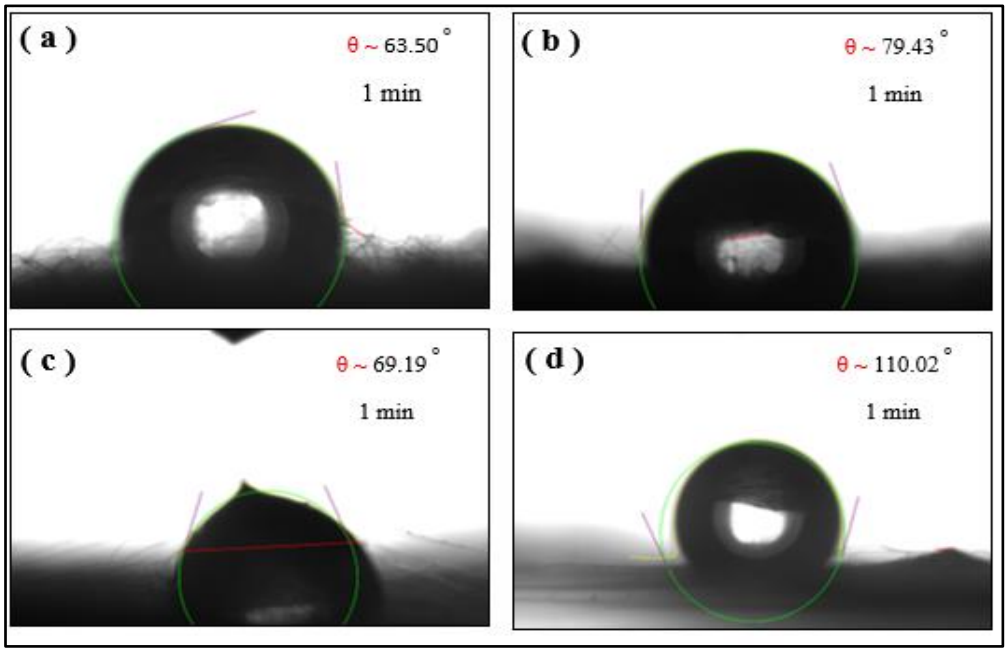

Figure (4.7) Contact angle results for four samples (16 wt.% PSNF) in which (a) Pure PSNF (b) PSNF/0.06wt.% MWCNT (c) PSNF/0.08wt.% MWCNT (d) PSNF/0.125wt.% MWCNT

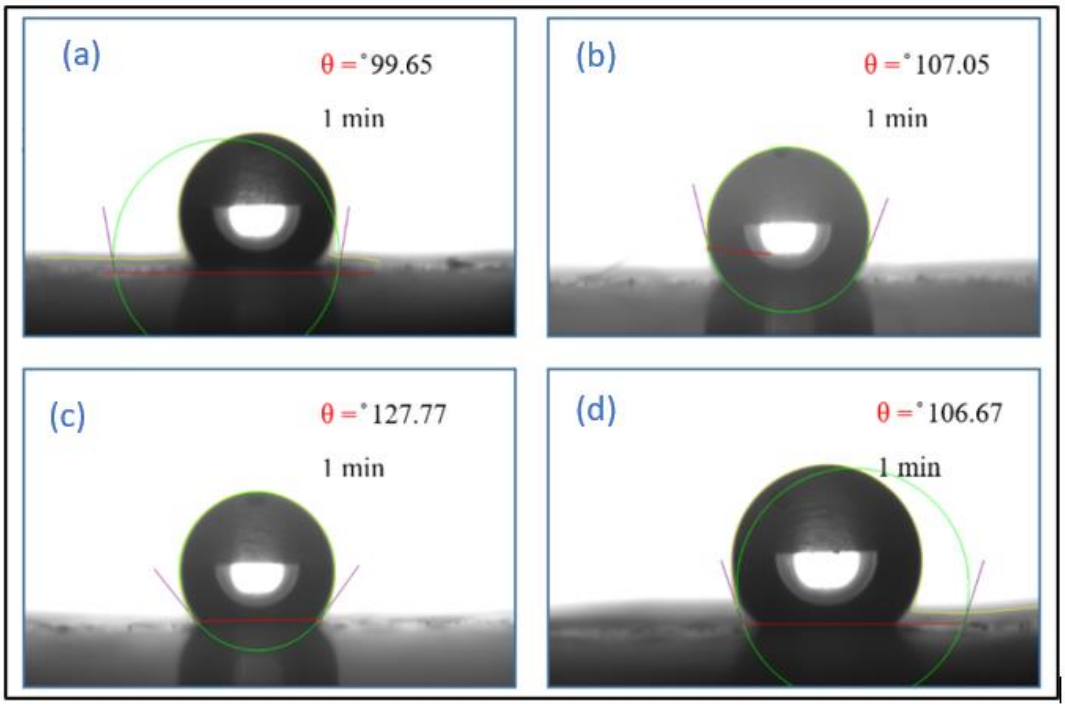

Figure (4.8) Contact angle results for four samples (12wt.% PSNF) +Dye) in which (a) Pure PSNF/Dye (b) PSNF/0.08wt.% MWCNT/Dye (c) PSNF/0.11wt.% MWCNT/Dye (d) PSNF/0.16wt.% MWCNT. /Dye

4.2.3 AFM Results

Atomic force microscopy results proved that for polymer concentration of (12 wt.% PS) The roughness average was (1.44 nm) for PSNF pure and decreased to (1.17nm) for (PSNF/0.08wt.% MWCNTs) and increased to (1.25 nm) for (PSNF/0.11wt.% MWCNT) and to (1.43 nm) of (0.16wt.% MWCNTs), the addition of MWCNT causes the average roughness to fall for the low percentages of it, and for higher percentage it leads the roughness average to grow gradually. The surface bearing index was improved from (0.47) to (1.44) this gives an indication of improvement in mechanical properties of the prepared nanofiber textiles. These results are depicted in the figure (4.9) and also in the table (4.3).

For group of (14 wt.% PS) group the roughness average was increased from 2.74 nm for the pure PSNF to 5.76 nm for (PSNF/0.14wt.% MWCNT) as the MWCNT concentration increased also the surface bearing index was

improved with MWCNT addition because the smoothness reduced for the prepared films as demonstrating in figure (4.10) also in Table (4.4).

As explained in chapter two the effect of polymeric concentration on the fiber diameter is that when increasing it will increase the fiber diameter and this will cause the surface roughness to decrease at higher polymer concentration from that of lower concentration groups

For the group (16 wt.% PS) the average roughness decreased and the surface tends to be smoother and the amount of the MWCNT has increased the roughness average slightly in MWCNT ratio (0.125wt.%) from the pure sample as shown in the figure (4.11)

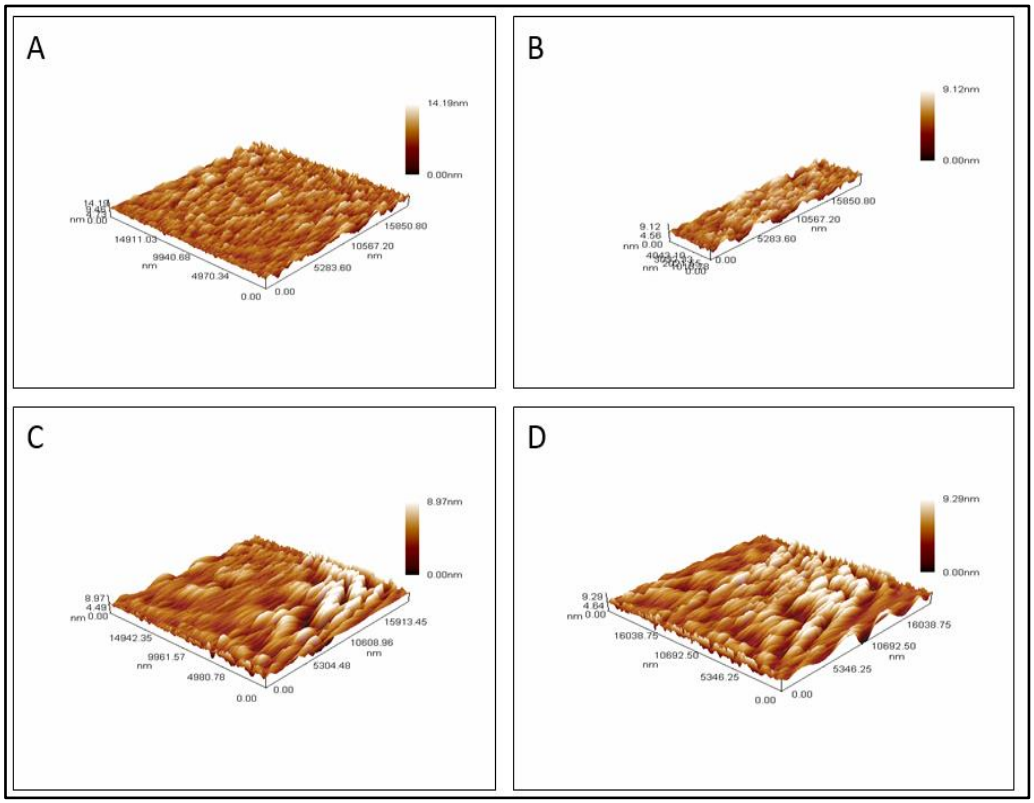

Figure (4.9) Atomic force microscopy test 2D and 3D images for (12wt.% PS) concentration where (a) Pure PSNF (b) PSNF/0.08wt.%. MWCNT (c) PSNF/0.11wt.% MWCNT (d) PSNF/0.16wt.% MWCNT

Table (4.3) Surface roughness analysis for (12 wt.% PS)

Sample	Roughness average (sa) nm	Roughness mean square (sq) nm	Surface area ratio (sdr)	Surface Bearing index (sbi)
Pure polystyrene	1.44	1.85	0.0428	0.475
PS/0.08 wt.% MWCNT	1.17	1.47	0.031	0.837
PS/0.11 wt.% MWCNT	1.25	1.71	0.0145	1.07
PS/0.16 wt.% MWCNT	1.43	1.86	0.022	1.44

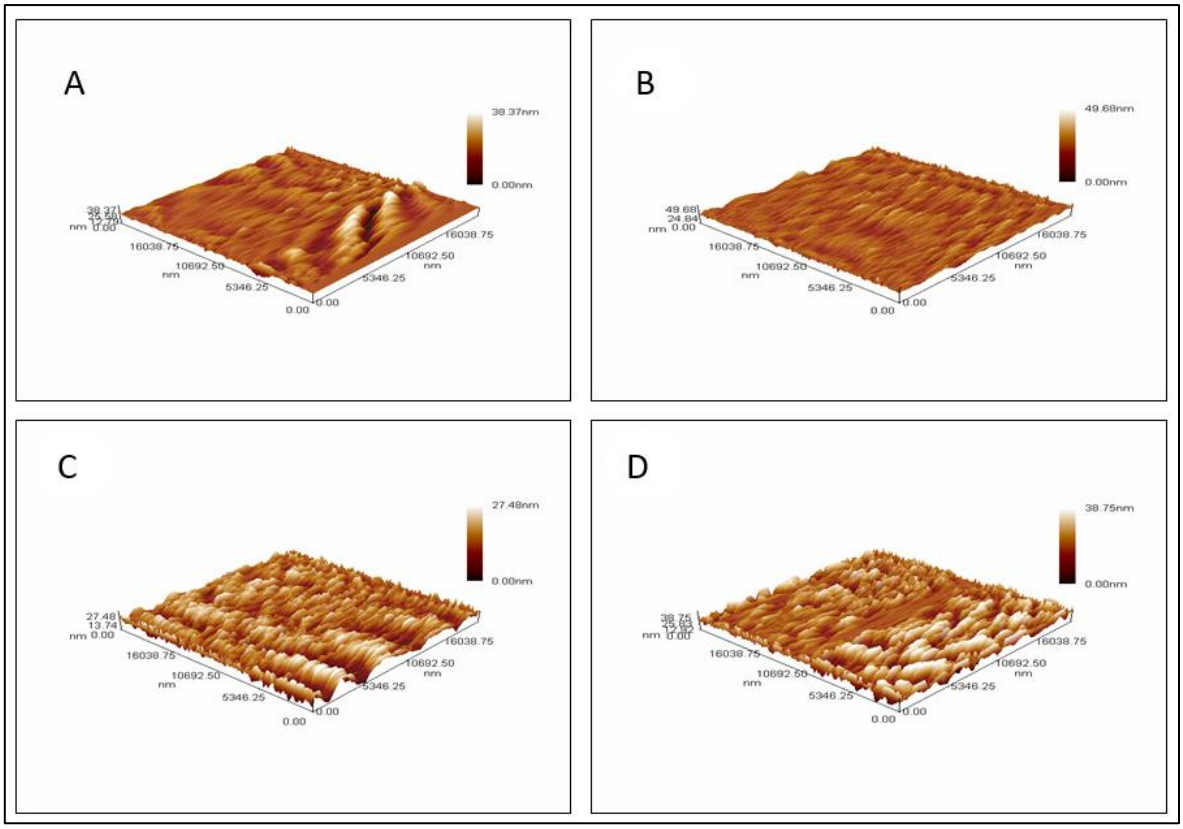

Figure (4.10) Atomic force microscopy test 2D and 3D images for (14wt.% PS) concentration where (a) Pure PSNF (b) PSNF/0.07wt.% MWCNT (c) PSNF/0.1wt.% MWCNT (d) PSNF/0.14wt.% MWCNT

Table (4.4) Surface roughness analysis for (14 wt.% PS)

Sample	Roughness average (sa) nm	Roughness mean square (sq) nm	Surface area ratio (sdr)	Surface Bearing index (sbi)
Pure polystyrene	2.74	2.74	0.0481	0.361
PS/0.07 wt.% MWCNT	2.68	3.47	0.123	0.232
PS/0.1 wt.% MWCNT	3.92	4.93	0.196	0.901
PS/0.14 wt.% MWCNT	5.76	7.55	0.475	1.2

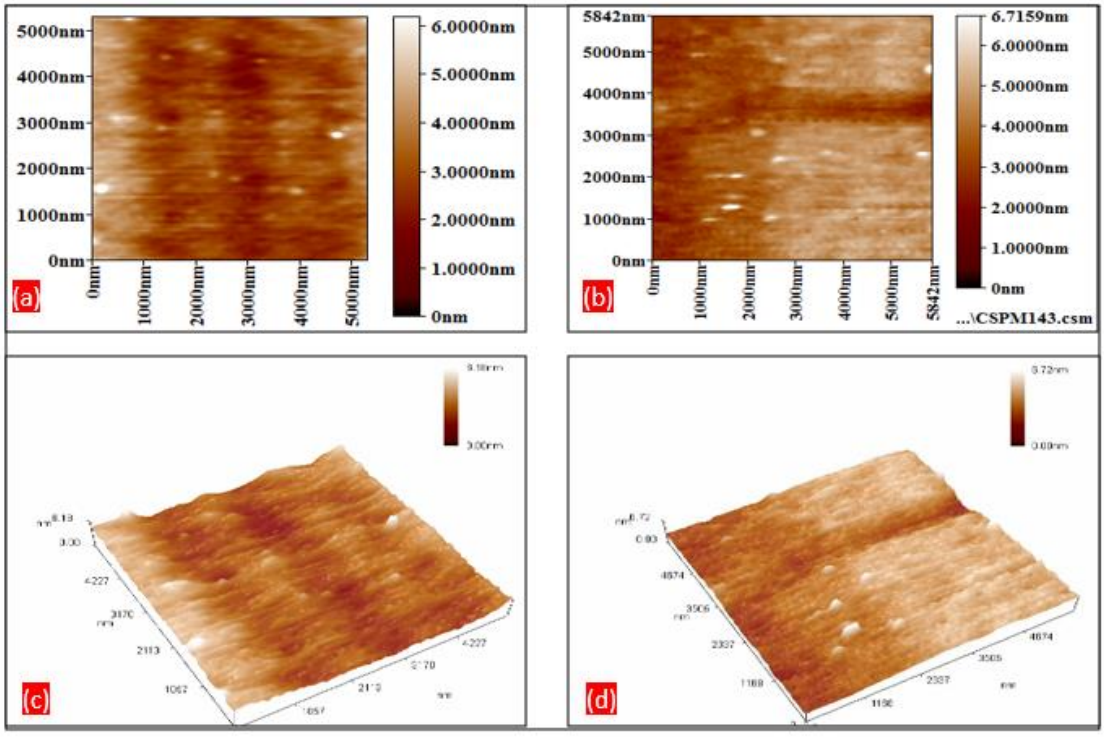

Figure (4.11) Atomic force microscopy test 2D and 3D images for (16wt.% PS) concentration where (a) pure PSNF (b) PSNF/0.125wt.% MWCNT, (c), (d) are the 3d image for pure PSNF and PSNF/0.125wt.% MWCNT respectively

4.2.4 FESEM Results

For group of (12 wt.%) we notice that the average fibers diameter reduced because of small concentration of polystyrene but this leads to beads formation because of the molecule of the solvents will be higher than polystyrene molecules so that they will exhibit a dipole moment and this leads to increase the ionic charges leading to increase the electrical conductivity of the solutions and this will give a smoother fibers with some beads due to higher solvent molecules and remaining solvents not evaporated easily due to its higher boiling point ~158℃ this is discussed by [86]. As shown in the figures (4.12, 4.16, 4.20)

The results from (14 wt.% PS) group show the increasing MWCNT concentration leads to reduce the average nanofiber diameter, this is because the addition of MWCNT leads to increase the conductivity of solution media which leads to reduce the nanofibers diameter, the raise in the electrical conductivity via MWCNT addition leads to increase the charge carrier capacity of the polymer solution. As well as, the addition of MWCNT leads to decrease the viscosity of solution media which leads to decrease of nanofibers diameters too, this is agreed with (Baumgarten equation) [73].

On the other hand, the addition of MWCNT to polymer solution affects the fiber alignments and made improve in the surface roughness of the fibers. this is also proved via atomic force and EDX test as shown in the figures (4.13, 4.17, 4.21).

We also notice from FESEM results of (16wt.% PS) group that the samples have small beads, this is because the ratio of polymer concentration is too high and will reduce the effect of MWCNT on the electrical conductivity so that it reduced charge carrier capacity of polymer solution leading to increasing fiber diameters as shown in the figures (4.14, 4.18, 4.22).

It can also be notice that the group of (12 wt.% PS/ (0.063 g natural dye) the addition of natural dye leads to increase the electrical conductivity too, due to present more free ions to increase the value of electrical conductivity up to (36 S/cm) this make the fibers smoother and fewer beads from addition MWCNT alone the average fibers diameter values were (0.746 µm) for pure polystyrene nanofiber with (0.063g) natural dye and (0.420 µm) for PSNF/0.16 wt.% MWCNT/0.063g natural dye. The FESEM and average fibers diameter are shown in the figures (4.15, 4.23) respectively. Also, the elements present in the nano textiles samples are shown in figure (4.19). Adding of dye to the prepared solutions leads to enhance the stability of electrospinning process via enhancement of viscosity and surface tension as well as conductivity of solutions, and this leads to fewer beads nanofibers formed in contrast to solutions free dye as in figure (4.12). The averages fiber diameter values of all prepared samples are mentioned in table (4.5).

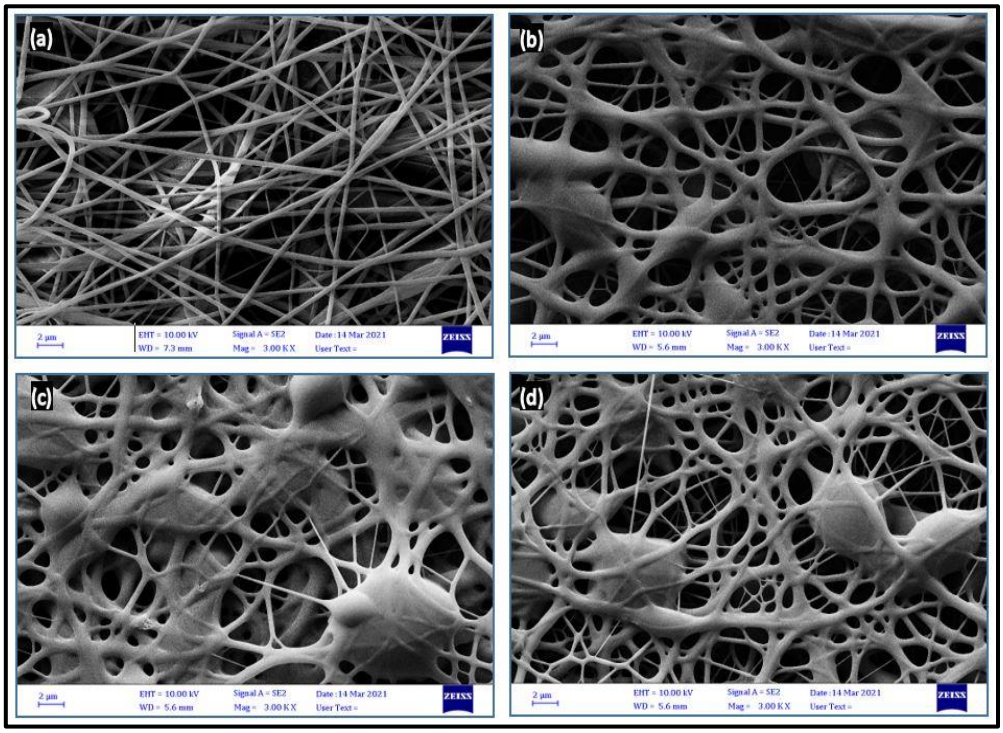

Figure (4.12) FESEM images for (12 wt.% PS) where(a) Pure PSNF (b) PSNF/0.08wt.% MWCNT (c) PSNF/0.11wt.% MWCNT (d) PSNF/0.16wt.% MWCNT

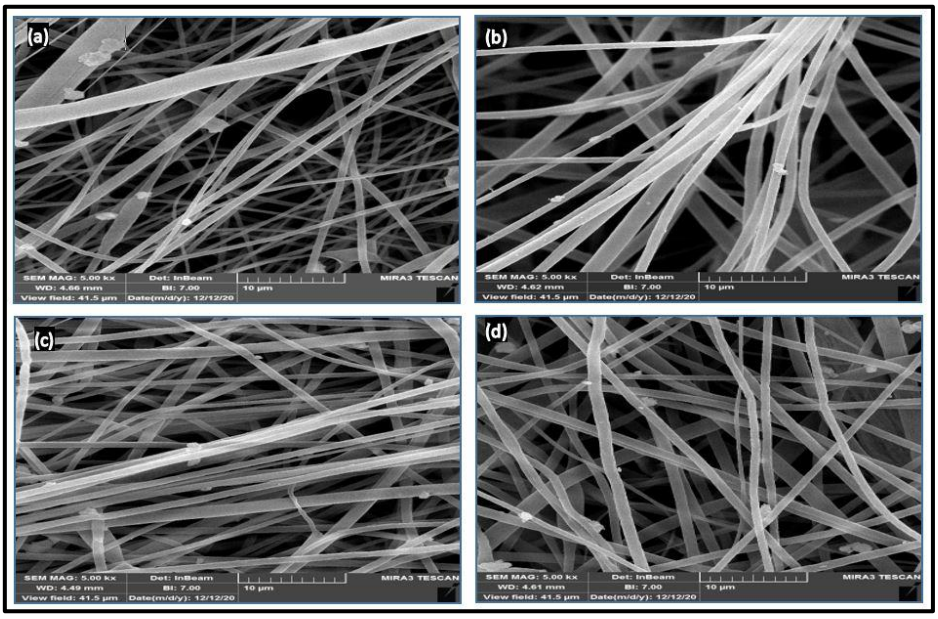

Figure (4.13) FESEM images for (14 wt.% Ps) where (a) Pure PSNF (b) PSNF/0.07wt.% MWCNT (c) PSNF/0.1wt.% MWCNT (d) PSNF/0.14wt.% MWCNT

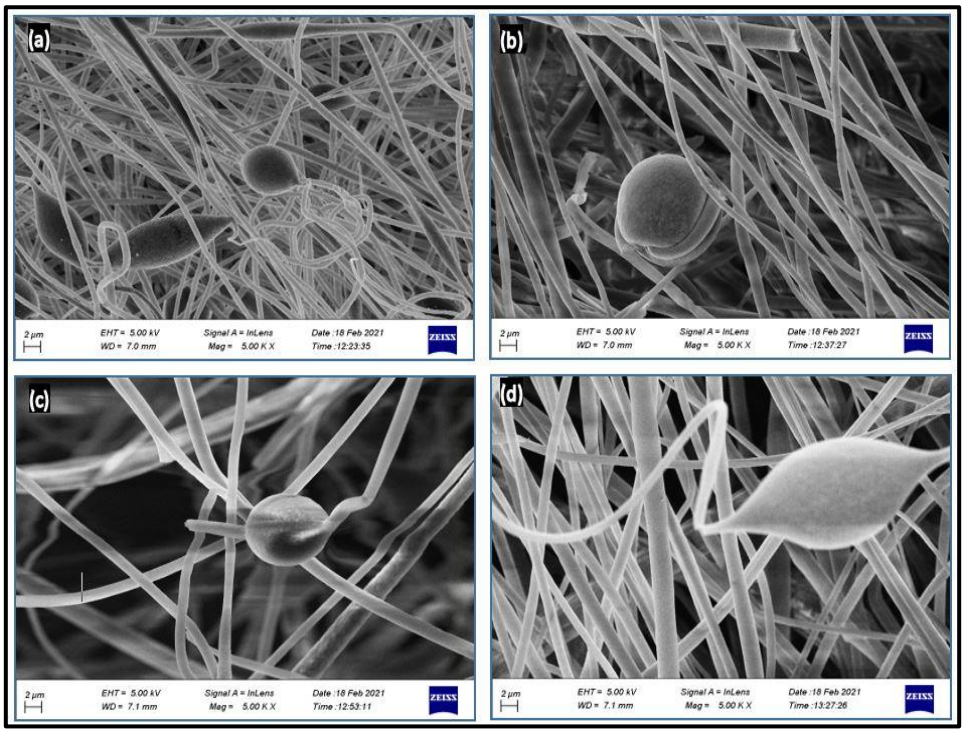

Figure (4.14) FESEM images for (16 wt.% Ps) where a) Pure PSNF (b) PSNF/0.06wt.% MWCNT (c) PSNF/0.08wt.% MWCNT (d) PSNF/0.125wt.% MWCNT

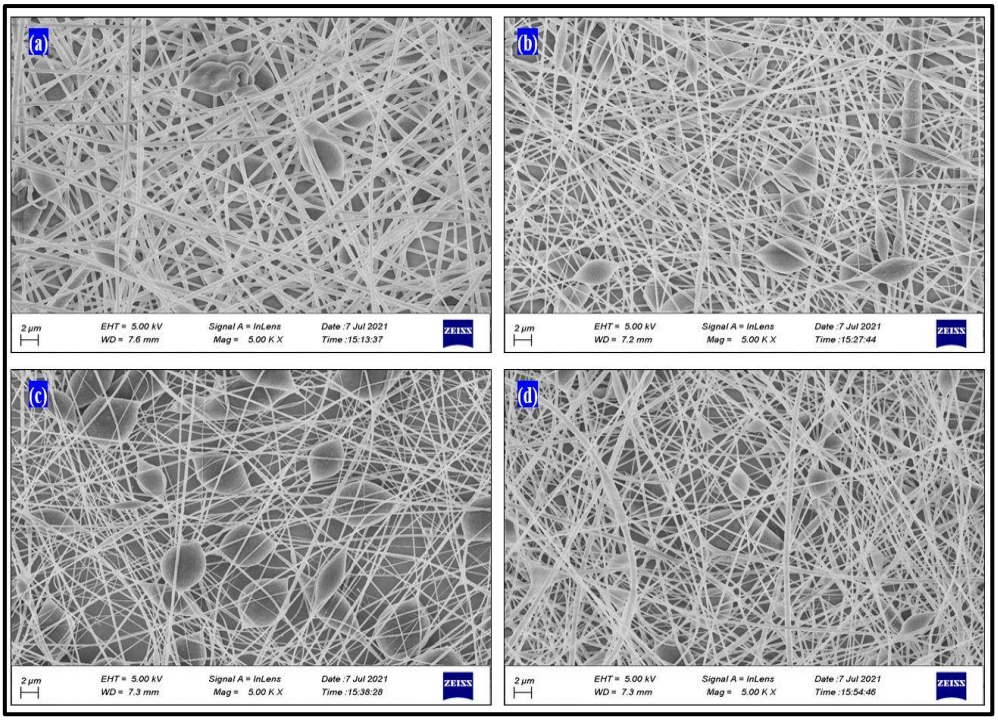

Figure (4.15) FESEM images for (12 wt.% PSNF/ 0.063 g dye) where (a) Pure PSNF/Dye (b) PSNF/0.08wt.% MWCNT/Dye (c) PSNF/0.11wt.% MWCNT/Dye (d) PSNF/0.16wt.% MWCNT. /Dye

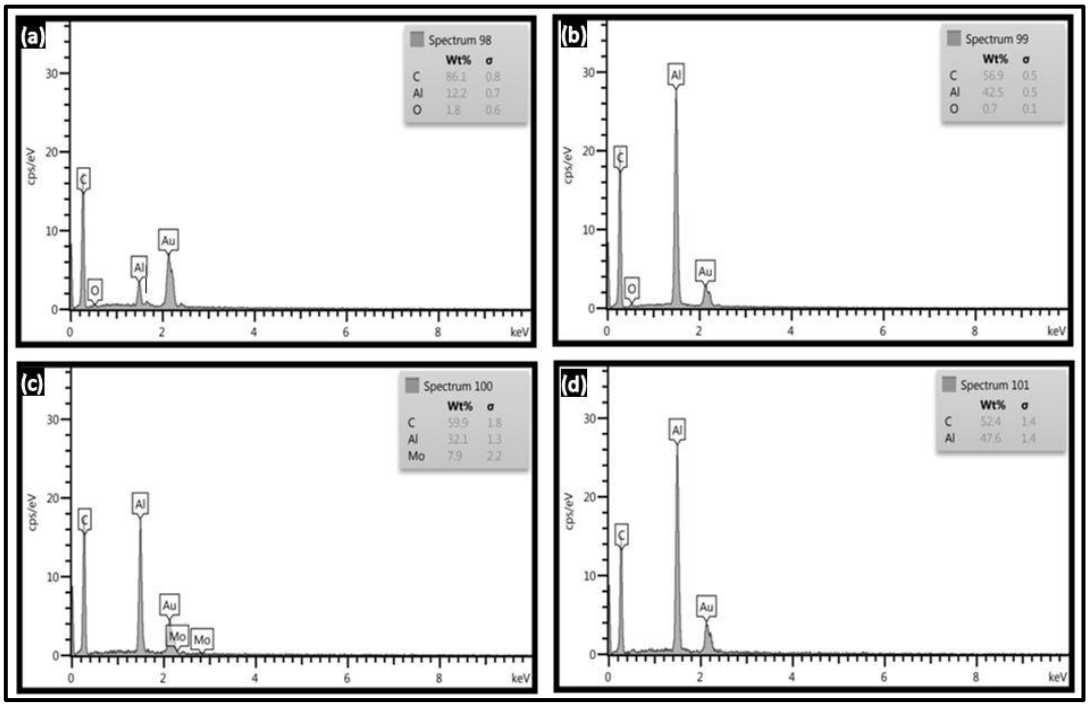

Figure (4.16) EDX results for (12 wt.% PS) where(a) Pure PSNF (b) PSNF/0.08wt.% MWCNT (c) PSNF/0.11wt.% MWCNT (d) PSNF/0.16wt.% MWCNT

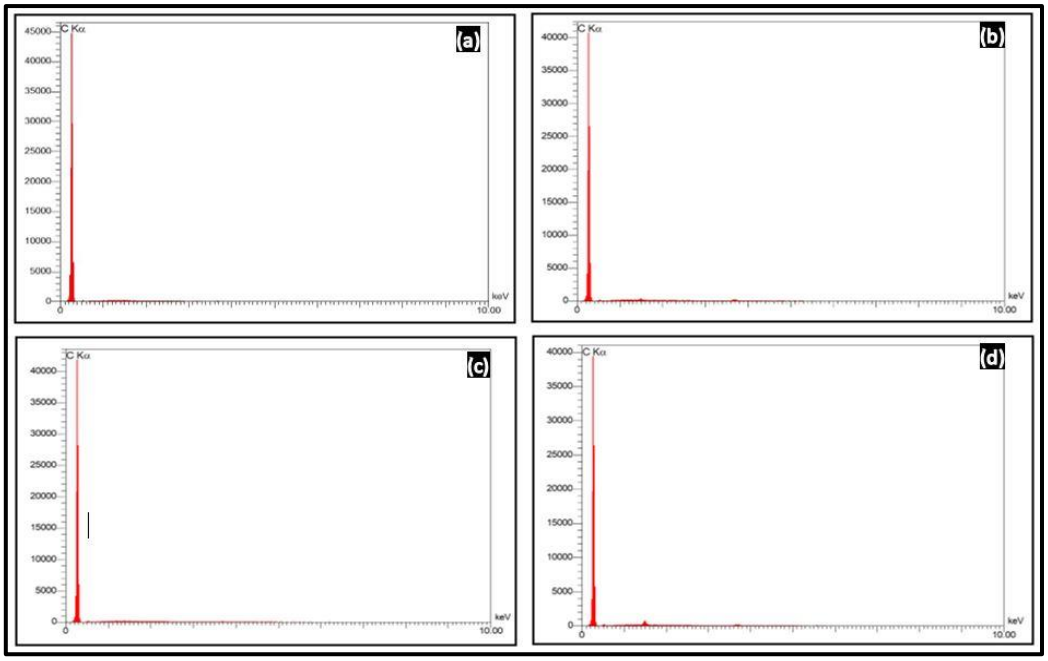

Figure (4.17) EDX results for (14 wt.% PS) where (a) Pure PSNF (b) PSNF/0.07wt.% MWCNT (c) PSNF/0.1wt.% MWCNT (d) PSNF/0.14wt.% MWCNT

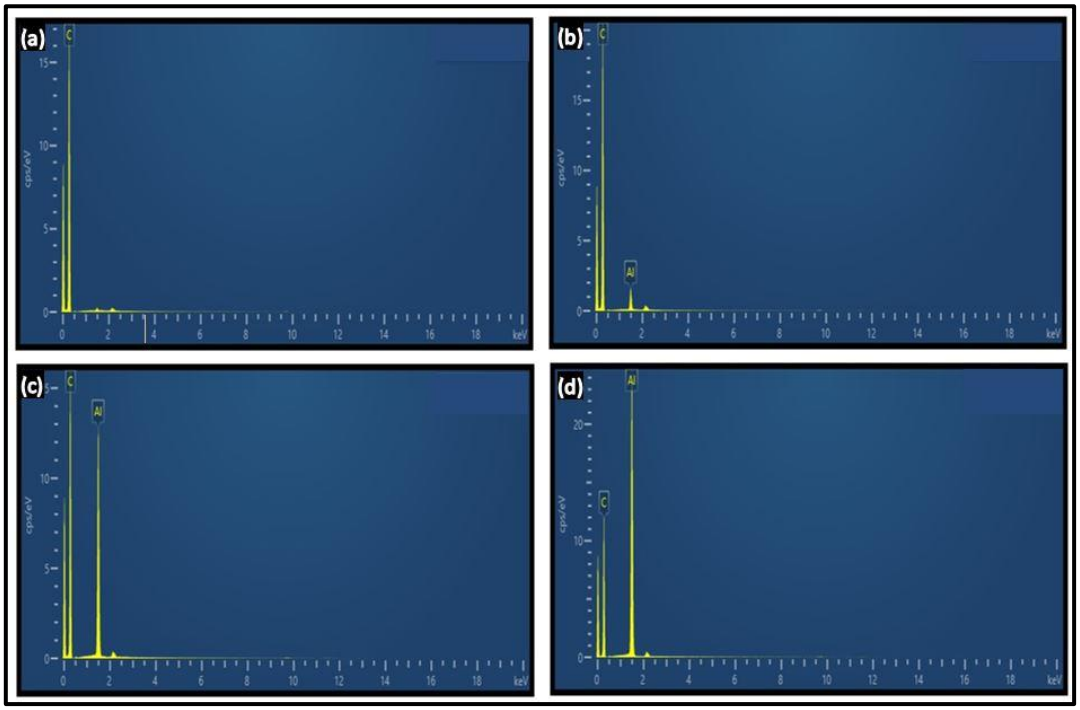

Figure (4.18) EDX results for (16 wt.% Ps) where a) Pure PSNF (b) PSNF/0.06wt.% MWCNT (c) PSNF/0.08wt.% MWCNT (d) PSNF/0.125wt.% MWCNT

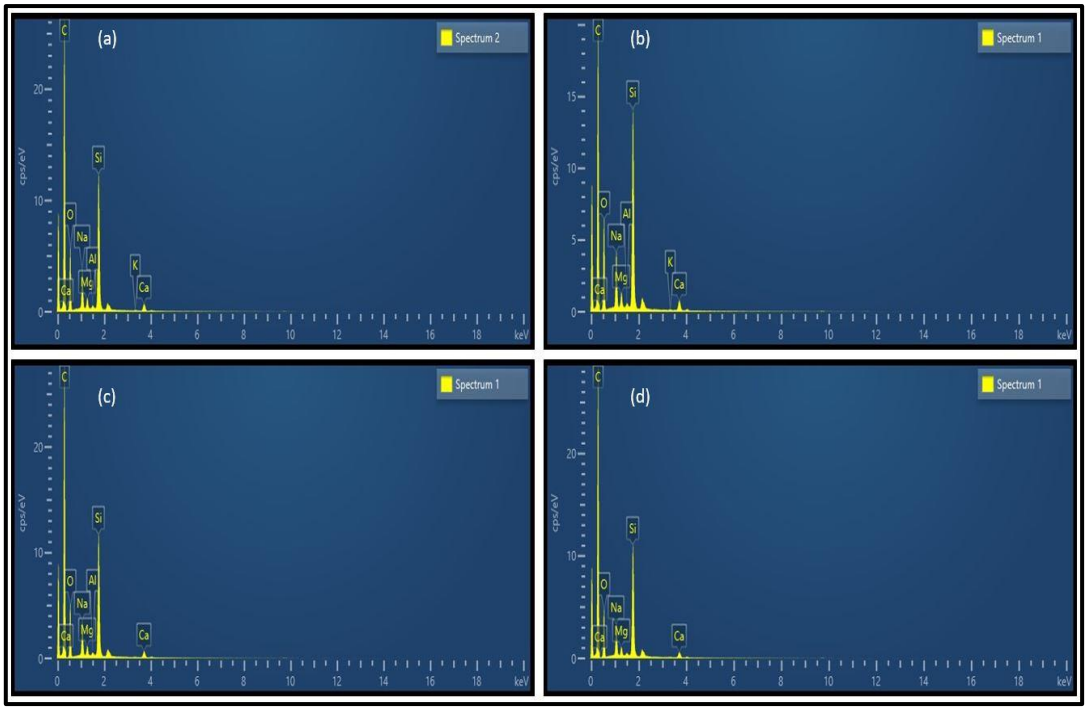

Figure (4.19) EDX images for (12 wt.% PSNF/ 0.063 g dye) where (a) Pure PSNF/Dye (b) PSNF/0.08wt.% MWCNT/Dye (c) PSNF/0.11wt.% MWCNT/Dye (d) PSNF/0.16wt.% MWCNT /Dye

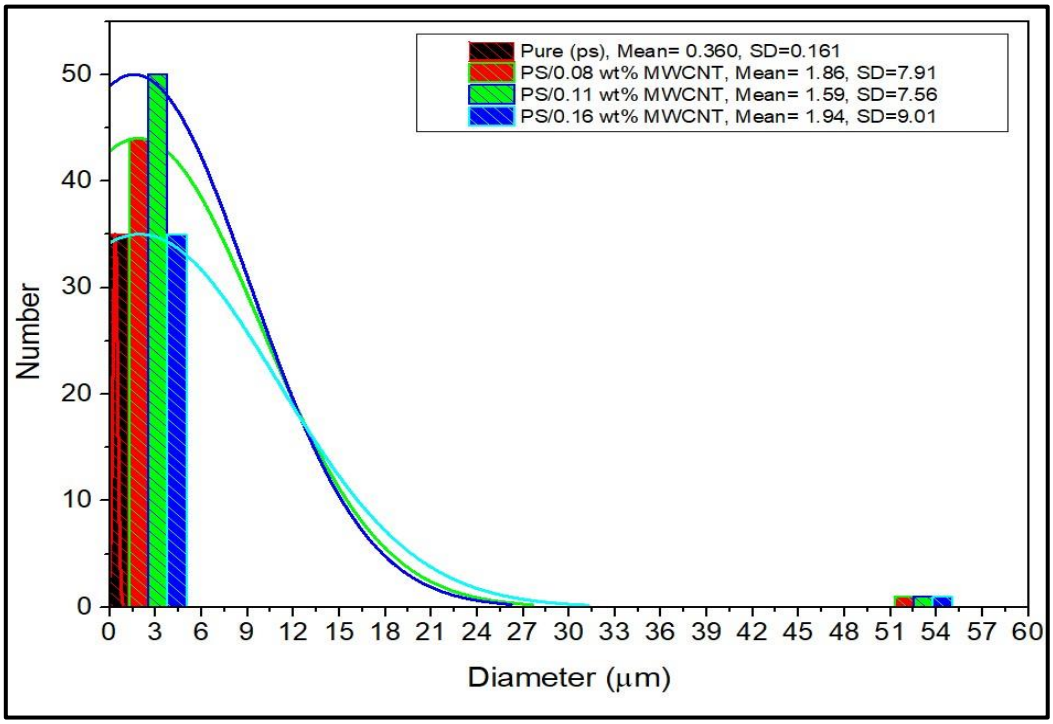

Figure (4.20) Average fibers diameter for four samples with (12 wt.% PSNF)

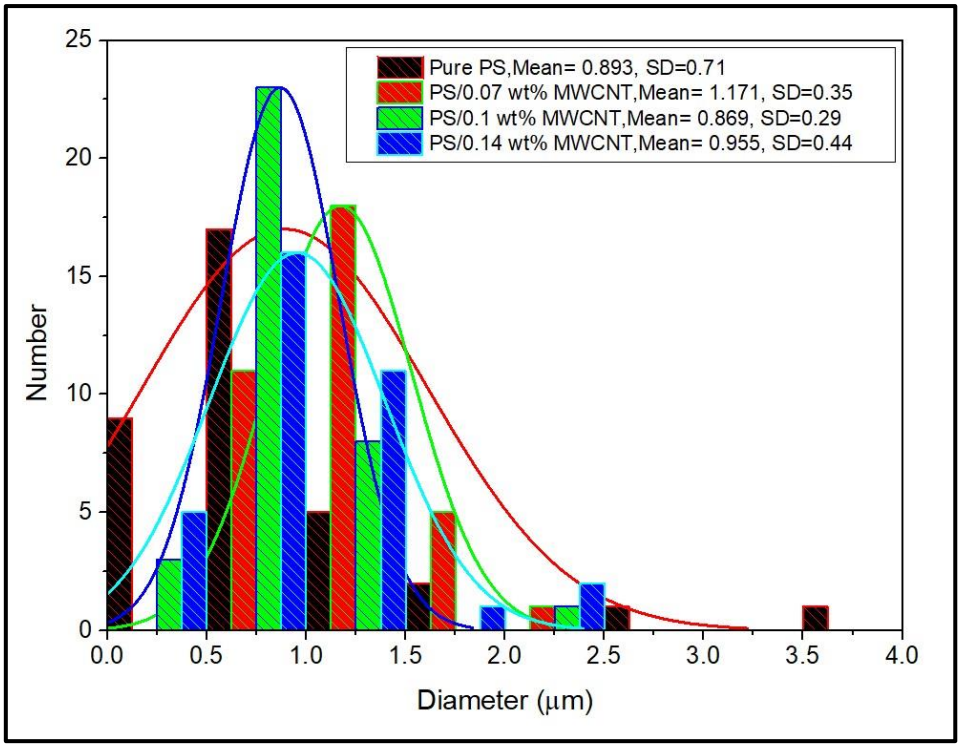

Figure (4.21) Average fibers diameter for four samples with (14 wt.% PSNF)

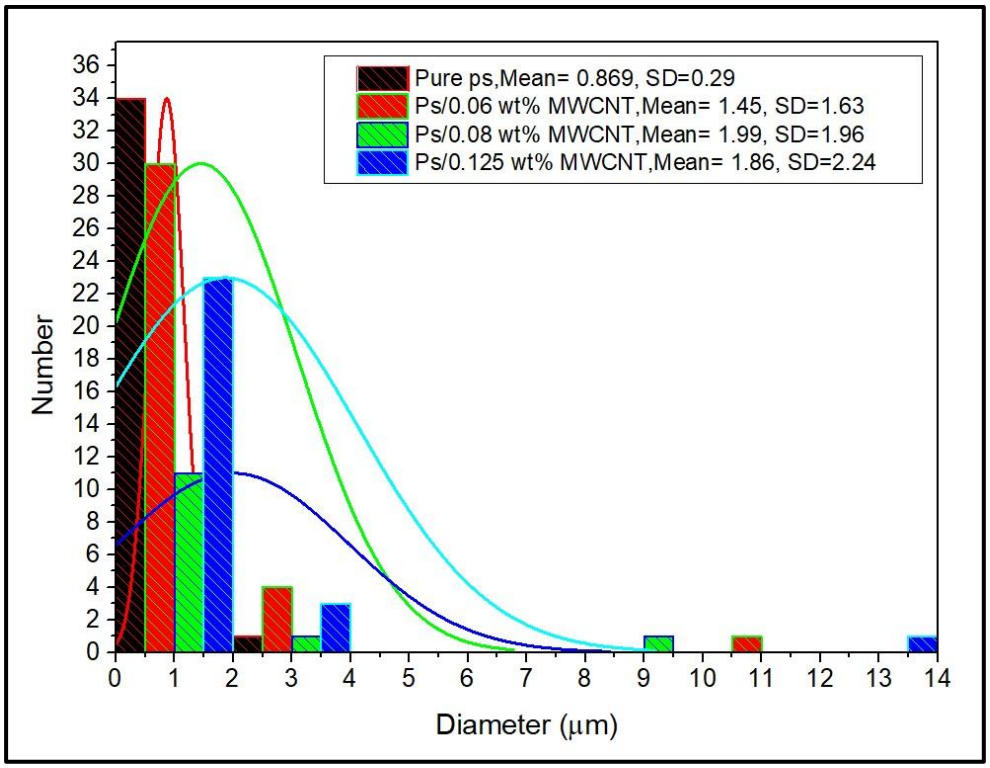

Figure (4.22) Average fibers diameter for four samples with (16 wt.% PSNF)

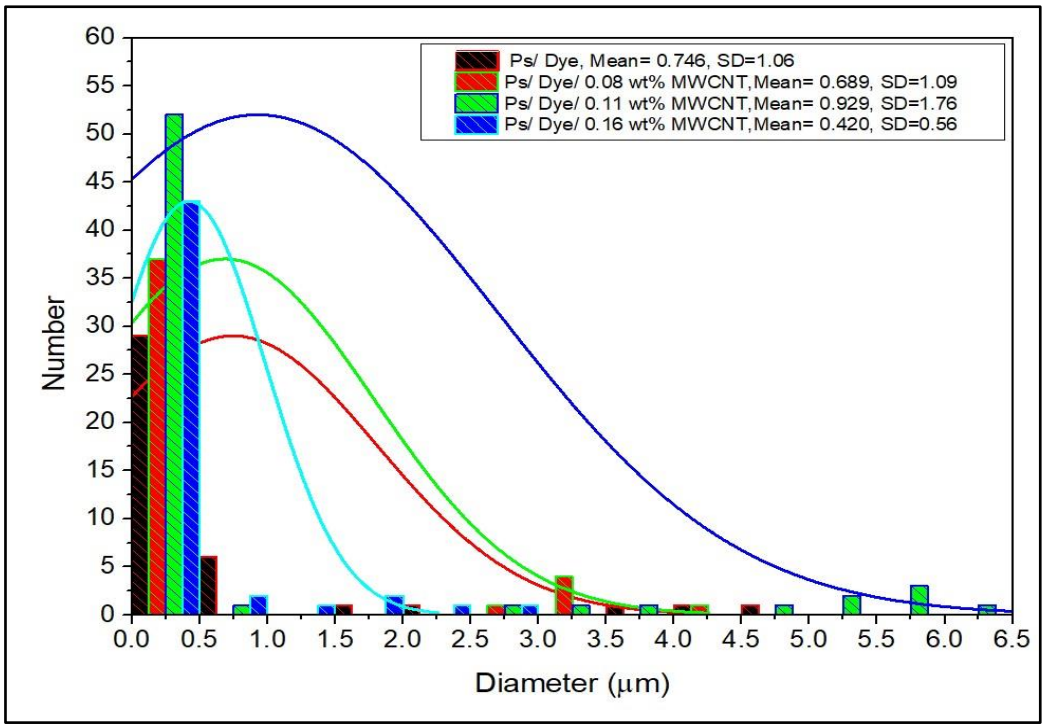

Figure (4.23) Average fibers diameter for four samples with (12 wt.% PSNF/0.063g natural dye)

Table (4.5) Average fibers diameters of four groups

(12wt.%PSNF)		
Sample	**Average fiber diameter (μm)**	**Morphology of nanofibers**
Pure PSNF	0.360	No beads
PSNF/0.08wt.% MWCNT	1.86	Beads
PSNF/0.11wt.% MWCNT	1.59	Beads
PSNF/0.16wt.% MWCNT	1.94	Beads
(14wt.%PSNF)		
Sample	**Average fiber diameter (μm)**	**Morphology of nanofibers**
Pure PSNF	0.893	No beads
PSNF/0.07wt.% MWCNT	1.17	No beads
PSNF/0.1wt.% MWCNT	0.869	No beads
PSNF/0.14wt.% MWCNT	0.955	No beads
(16wt.%PSNF)		
Sample	**Average fiber diameter (μm)**	**Morphology of nanofibers**
Pure PSNF	0.869	Little beads
PSNF/0.06wt.% MWCNT	1.45	Little beads
PSNF/0.08wt.% MWCNT	1.99	Little beads
PSNF/0.125wt.% MWCNT	1.86	Little beads
(12 wt.% PSNF, 0.063g natural Dye)		
Sample	**Average fiber diameter (μm)**	**Morphology of nanofibers**
Pure PSNF	0.746	Little beads
PSNF/0.08wt.% MWCNT	0.689	Little beads
PSNF/0.11wt.% MWCNT	0.929	Beads
PSNF/0.16wt.% MWCNT	0.420	Little beads

4.2.5 Directionality Calculations

Orientation of the fibers was measured by using the Fiji Software to the FESEM images the directionality values extracted in a gaussian method where for (12 wt.%) (°22, °-2.68, °-18.21, °31.91) for pure polystyrene nanofiber, PSNF/0.08wt.%. MWCNT, PSNF/0.11wt.%MWCNT, PSNF/0.16wt.% MWCNT) respectively as shown in the figure (4.24). And for the group of (14 wt.%) the results where (°49.63, °5.36, °20.04, °-15329.15) for, PSNF/0.07wt.%. MWCNT, PSNF/0.1wt.% MWCNT, PSNF/0.14wt.% MWCNT) respectively. as shown in figure (4.25). And for polymer concentration group of (16 wt.%) the results where (° -50.47, ° -52.53, ° 86.71, ° -75.67) for, PSNF/0.06wt.%. MWCNT, PSNF/0.08wt.%MWCNT, PSNF/0.125wt.% MWCNT) respectively. as shown in figure (4.26). From these results, we notice the group of (14 w.%) has the best orientation followed by group (12wt.%) which has good orientation and group of (16 wt.%) has the lowest orientation. This was confirmed through FESEM test results. When we added natural dye by (0.063 g) to the first group of (12 wt.% PSNF) the angles were (°31.83, °-33.72, °32.87, °-67.94) for PSNF/0.08wt.%. MWCNT, PSNF/0.11wt.% MWCNT, PSNF/0.16wt.% MWCNT) respectively. This means that the natural dye has caused to reduce the directionality of the (12 wt.%) group as shown in the figure (4.27).

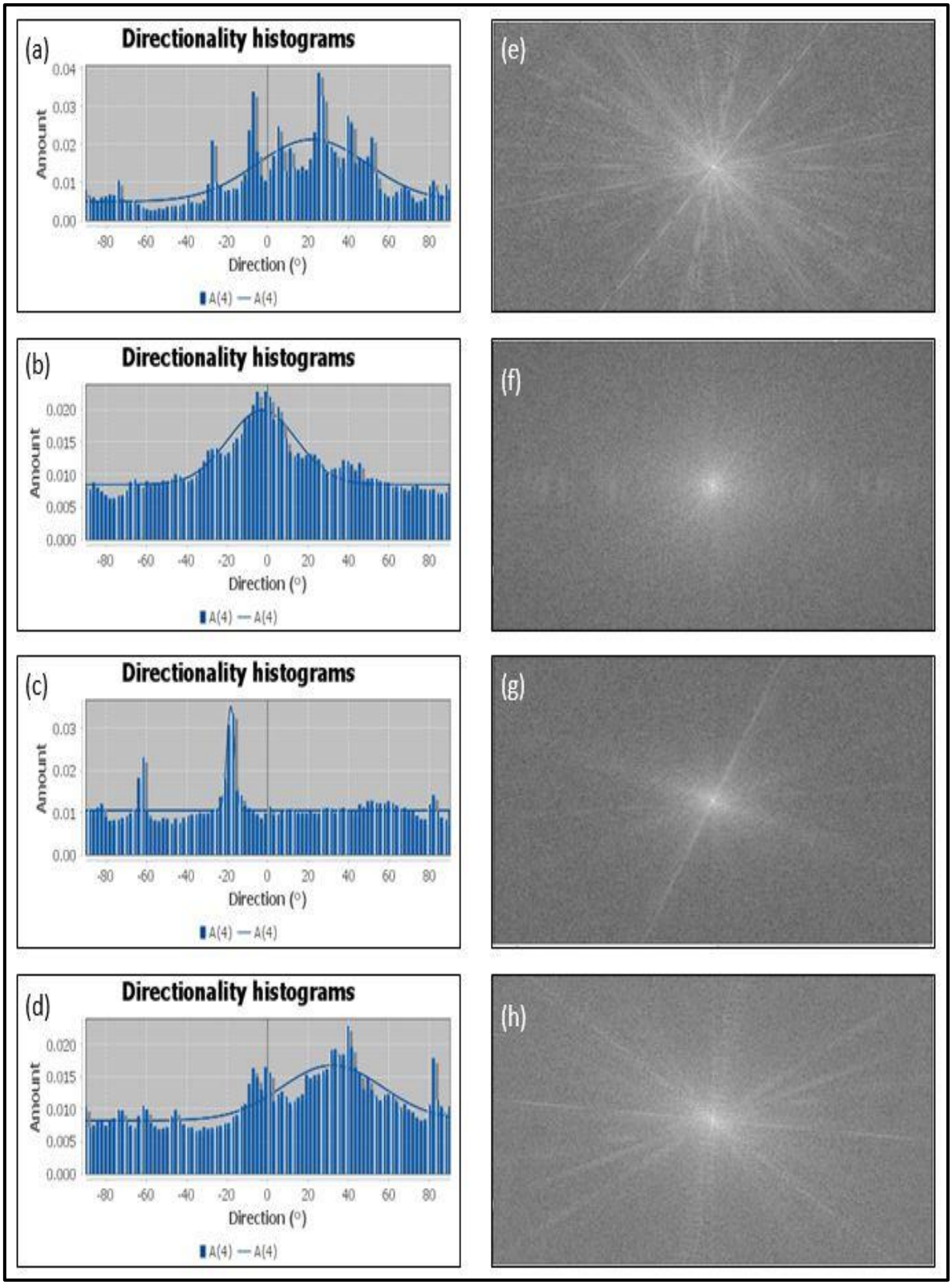

Figure (4.24) Directionality results for (12 wt.%) Polystyrene group where (a-d) are (pure PS, PS/0.08wt.%. MWCNT, PS/0.11wt.% MWCNT, PS/0.16wt.% MWCNT) respectively and their 2D-FFT from (e-h) respectively

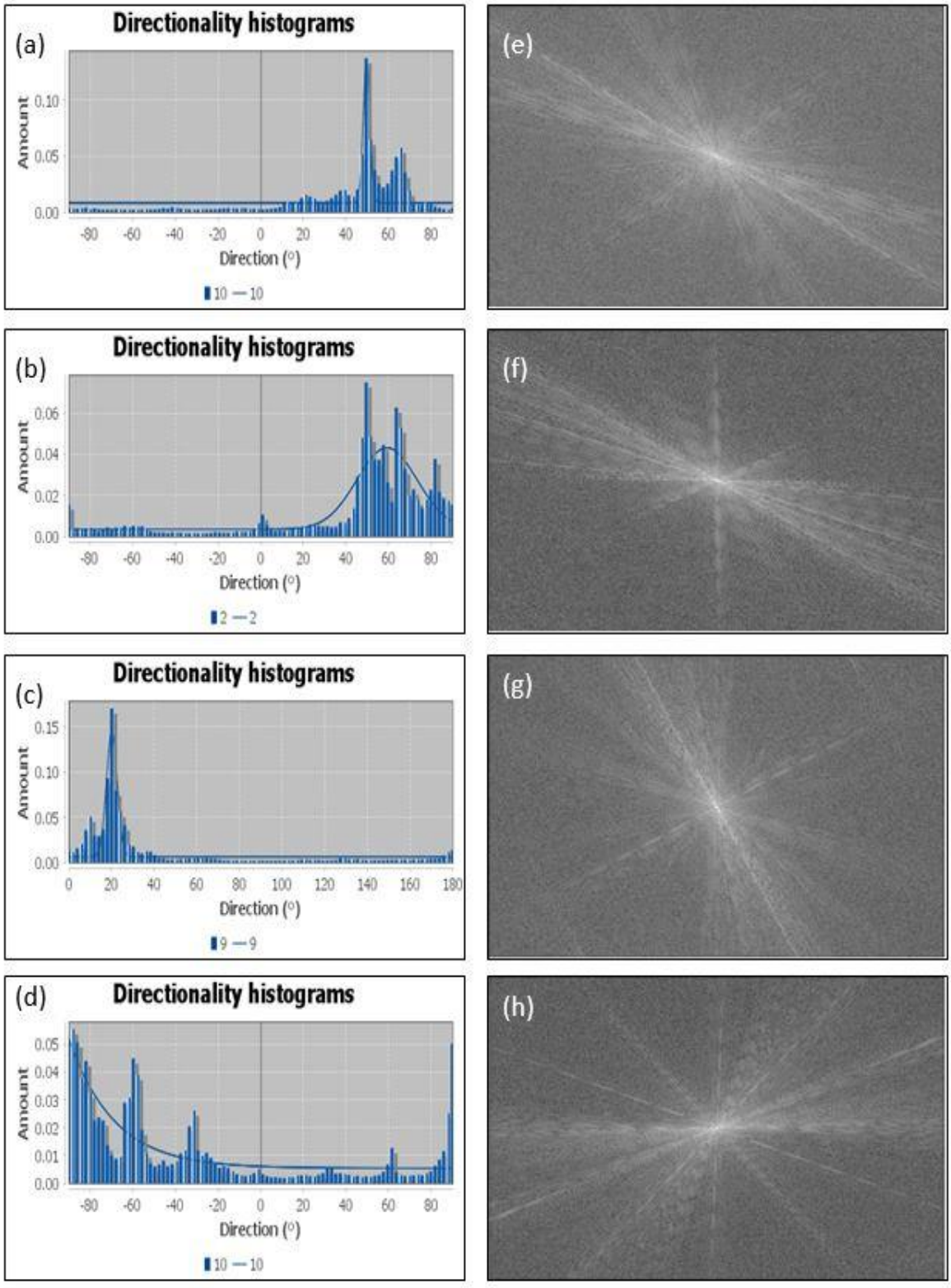

Figure (4.25) Directionality results for (14 wt.%) Polystyrene group where (a-d) are (pure PS, PS/0.07wt.%. MWCNT, PS/0.1wt.% MWCNT, PS/0.14wt.% MWCNT) respectively and their 2D-FFT from (e-h) respectively

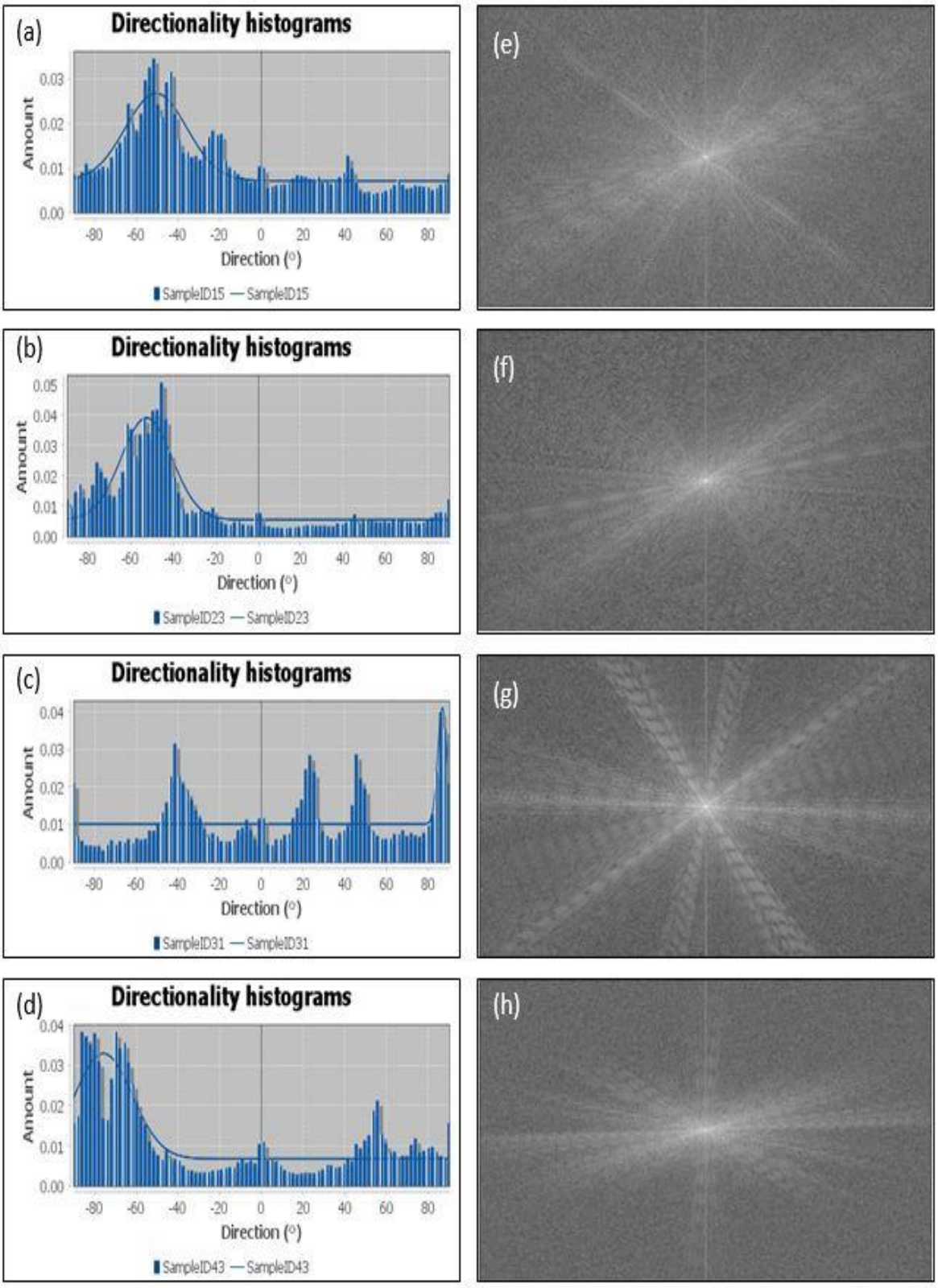

Figure (4.26) Directionality results for (16 wt.%) Polystyrene group where (a-d) are (pure PS, PS/0.06wt.%. MWCNT, PS/0.08wt.% MWCNT, PS/0.125wt.% MWCNT) respectively and their 2D-FFT from (e-h) respectively

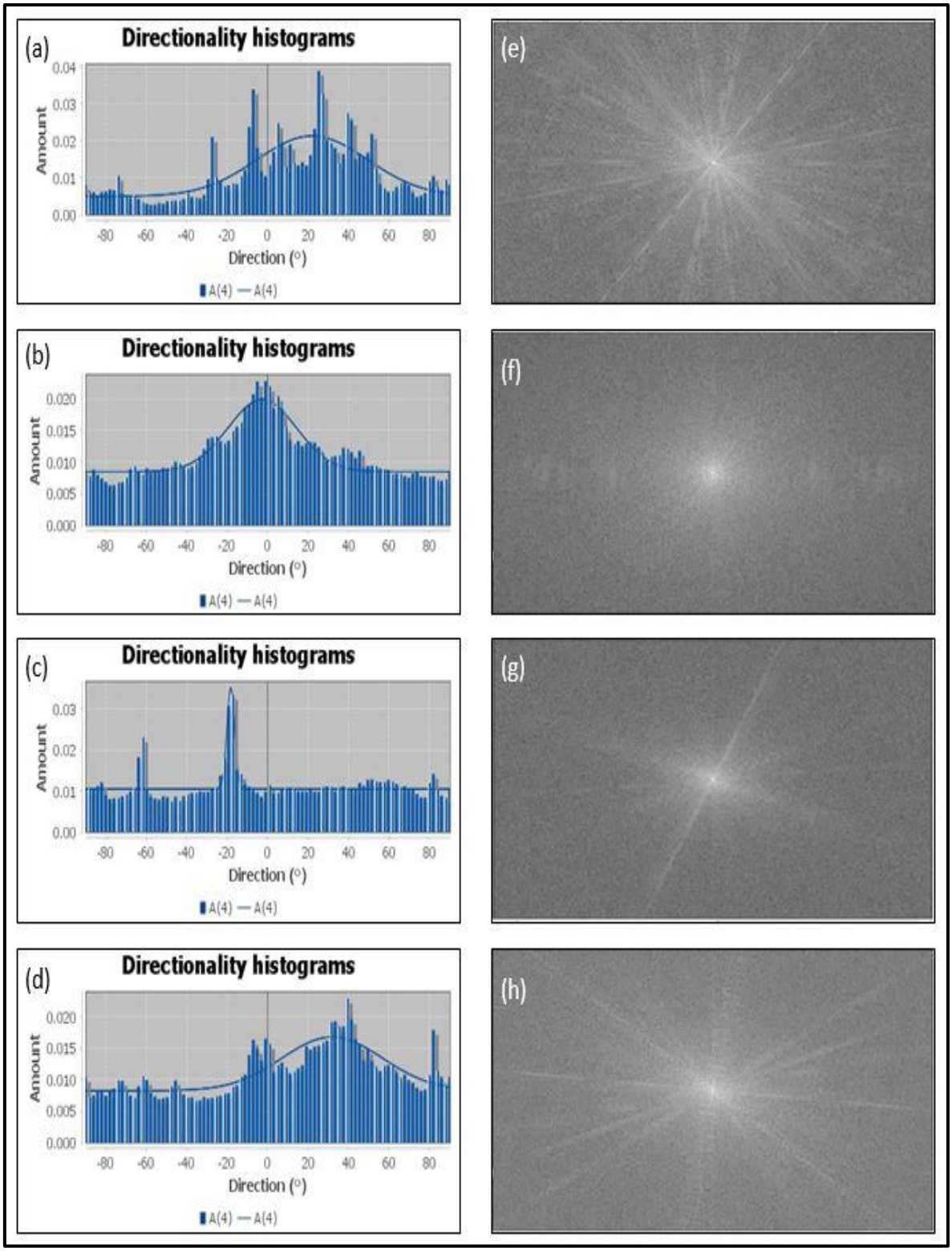

Figure (4.27) Directionality results for (12 wt.%+Natural Dye) Polystyrene group where (a-d) are (pure PS, PS/0.08wt.%. MWCNT, PS/0.11wt.% MWCNT, PS/0.16wt.% MWCNT) respectively and their 2D-FFT from (e-h) respectively

4.2.6 UV-Visible Spectroscopy results

4.2.6.1 Energy gap

The results from UV-visible and using (origin pro-9.0) to draw a (tauc plot) showed that for (12 wt.% PS) group there is a minimum bandgap than other groups .This is because that in the group of (12 wt.% PS), the polymer concentration is lower than other groups, which permit to MWCNT to be effective in increasing the electrical sensitivity to the prepared nanofibers textiles, while the other groups have higher polymer concentration and the MWCNT has little effect on electrical sensitivity improvement of the prepared nanofibers textiles .The best group is (12 wt.% PS). As shown in the figures (4.28, 4.29, 4.30) and table (4.6)

On the other hand, more work done to reduce the bandgap of the (12 wt.%) to improve its electrical sensitivity, by added a natural dye extracted from flower leaves in DMF by 0.62 wt.% Dye concentration and added two drops (0.063 g) to each sample in the (12 wt.% ps) group, adding this dye improved electrical conductivity of the solutions up to (36 S/cm) due to the presence of ions as shown in the table (3.3) from chapter three in which the elements made the electrospinning jet more easily and faster and improves the electrical sensitivity of the final prepared samples by reducing their Energy bandgap from (1.18 ev) for pure polystyrene/ 0.063g dye to (0.2 ev) for (PS/0.16wt.% MWCNT /0.063g Dye) This is due to the yellow dye has little energy gap value and it works on supporting the electron to travel from valence band to the conduction band with very depressed energy and very little time, this produces high sensitivity solar cells with high activity. This deals with [89], this will give excellent electrical sensitivity of the prepared nano textiles as shown in the figure (4.31) and table (4.6)

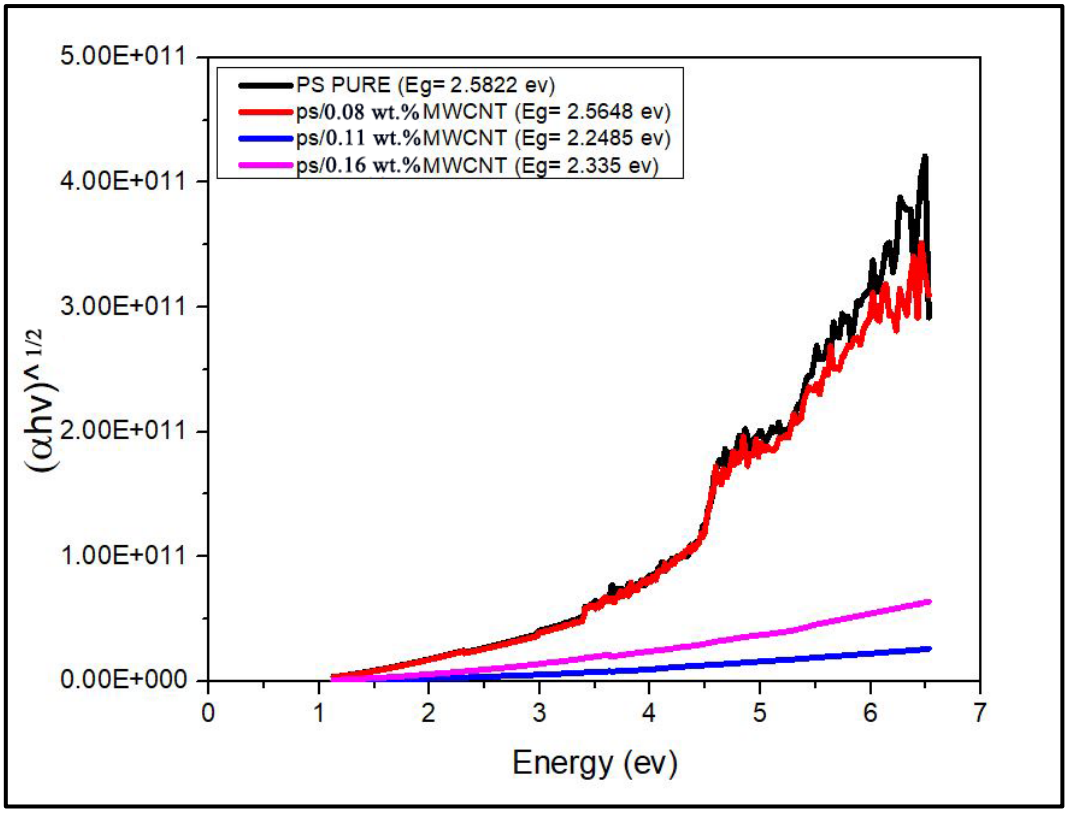

Figure (4.28) Tauc plot energy bandgap of (12 wt.% PS) group

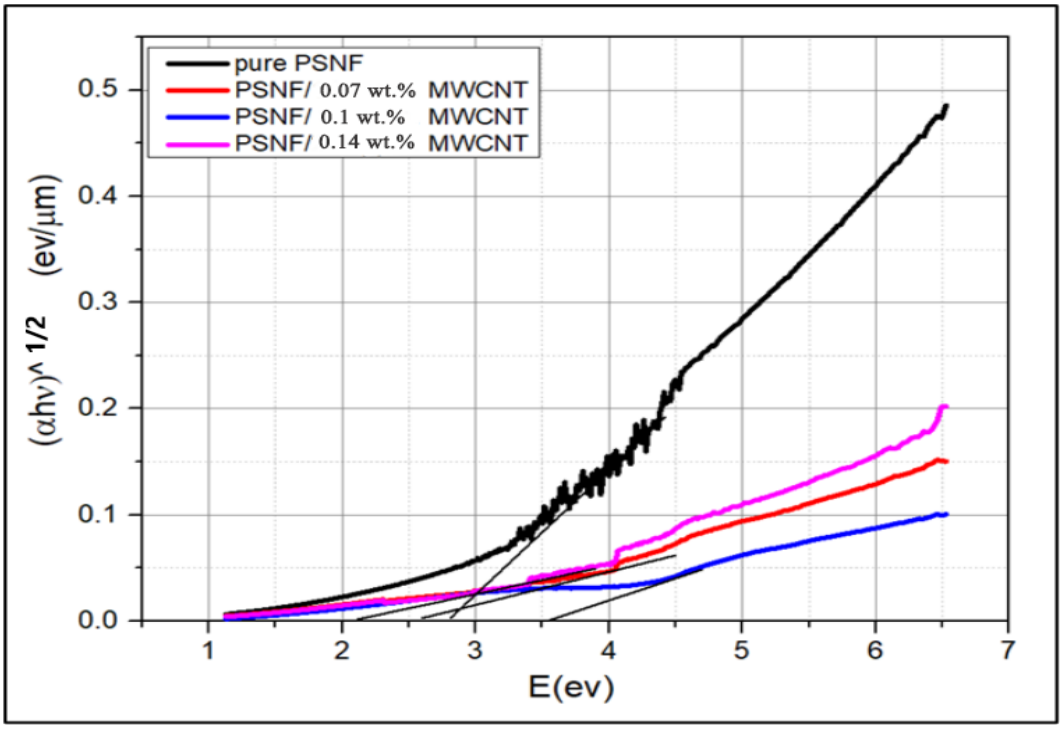

Figure (4.29) Tauc plot energy bandgap of (14 wt.% PS) group

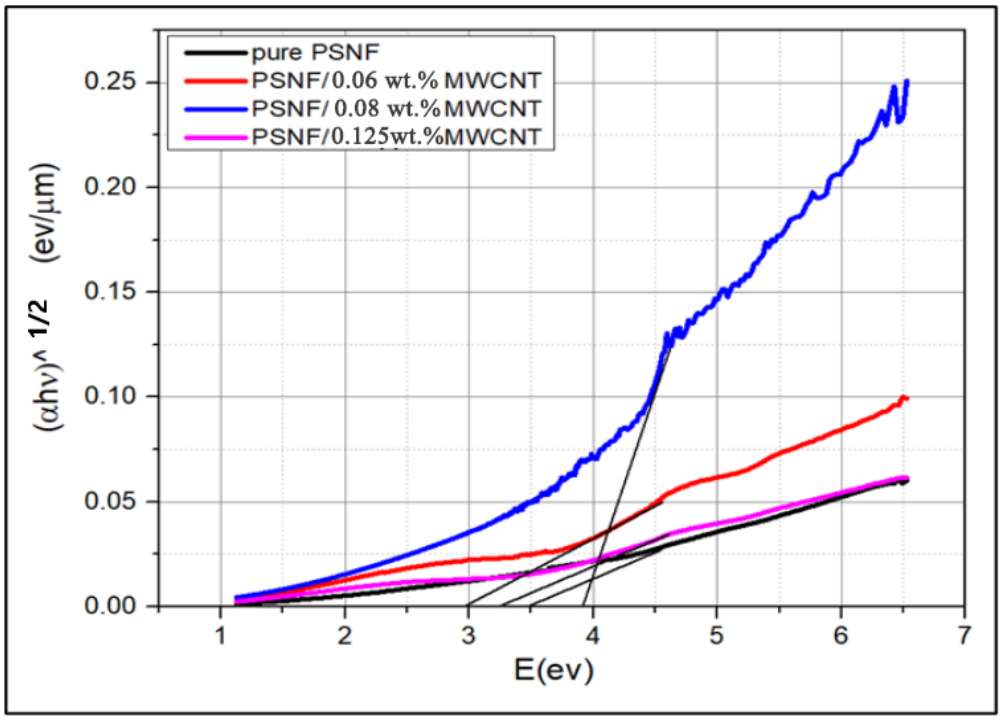

Figure (4.30) Tauc plot energy bandgap of (16 wt.% PS) group

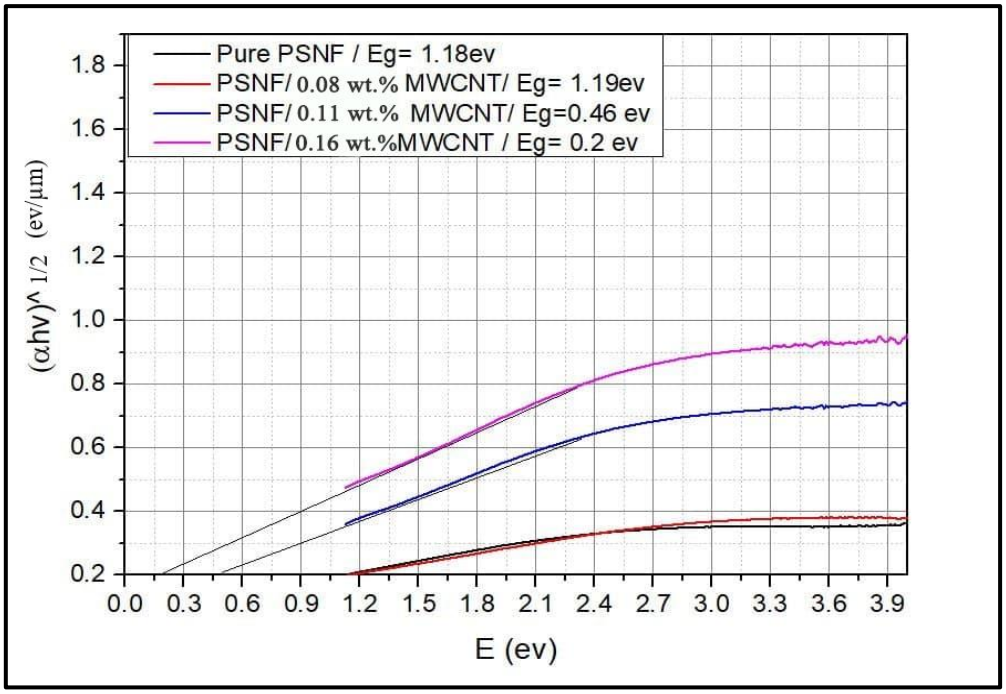

Figure (4.31) Tauc plot energy bandgap of (12 wt.% PS/Natural Dye) group

Table (4.6) Energy bandgaps for all the prepared samples

(12wt.%PSNF)	
Sample	**Bandgap (ev)**
Pure PSNF	2.582
PSNF/0.08wt.% MWCNT	2.564
PSNF/0.11wt.% MWCNT	2.248
PSNF/0.16wt.% MWCNT	2.335
(14wt.%PSNF)	
Sample	**Bandgap (ev)**
Pure PSNF	2.7
PSNF/0.07wt.% MWCNT	2.6
PSNF/0.1wt.% MWCNT	3.5
PSNF/0.14wt.% MWCNT	2.2
(16wt.%PSNF)	
Sample	**Bandgap (ev)**
Pure PSNF	3.4
PSNF/0.06wt.% MWCNT	2.9
PSNF/0.08wt.% MWCNT	3.8
PSNF/0.125wt.% MWCNT	3.25
(12 wt.% PSNF, 0.063g natural Dye)	
Sample	**Bandgap (ev)**
Pure PSNF	1.18
PSNF/0.08wt.% MWCNT	1.19
PSNF/0.11wt.% MWCNT	0.46
PSNF/0.16wt.% MWCNT	0.2

4.2.6.2 Absorption

From the figure (4.32), the addition of multiwall carbon nanotubes lowered the absorption of the prepared nanofibers in the visible and ultraviolet and IR range. This is due to the structure of nanofibers has many beads as shown in the figure (4.12). This will facilitate the passage of electromagnetic radiation through it because of increasing the spaces between nanofibers. On the other hand, it should be noted from figure (4.33), that when the natural dye was added, it makes reversible effect of adding MWCNT in which the absorption was increased, this is because the natural dye has changed the electronic energy levels and the diameter of nanofibers and also produce nanofibers with lesser beads and higher density so that the radiation passage is very hard through it. This is good to have nanofibers possess ability to absorb the harmful radiation and dissipate it into harmless energy as a heat dissipated through it and this also

enhances the service time of the prepared samples under severe environmental conditions.

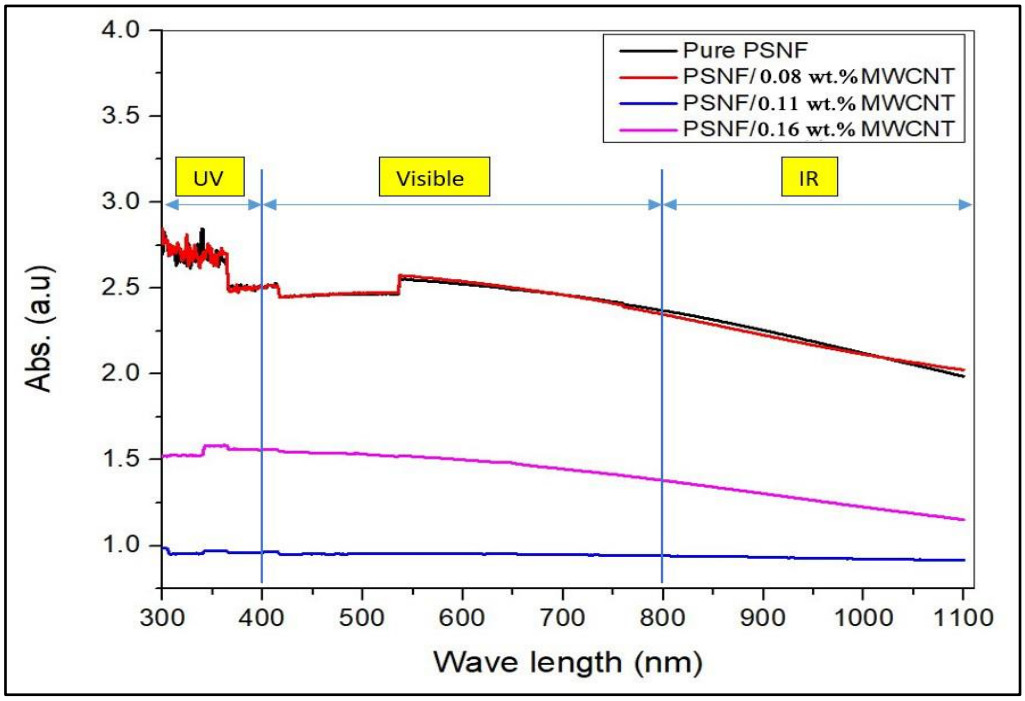

Figure (4.32) Absorption versus wavelength for 12wt.% PSNF/MWCNT

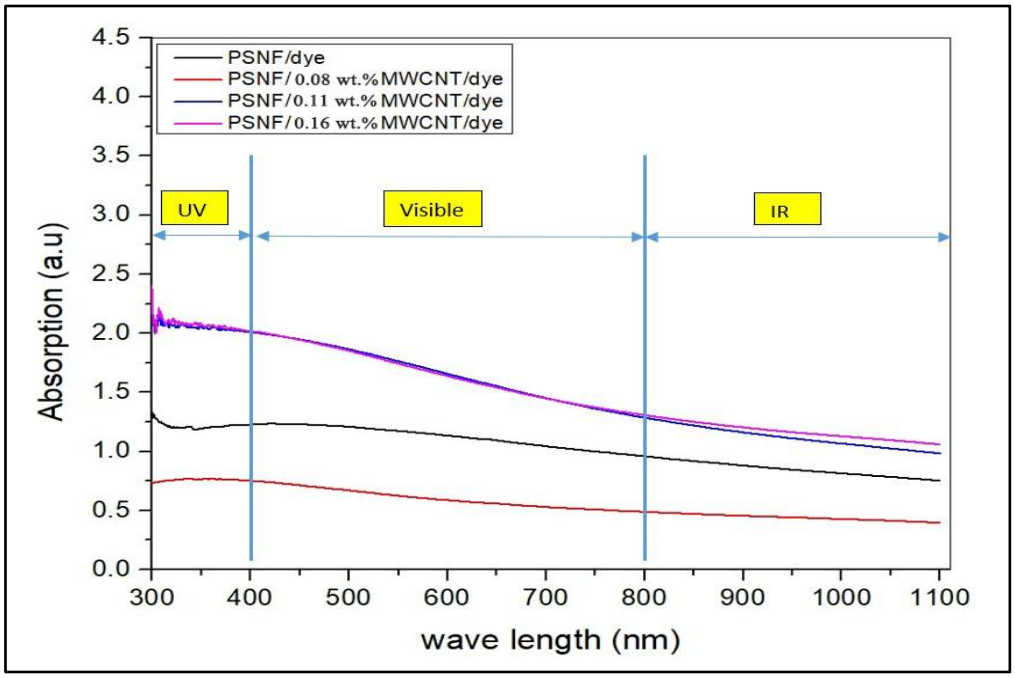

Figure (4.33) Absorption versus wavelength for 12wt.% PSNF group/MWCNT/ natural dye

4.2.6.3 Extinction coefficient

The results of the extinction coefficient obtained from the uv-vis test depending on the absorption and wavelength values the results extracted indicate how strongly a chemical substance absorbs light or the amount of absorption loss when electromagnetic wave propagates through a sample. We see from figure (4.34) the extinction coefficient was higher for sample with (0.16 wt.% MWCNT) followed by sample with (0.11wt.% MWCNT), this indicate that the sample of (0.16 wt.% MWCNT) absorbs higher amount of light or energy than the other samples so the fraction of light will be lost during absorption and scattering this is deals with absorption results as explained in [94].

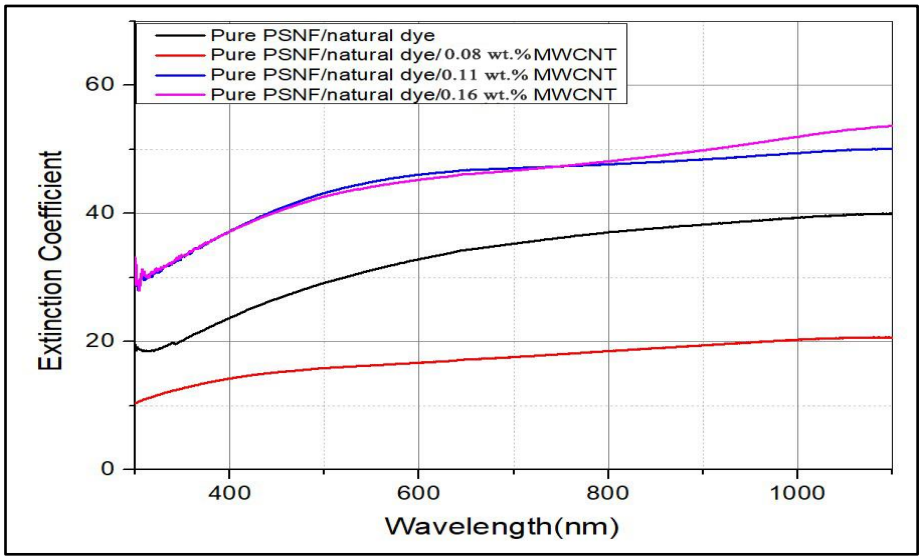

Figure (4.34) Extinction coefficient for 12wt.% PSNF group/MWCNT/ natural dye

4.2.6.4 Refractive index (n)

The ratio between the speed of light in the vacuum to the speed inside the sample called refractive index (n). As shown in the figure (4.35) we see the refractive index decrease with increasing the photon energy this indicates that polymeric nanocomposites samples represent normal dispersion behavior. The change between values of (n) represent that there is interaction between the photons and the electrons, thus the prepared samples can be used for

optoelectronics devices by estimating the photon energy as internal energy of device depends on photon energy as stated in [94]

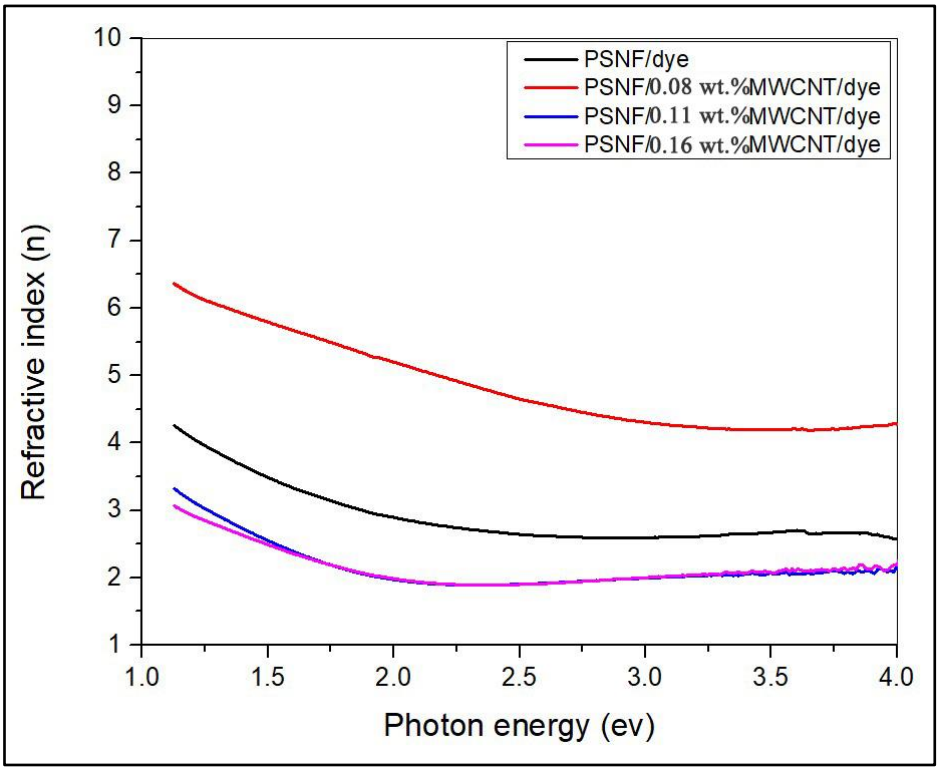

Figure (4.35) Refractive index versus photon energy for (12wt.%PSNF/MWCNT/dye) group

4.2.6.5 Optical conductivity (σ)

Optical conductivity is the property of a material which gives the relationship between the induced current density in the material and the magnitude of the inducing electric field for arbitrary frequencies. This linear response function is a generalization of the electrical conductivity, which is usually considered in the static limit, i.e., for time-independent or slowly varying electric fields [95].

We notice from the results in figure (4.36) that the optical conductivity was at higher values in the wave length (300-400 nm) it reached ($6.58x10^6$ S^{-1}) for the sample containing (12wt.%PSNF/0.16 wt.% MWCNT /dye) and ($6 x10^6$ S^{-1}) for sample (12wt.%PSNF/0.11 wt.% MWCNTs/dye) and ($4.7x10^6$ S^{-1}) for (PSNF/dye) and ($4.85x10^6$ S^{-1}) for (12wt.%PSNF/0.08wt.% MWCNT/dye). The optical conductivity decreased at wavelength (400-700nm) and start

increase after (700nm) these results deals with bandgap results and we conclude that the sample (12wt.%PSNF/0.16 wt.% MWCNT/dye) has higher optical conductivity and higher electrical conductivity from the prepared samples and can be used as optical sensor.

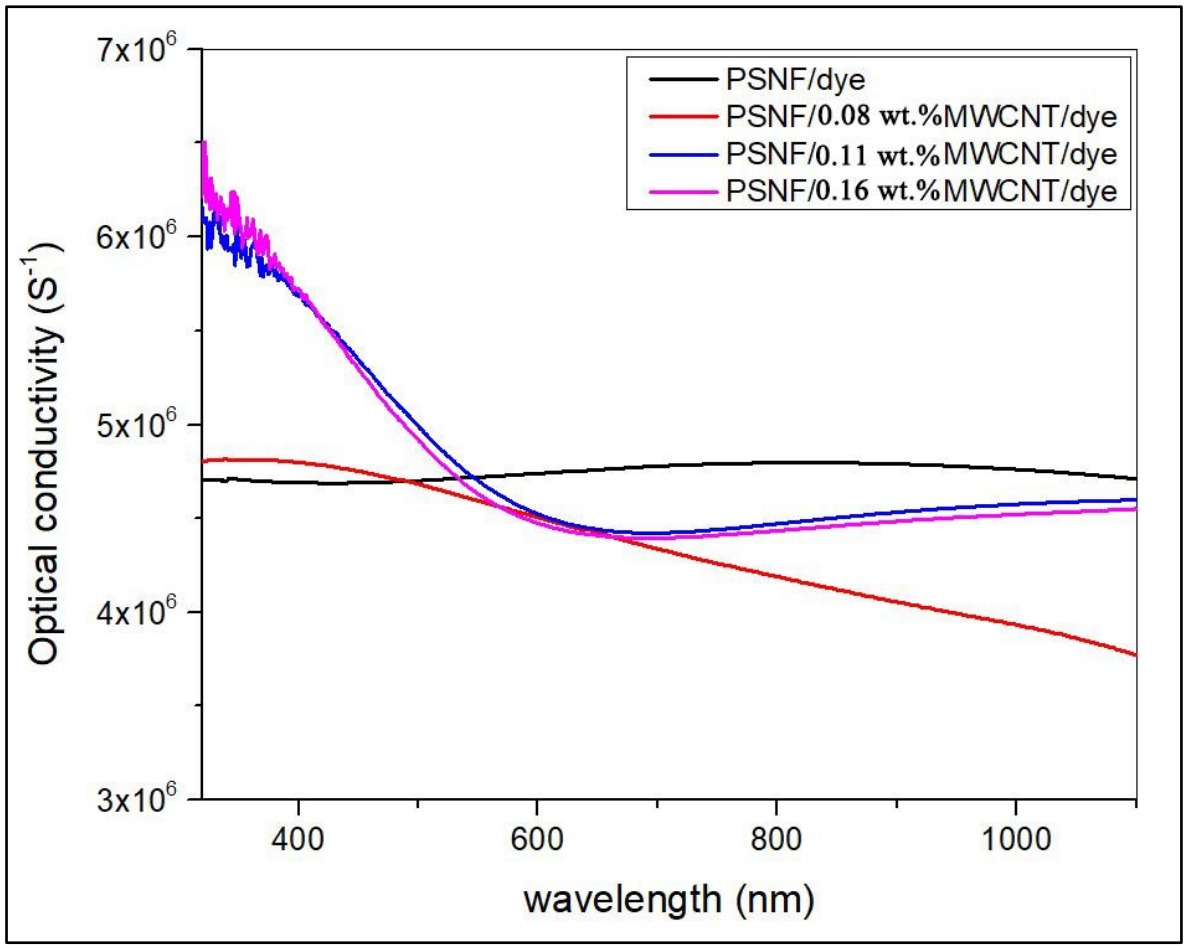

Figure (4.36) Optical conductivity versus wavelength for (12wt.%PSNF/MWCNT/dye) group

Chapter 5

Conclusions & Recommendations

5.1 Conclusions

1-The surface tension was approximately constant and increased slightly in the (natural dye /12wt.% group).

2- The viscosity of solutions increased with increasing polymer concentration, it decreased when adding MWCNT and slightly increased when adding the natural dye.

3- The interaction between components is physical.

4- The fabricated nanofibers became hydrophilic in groups of (14, 16 wt.%) and hydrophobic in group of (12wt.%) polystyrene, also when added natural dye to the group of (12wt.% ps).

5- The roughness average value increased with increasing the MWCNT and this addition also improved the surface bearing index which will improves the mechanical properties of the prepared textiles.

6- Average fiber diameter reduced with increasing the addition of MWCNT concentration, natural dye (because of improving the electrical conductivity of solutions). And increased with polystyrene concentration and lower values recorded in the group of polystyrene concentration (12wt.%). Orientation of nanofibers has best results in the group of polymer concentration of (14wt.%) followed by group of (16wt.%).

7- The energy bandgap improved when natural pigment with (0.063g) was added to the group (12 wt.%) and give us a value (0.2 ev) for sample (12 wt.% PS / 0.16wt.% MWCNT/0.063g natural dye) and (0.4 ev) for sample (12 wt.% PS / 0.11 wt.% MWCNT/0.063g natural dye) which is an indicator to increasing its electrical conductivity.

8- Prepared samples can be used as optical sensors from the results of UV-Visible parameters (σ, n, k, Abs., Bg).

5.2 Recommendations

1- Use another polymer type, such as poly aniline or polyvinyl difluoride.

2- Use another nanofiller, such as zinc oxide, titanium oxide, …etc.

3- Use surface tunneling microscope (STM) to test the sample and the raw materials to have accurate roughness, size distribution and many other parameters and use Transmission electron microscopy (TEM) to show the morphology and distribution of nanofillers within the nanofibers.

References

References

[1] D. Aussawasthien, “Electrospun Conducting Nanofiber–Based Materials and Their Characterizations: Effects of Fiber Characteristics on Properties and Applications a.” p. 259, 2006.

[2] J. F. Sargent, “The National Nanotechnology Initiative: Overview, reauthorization, and appropriations issues,” Nanotechnol. USA Dev. Policies Issues, pp. 47–87, 2009.

[3] Y. Dzenis, “Spinning continuous fibers for nanotechnology,” *Science (80-.).*, vol. 304, no. 5679, pp. 1917–1919, 2004, doi: 10.1126/science.1099074.

[4] E. T. Thostenson, C. Li, and T.-W. Chou, “Nanocomposites in context,” Compos. Sci. Technol., vol. 65, no. 3–4, pp. 491–516, 2005.

[5] A. R. Jabur, “Multiwall Carbon Nanotube / Polyvinyl Alcohol Nanofibers Film, Electrical Conductivity Improvement,” *Eng. Technol. J.*, vol. 38, no. 3A, pp. 431–439, 2020, doi: 10.30684/etj.v38i3a.530.

[6] A. G. MacDiarmid, “‘Synthetic Metals’: A Novel Role for Organic Polymers (Nobel Lecture) Copyright((c)) The Nobel Foundation 2001. We thank the Nobel Foundation, Stockholm, for permission to print this lecture.,” Angew. Chem. Int. Ed. Engl., vol. 40, no. 14, pp. 2581–2590, Jul. 2001.

[7] A. R. Jabur, M. H. Abdulmajeed, and S. Y. Abd, “Effect of Cu nanoparticles addition on improving the electrical conductivity and mechanical properties of PVA electrospun polymeric film,” in AIP Conference Proceedings, 2018, vol. 1968, no. 1, p. 30016.

[8] R. R. Parajuli, “Developing conducting polymer nanocomposites with carbon nanomaterials for molecular detection and fuel cell applications.” Rutgers University-Graduate School-Newark, 2011.

[9] S. Gul, A. Shah, and S. Bilal, “Calculation of activation energy of degradation of polyaniline-dodecylbenzene sulfonic acid salts via TGA,” J.

Sci. Innov. Res., vol. 2, pp. 673–684, 2013.

[10] W. S. Khan, R. Asmatulu, and M. M. Eltabey, “Electrical and thermal characterization of electrospun PVP nanocomposite fibers,” J. Nanomater., vol. 2013, 2013.

[11] X. D. Zhu, Q. J. Jiao, C. G. Zang, and X. P. Cao, “Effects of functionalization MWCNTs on the mechanical and electrical properties of nylon-6 composites,” in Advanced Materials Research, 2013, vol. 750, pp. 127–131.

[12] T. Blachowicz and A. Ehrmann, “Conductive electrospun nanofiber mats,” Materials (Basel)., vol. 13, no. 1, 2020, DOI: 10.3390/ma13010152.

[13] C. Salas, Solution electrospinning of nanofibers. Elsevier Ltd., 2017.

[14] M. Halabi et al., “Electrospun anion-conducting ionomer fibers-effect of humidity on final properties,” Polymers (Basel)., vol. 12, no. 5, pp. 1–12, 2020, doi: 10.3390/POLYM12051020.

[15] W. E. Teo and S. Ramakrishna, “A review on electrospinning design and nanofibre assemblies,” Nanotechnology, vol. 17, no. 14, p. R89, 2006.

[16] X. Shi et al., “Electrospinning of nanofibers and their applications for energy devices,” J. Nanomater., vol. 2015, 2015.

[17] S. Mazinani, A. Ajji, and C. Dubois, “Morphology, structure and properties of conductive PS/CNT nanocomposite electrospun mat,” Polymer (Guildf)., vol. 50, no. 14, pp. 3329–3342, 2009.

[18] K. Ketpang and J. S. Park, “Electrospinning PVDF / PPy / MWCNTs conducting composites,” Synth. Met., vol. 160, no. 15–16, pp. 1603–1608, 2010, DOI: 10.1016/j.synthmet.2010.05.022.

[19] F. A. Chayad, A. R. Jabur, and N. M. Jalal, “ScienceDirect Effect of MWCNT addition on improving the electrical conductivity and activation energy of electrospun nylon films,” Karbala Int. J. Mod. Sci., vol. 1, no. 4,

pp. 187–193, 2015, DOI: 10.1016/j.kijoms.2015.10.004.

[20] S. A Hosseini Ravandi and N. Pan, “Morphological characterization of individual polyacrylonitrile nanofibers,” *Curr. Nanosci.*, vol. 7, no. 3, pp. 415–419, 2011.

[21] P. Gupta, “Processing-Structure-Property Studies of: I) Submicron Polymeric Fibers Produced By Electrospinning and II) Films Of Linear Low Density Polyethylenes As Influenced By The Short Chain Branch Length In Copolymers Of Ethylene/1-Butene, Ethylene/1-Hexene & Et.” Virginia Tech, 2004.

[22] V. Beachley and X. Wen, “Polymer nanofibrous structures: Fabrication, biofunctionalization, and cell interactions,” *Prog. Polym. Sci.*, vol. 35, no. 7, pp. 868–892, 2010.

[23] P. Kumar, “Effect of colletor on electrospinning to fabricate aligned nano fiber.” 2012.

[24] W. E. Teo and S. Ramakrishna, “A review on electrospinning design and nanofibre assemblies,” *Nanotechnology*, vol. 17, no. 14, p. R89, 2006.

[25] N. G. Rim, C. S. Shin, and H. Shin, “Current approaches to electrospun nanofibers for tissue engineering,” Biomed. Mater., vol. 8, no. 1, 2013, doi: 10.1088/1748-6041/8/1/014102.

[26] B. Zaarour, L. Zhu, C. Huang, and X. Jin, “Controlling the Secondary Surface Morphology of Electrospun PVDF Nanofibers by Regulating the Solvent and Relative Humidity,” Nanoscale Res. Lett., vol. 13, 2018, doi: 10.1186/s11671-018-2705-0.

[27] X. Zhang and Y. Lu, “Centrifugal spinning: an alternative approach to fabricate nanofibers at high speed and low cost,” *Polym. Rev.*, vol. 54, no. 4, pp. 677–701, 2014.

[28] P. Kumar, “Effect of colletor on electrospinning to fabricate aligned nano

fiber.” 2012.

[29] I. Alghoraibi and S. Alomari, “Different methods for nanofiber design and fabrication,” *Handb. nanofibers*, pp. 1–46, 2018.

[30] S. Ramakrishna, *An introduction to electrospinning and nanofibers*. World Scientific, 2005.

[31] P. Gupta, “Processing-Structure-Property Studies of: I) Submicron Polymeric Fibers Produced By Electrospinning and II) Films Of Linear Low Density Polyethylenes As Influenced By The Short Chain Branch Length In Copolymers Of Ethylene/1-Butene, Ethylene/1-Hexene & Ethylene/1-Octene Synthesized By A Single Site Metallocene Catalyst.” Virginia Tech, 2004.

[32] J. Yun, J. S. Im, Y. S. Lee, and H. Il Kim, “Electro-responsive transdermal drug delivery behavior of PVA/PAA/MWCNT nanofibers,” *Eur. Polym. J.*, vol. 47, no. 10, pp. 1893–1902, 2011, doi: 10.1016/j.eurpolymj.2011.07.024.

[33] J. C. C. Lima, W. A. Nascimento, P. Agrawal, and H. L. Lira, “19º Congresso Brasileiro de Engenharia e Ciência dos Materiais – CBECiMat, 21 a 25 de novembro de 2010, Campos do Jordão, SP, Brasil,” pp. 9060–9067, 2010.

[34] G. A. Zamora-P?rez, C. O. Gonz?lez-Mor?n, and E. Suaste-G?mez, “Humidity sensor for biological applications via electrospinning | Sensor de humedad para aplicaciones biol?gicas v?a electrospinning,” *2012 Pan Am. Heal. Care Exch. PAHCE 2012 - Conf. Work. Exhib. Coop. / Linkages An Indep. Forum Patient AareTechnol.Support*, pp. 97–100, 2012, doi: 10.1109/PAHCE.2012.6233449.

[35] Z. Oxide, N. Gas, and S. Via, “Zinc Oxide Nanofiber Gas Sensors Via Electrospinning,” vol. 3819, no. 25169, pp. 3817–3819, 2008, doi: 10.1111/j.1551-2916.2008.02765.x.

[36] N. Amariei, L. R. Manea, A. P. Bertea, R. Cramariuc, A. Bertea, and O. Cramariuc, “Electrospinning Polyaniline for Sensors,” *IOP Conf. Ser. Mater. Sci. Eng.*, vol. 209, no. 1, 2017, doi: 10.1088/1757-899X/209/1/012091.

[37] Z. Zhang, X. Li, C. Wang, L. Wei, Y. Liu, and C. Shao, "ZnO hollow nanofibers: Fabrication from facile single capillary electrospinning and applications in gas sensors," *J. Phys. Chem. C*, vol. 113, no. 45, pp. 19397–19403, 2009, doi: 10.1021/jp9070373.

[38] S. Ponce-Alcántara, D. Martín-Sánchez, A. Pérez-Márquez, J. Maudes, N. Murillo, and J. García-Rupérez, "Optical sensors based on polymeric nanofibers layers created by electrospinning," *Opt. Mater. Express*, vol. 8, no. 10, p. 3163, 2018, doi: 10.1364/ome.8.003163.

[39] S. Kohn, D. Wehlage, I. J. Junger, and A. Ehrmann, "Electrospinning a dye-sensitized solar cell," *Catalysts*, vol. 9, no. 12, pp. 1–9, 2019, doi: 10.3390/catal9120975.

[40] H. J. Alesa, B. M. Aldabbag, and R. M. Salih, "Natural pigment -poly vinyl alcohol nano composites thin films for solar cell," *Baghdad Sci. J.*, vol. 17, no. 3, pp. 832–840, 2020, doi: 10.21123/bsj.2020.17.3.0832.

[41] H. Hou *et al.*, "Electrospun polyacrylonitrile nanofibers containing a high concentration of well-aligned multiwall carbon nanotubes," *Chem. Mater.*, vol. 17, no. 5, pp. 967–973, 2005, doi: 10.1021/cm0484955.

[42] T. Uyar and F. Besenbacher, "Electrospinning of uniform polystyrene fibers: The effect of solvent conductivity," *Polymer (Guildf).*, vol. 49, no. 24, pp. 5336–5343, 2008, doi: 10.1016/j.polymer.2008.09.025.

[43] J. Lyons, C. Li, and F. Ko, "Melt-electrospinning part I: Processing parameters and geometric properties," *Polymer (Guildf).*, vol. 45, no. 22, pp. 7597–7603, 2004, doi: 10.1016/j.polymer.2004.08.071.

[44] American Polymers Service Inc.APS

[45] c. J. Buchko, L. C. Chen, Y. Shen, and D. C. Martin, "Processing and microstructural characterization of porous biocompatible protein polymer thin films," Polymer (Guildf)., vol. 40, no. 26, pp. 7397–7407, 1999.

[46] S. L. Shenoy, W. D. Bates, H. L. Frisch, and G. E. Wnek, “Role of chain entanglements on fiber formation during electrospinning of polymer solutions: good solvent, non-specific polymer–polymer interaction limit,” *Polymer (Guildf).*, vol. 46, no. 10, pp. 3372–3384, 2005.

[47] J. Kameoka *et al.*, “A scanning tip electrospinning source for deposition of oriented nanofibres,” *Nanotechnology*, vol. 14, no. 10, p. 1124, 2003.

[48] X. Zong, K. Kim, D. Fang, S. Ran, B. S. Hsiao, and B. Chu, “Structure and process relationship of electrospun bioabsorbable nanofiber membranes,” *Polymer (Guildf).*, vol. 43, no. 16, pp. 4403–4412, 2002.

[49] P. Schümmer and K. H. Tebel, “A new elongational rheometer for polymer solutions,” J. Nonnewton. Fluid Mech., vol. 12, no. 3, pp. 331–347, 1983.

[50] Y. Christanti and L. M. Walker, “Surface tension driven jet break up of strain-hardening polymer solutions,” J. Nonnewton. Fluid Mech., vol. 100, no. 1–3, pp. 9–26, 2001.

[51] V. Morozov, T. Morozova, and N. Kallenbach, “Atomic force microscopy of structures produced by electrospraying polymer solutions,” *Int. J. Mass Spectrom.*, vol. 178, no. 3, pp. 143–159, 1998.

[52] J. S. Choi *et al.*, “Effect of organosoluble salts on the nanofibrous structure of electrospun poly (3-hydroxybutyrate-co-3-hydroxyvalerate),” *Int. J. Biol. Macromol.*, vol. 34, no. 4, pp. 249–256, 2004.

[53] W. K. Son, J. H. Youk, T. S. Lee, and W. H. Park, “Electrospinning of ultrafine cellulose acetate fibers: studies of a new solvent system and deacetylation of ultrafine cellulose acetate fibers,” *J. Polym. Sci. Part B Polym. Phys.*, vol. 42, no. 1, pp. 5–11, 2004.

[54] T. Jarusuwannapoom *et al.*, “Effect of solvents on electro-spinnability of polystyrene solutions and morphological appearance of resulting electrospun polystyrene fibers,” *Eur. Polym. J.*, vol. 41, no. 3, pp. 409–421, 2005.

[55] S. A. Theron, E. Zussman, and A. L. Yarin, "Experimental investigation of the governing parameters in the electrospinning of polymer solutions," *Polymer (Guildf).*, vol. 45, no. 6, pp. 2017–2030, 2004.

[56] M. Prego, O. Cabeza, E. Carballo, C. F. Franjo, and E. Jime, "Measurement and interpretation of the electrical conductivity of 1-alcohols from 273 K to 333 K," *J. Mol. Liq.*, vol. 89, no. 1–3, pp. 233–238, 2000.

[57] K. H. Lee, H. Y. Kim, M. S. Khil, Y. M. Ra, and D. R. Lee, "Characterization of nano-structured poly (ε-caprolactone) nonwoven mats via electrospinning," *Polymer (Guildf).*, vol. 44, no. 4, pp. 1287–1294, 2003.

[58] C. Hsu and S. Shivkumar, "N, N-Dimethylformamide Additions to the Solution for the Electrospinning of Poly (ε-caprolactone) Nanofibers," *Macromol. Mater. Eng.*, vol. 289, no. 4, pp. 334–340, 2004.

[59] L. Wannatong, A. Sirivat, and P. Supaphol, "Effects of solvents on electrospun polymeric fibers: preliminary study on polystyrene," *Polym. Int.*, vol. 53, no. 11, pp. 1851–1859, 2004.

[60] C. Berkland, D. W. Pack, and K. K. Kim, "Controlling surface nano-structure using flow-limited field-injection electrostatic spraying (FFESS) of poly (D, L-lactide-co-glycolide)," *Biomaterials*, vol. 25, no. 25, pp. 5649–5658, 2004.

[61] Q. Yang *et al.*, "Influence of solvents on the formation of ultrathin uniform poly (vinyl pyrrolidone) nanofibers with electrospinning," *J. Polym. Sci. Part B Polym. Phys.*, vol. 42, no. 20, pp. 3721–3726, 2004.

[62] G. I. Taylor, "Disintegration of water drops in an electric field," *Proc. R. Soc. London. Ser. A. Math. Phys. Sci.*, vol. 280, no. 1382, pp. 383–397, 1964.

[63] S. Megelski, J. S. Stephens, D. B. Chase, and J. F. Rabolt, "Micro-and nanostructured surface morphology on electrospun polymer fibers," *Macromolecules*, vol. 35, no. 22, pp. 8456–8466, 2002.

[64] S. Zhao, X. Wu, L. Wang, and Y. Huang, "Electrospinning of ethyl–cyanoethyl

cellulose/tetrahydrofuran solutions," *J. Appl. Polym. Sci.*, vol. 91, no. 1, pp. 242–246, 2004.

[65] M. M. Demir, I. Yilgor, E. Yilgor, and B. Erman, "Electrospinning of polyurethane fibers," *Polymer (Guildf).*, vol. 43, no. 11, pp. 3303–3309, 2002, doi: 10.1016/S0032-3861(02)00136-2.

[66] C. Mit-uppatham, M. Nithitanakul, and P. Supaphol, "Ultrafine electrospun polyamide-6 fibers: effect of solution conditions on morphology and average fiber diameter," *Macromol. Chem. Phys.*, vol. 205, no. 17, pp. 2327–2338, 2004.

[67] R. Kessick and G. Tepper, "Microscale polymeric helical structures produced by electrospinning," *Appl. Phys. Lett.*, vol. 84, no. 23, pp. 4807–4809, 2004.

[68] H. Liu and Y. Hsieh, "Ultrafine fibrous cellulose membranes from electrospinning of cellulose acetate," *J. Polym. Sci. Part B Polym. Phys.*, vol. 40, no. 18, pp. 2119–2129, 2002.

[69] M. Vlachou, A. Siamidi, and S. Kyriakou, "Electrospinning and Drug Delivery," *Electrospinning Electrospraying - Tech. Appl.*, 2019, doi: 10.5772/intechopen.86181.

[70] X. M. Mo, C. Y. Xu, M. E. A. Kotaki, and S. Ramakrishna, "Electrospun P (LLA-CL) nanofiber: a biomimetic extracellular matrix for smooth muscle cell and endothelial cell proliferation," *Biomaterials*, vol. 25, no. 10, pp. 1883–1890, 2004.

[71] M. Bognitzki *et al.*, "Nanostructured fibers via electrospinning," *Adv. Mater.*, vol. 13, no. 1, pp. 70–72, 2001.

[72] J. Y. Park and I. H. Lee, "Relative humidity effect on the preparation of porous electrospun polystyrene fibers," *J. Nanosci. Nanotechnol.*, vol. 10, no. 5, pp. 3473–3477, 2010, doi: 10.1166/jnn.2010.2349.

[73] P. K. Baumgarten, "Electrostatic spinning of acrylic microfibers," *J. Colloid*

Interface Sci., vol. 36, no. 1, pp. 71–79, 1971, doi: 10.1016/0021-9797(71)90241-4.

[74] S. Christie, E. Scorsone, K. Persaud, and F. Kvasnik, "Remote detection of gaseous ammonia using the near infrared transmission properties of polyaniline," *Sensors Actuators B Chem.*, vol. 90, no. 1–3, pp. 163–169, 2003.

[75] B. Ding, J. Kim, Y. Miyazaki, and S. Shiratori, "Electrospun nanofibrous membranes coated quartz crystal microbalance as gas sensor for NH3 detection," *Sensors Actuators B Chem.*, vol. 101, no. 3, pp. 373–380, 2004.

[76] B. Ding, M. Yamazaki, and S. Shiratori, "Electrospun fibrous polyacrylic acid membrane-based gas sensors," *Sensors Actuators B Chem.*, vol. 106, no. 1, pp. 477–483, 2005.

[77] P. I. Gouma, "Nanostructured polymorphic oxides for advanced chemosensors," *Rev. Adv. Mater. Sci*, vol. 5, no. 123, p. 122, 2003.

[78] M. Zhao, X. Wang, L. Ning, J. Jia, X. Li, and L. Cao, "Electrospun Cu-doped ZnO nanofibers for H2S sensing," *Sensors Actuators B Chem.*, vol. 156, no. 2, pp. 588–592, 2011.

[79] D. Zhao, Y. Lu, Y. Ding, and R. Fu, "An amperometric l-tryptophan sensor platform based on electrospun tricobalt tetroxide nanoparticles decorated carbon nanofibers," *Sensors Actuators B Chem.*, vol. 241, pp. 601–606, 2017.

[80] P. Zhang *et al.*, "Electrospun doping of carbon nanotubes and platinum nanoparticles into the β-phase polyvinylidene difluoride nanofibrous membrane for biosensor and catalysis applications," *ACS Appl. Mater. Interfaces*, vol. 6, no. 10, pp. 7563–7571, 2014.

[81] Z. Su, J. Ding, and G. Wei, "Electrospinning: A facile technique for fabricating polymeric nanofibers doped with carbon nanotubes and metallic nanoparticles for sensor applications," *Rsc Adv.*, vol. 4, no. 94, pp. 52598–52610, 2014.

[82] W. Jia, L. Su, and Y. Lei, "Pt nanoflower/polyaniline composite nanofibers

based urea biosensor," *Biosens. Bioelectron.*, vol. 30, no. 1, pp. 158–164, 2011.

[83] S.-H. Lee, B.-C. Ku, X. Wang, L. A. Samuelson, and J. Kumar, "Design, synthesis and electrospinning of a novel fluorescent polymer for optical sensor applications," *MRS Online Proc. Libr.*, vol. 708, no. 1, pp. 10451–10456, 2001.

[84] X. Wang, Y.-G. Kim, C. Drew, B.-C. Ku, J. Kumar, and L. A. Samuelson, "Electrostatic assembly of conjugated polymer thin layers on electrospun nanofibrous membranes for biosensors," *Nano Lett.*, vol. 4, no. 2, pp. 331–334, 2004.

[85] S. J. Kwoun, R. M. Lec, B. Han, and F. K. Ko, "A novel polymer nanofiber interface for chemical sensor applications," in *Proceedings of the 2000 IEEE/EIA International Frequency Control Symposium and Exhibition (Cat. No. 00CH37052)*, 2000, pp. 52–57.

[86] T. Jarusuwannapoom *et al.*, "Effect of solvents on electro-spinnability of polystyrene solutions and morphological appearance of resulting electrospun polystyrene fibers," *Eur. Polym. J.*, vol. 41, no. 3, pp. 409–421, 2005.

[87] U. Miftah K. Raghava and T. Snguanwongchai. "Polymer brush synthesis on surface modified carbon nanotubes via in situ emulsion polymerization" . Colloid Polym Sci 294(10) . 2016

[88] A. Durigon, M. M., da Silveira, G. D., Sokal, F. R., Pires, R. A. C. V., & Dias, D. (2020). Food dyes screening using electrochemistry approach in solid state: the case of sunset yellow dye electrochemical behavior. Journal of Solid State Electrochemistry. doi:10.1007/s10008-020-04678-z

[89] Ruihan W. , Ji-Hong Ch., Jan D. H ." On the Relationship Between Viscosity and Surface Tension ", Journal of Emerging Investigators September 16, 2014

[90] Sunita T., Pramod Kumar Sh. and Rishabha M. " Influence of Concentration on Surface Tension & Viscosity of Tamarind (Tamarindus Indica) Seed Gum

". Nanoscale Research Letters . 7(226) . (2012)

[91] J. Chen, L. Yan, W. Song, and D. Xu, “Interfacial characteristics of carbon nanotube-polymer composites: A review,” Compos. Part A Appl. Sci. Manuf., vol. 114, no. August, pp. 149–169, 2018, doi: 10.1016/j.compositesa.2018.08.021.

[92] A. K. Kota et al., “Electrical and rheological percolation in polystyrene/MWCNT nanocomposites,” Macromolecules, vol. 40, no. 20, pp. 7400–7406, 2007, doi: 10.1021/ma0711792.

[93] M. Kaseem, K. Hamad, and Y. G. Ko, “Fabrication and materials properties of polystyrene/carbon nanotube (PS/CNT) composites: A review,” Eur. Polym. J., vol. 79, pp. 36–62, 2016, doi: 10.1016/j.eurpolymj.2016.04.011.

[94] N. S. Wadatkar and S. A. Waghuley, “Complex optical studies on conducting polyindole as-synthesized through chemical route,” Egypt. J. Basic Appl. Sci., vol. 2, no. 1, pp. 19–24, 2015.

[95] J. S. Brooks and J. R. Schrieffer, Handbook of High -Temperature Superconductivity: Theory and Experiment. Springer New York, 2007.

[96] John Scheirs; Duane Priddy (28 March 2003). Modern Styrenic Polymers: Polystyrenes and Styrenic Copolymers. John Wiley & Sons. p. 3. ISBN 978-0-471-49752-3.

[97] Common Plastic Resins Used in Packaging". Introduction to Plastics Science Teaching Resources. American Chemistry Council, Inc. Retrieved 24 December 2012.

[98] T. Maharana, Y. S. Negi, and B. Mohanty, “Review article: Recycling of polystyrene,” Polym. - Plast. Technol. Eng., vol. 46, no. 7, pp. 729–736, 2007

[99] C. L. Huang, Y. C. Chen, T. J. Hsiao, J. C. Tsai, and C. Wang, “Effect of tacticity on viscoelastic properties of polystyrene,” Macromolecules, vol. 44, no. 15, pp. 6155–6161, 2011.

[100] K. Grigoriadi, J. B. H. M. Westrik, G. G. Vogiatzis, L. C. A. van Breemen, P. D. Anderson, and M. Hütter, “Physical Ageing of Polystyrene: Does Tacticity Play a Role?,” Macromolecules, vol. 52, pp. 5948–5954, 2019.

[101] A. G. Adeniyi, S. A. Abdulkareem, J. O. Ighalo, D. V. Onifade, S. A. Adeoye, and A. E. Sampson, “Morphological and thermal properties of polystyrene composite reinforced with biochar from elephant grass (Pennisetum purpureum),” J. Thermoplast. Compos. Mater., no. July 2021, 2020, doi: 10.1177/0892705720939169.

[102] C. Goze-Bac, “NMR studies of carbon nanotubes and derivatives,” no. January, pp. 1–132, 2008, [Online]. Available: https://tel.archives-ouvertes.fr/tel-00550837.

[103] Thermal and Electrical Conductivity of Single and Multi-Walled Carbon Nanotube-Epoxy Composites, A Moisala et.al., Compos. Sci. Technol., 66, 1285-1288 (2006)

[104] O. Shepelev, S. Kenig, and H. Dodiuk, Nanotechnology Based Thermosets, Third Edition. Elsevier Inc., 2014.

[105] Journet C, Maser W, Bernier P, Loiseau A, Lamy de Chapelle M, Lefrant S. Large-scale production of single-walled carbon nanotubes by the electric-arc technique. Nature 1997;388:7568.

[106] Ren ZF, Huang ZP, Xu JW, Wang JH, Bush P, Siegal MP. Synthesis of large arrays of well-aligned carbn nanotubes on glass. Science 1998;282:11057.

الخلاصة

تم في العمل الحالي استخدام تقنية البرم الكهربائي لتصنيع الياف متراكبة نانوية من البولي ستايرين المذاب بالثنائي مثيل فورمول أمايد بنسب (١٢،١٤،١٦ % وزنا)، وتم أيضا إضافة الكاربون النانوي المتعدد الجدران للعينات المحضرة، لمعرفة تأثيره على المحاليل المحضرة وخواص الالياف الناتجة. كما وتم استخدام صبغة نباتية مستخلصة من ورق الازهار الصفراء على افضل العينات المحضرة لرؤية مدى تأثيرها على خصائص المحلول والالياف الناتجة .

تم اجراء العديد من الفحوصات منها فحوصات خاصة بالمحلول التي تشمل الشد السطحي واللزوجة وفحوصات للأغشية المحضرة التي تشمل ، فحص الاشعة تحت الحمراء لتبيان نوع التفاعل بين المكونات ولمعرفة الاواصر الناتجة والتركيب، فحص زاوية الترطيب لمعرفة هل ان الالياف المحضرة محبة للماء ام كارهه للماء، فحص مجهر القوى الذرية لمعرفة خشونة السطح وعامل تحمل السطح، فحص المجهر الالكتروني الماسح ذو الانبعاث بالمجال لدراسة مورفولوجية الالياف وتوزيعها وحساب معدل اقطارها وتوجيهها وهوية عناصرها, كما وتم استخدام تقنية الاشعة فوق البنفسجية لمعرفة الخصائص الفيزيائية للمادة مثل وفجوة الطاقة والموصلية الضوئية ومعامل الانكسار ومعامل الاخماد والامتصاصية.

أثبتت النتائج ان الشد السطحي زاد بزيادة تركيز البولي ستايرين من (١٢-١٤٪وزنا) وقل عند زيادة التركيز ال(١٦٪وزنا) ، أما إضافة الكاربون النانوي المتعدد الجدران قد أدت الى تقليل الشد السطحي في التراكيز القليلة ويزداد بالتراكيز العالية. أما إضافة الصبغة فقد أدت الى زيادة الشد السطحي.اثبتت النتائج أيضا ان الاغشية المحضرة أصبحت محبة للماء بزيادة تركيز البولي ستايرين وكارهه للماء عند إضافة الصبغة للمجموعة ذات تركيز البوليمر (١٢٪وزنا). أما خشونة السطح زادت عند زيادة نسبة البولي ستايرين وكذلك بزيادة الكاربون النانوي المتعدد الجدران. عامل تحمل السطح قد زاد أيضا مما يؤشر على زيادة الخواص الميكانيكية للاغشية المحضرة. نتائج فحص المجهر الالكتروني اثبتت ان معدل اقطار الالياف يزداد بزيادة تركيز البولي ستايررين وتزداد كمية البيدات بالتراكيز القليلة ، اما عند استخدام الصبغة فسوف يقل القطر للالياف الناتجة وكمية البيدات يقل أيضا وان الالياف المنتجه كانت اعلى توجيه بالنسبة للمجموعة ذات تركيز البولي ستايرين (١٤٪ وزنا) تلتها (١٦٪وزنا) ثم ((١٢٪وزنا/الصبغة) ثم (١٢٪وزنا). كذلك تم الاستدلال على العناصر المكونة للمواد من خلال منضومة تشتيت الاشعة السينية المرتبطة بالمجهر الالكتروني. نتائج فحص الاشعة فوق البنفسجية أوضحت ان فجوة الطاقة تزداد بزيادة تركيز البولي ستايرين وتقل بزيادة الكاربون النانوي المتعدد الجدران والصبغة النباتية حيث بلغت اقل فجوة طاقة مستحصلة حوال (٠,٢ الكترون فولت) للعينة ذات التركيز(١٢٪وزنا بولي ستايرين /٠,١٦٪وزنا كاربون نانوي متعدد

الجدران/٠,٠٦٣ غرام صبغة) وبلغت قيمة الموصلية الضوئية لها حوالي (٦,٨٥x١٠^{٦} سيمنز$^{-١}$). مما يدل على انها افضل عينة محضرة ولها الخصائص اللازمة لاستخدامها كمتحسس للضوء وان افضل مجموعة تم تحضيرها كانت مجموعة الصبغة لاحتوائها على اقل قيم فجوة طاقة وكذلك على اقل قيم لاقطار الالياف وكذلك لزوجة متوسطة وشد سطحي متوسط ومقاومة للرطوبة فيما لو قورنت مع باقي المجاميع المحضرة.

جمهورية العراق
وزارة التعليم العالي والبحث العلمي
جامعة بابل
كلية هندسة المواد
قسم البوليمر

تأثير أنابيب الكربون متعدد الجدران النانوية والصبغة الطبيعية على ألياف البولي ستايرين النانوية للتطبيقات عالية التحسس بأستخدام تقنية البرم الكهربائي

رسالة مقدمة الى مجلس كلية هندسة المواد/ جامعة بابل كجزء من متطلبات نيل درجة الماجستير في هندسة المواد/ البوليمر

اعدت من قبل:

احمد عامر فليح حسن

إشراف:

ا. د هناء جواد كاظم

٢٠٢١ م – ١٤٤٢ هـ